Investigation of the biosynthesis of lovastatin and cytochalasin E, two fungal polyketides assembled by iterative PKS-NRPS enzymes.

by

Justin A. J. Thuss

A thesis submitted in partial fulfillment of the requirements for the degree of

Doctor of Philosophy

Department of Chemistry,
University of Alberta

Abstract

Cytochalasin E and lovastatin are two fungal polyketides that have seen extensive use as an angiogenesis inhibitor and as a cholesterol-lowering agent, respectively. These structurally divergent compounds are synthesized by polymerization of acetate units with concomitant functionalization by two different polyketide synthases (PKSs), CcsA and LovB. Both of these fungal synthases belong to a unique class of enzymes called fungal iterative polyketide synthase-nonribosomal peptide synthetase hybrids (fungal iterative PKS-NRPSs). These enzymes are unique, as the PKS component contains a suite of reactive domains that are similar in architecture to fatty acid synthases (FASs) but construct much more functionalized acyl chains than the long saturated lipids made by FASs. The NRPS region typically facilitates attachment of an amino acid to the acyl chain and release from the synthase. The diversity of the natural products produced from PKS-NRPSs is astonishing, yet very little is understood about how the domains operate. The iterative nature of the domains means that they must display "inherent selectivity" that results in partial reduction on some sections of the polyketide chain. This is sometimes referred to as the "programming" of the synthase.

This thesis explores the biosynthesis of cytochalasin E by first investigating the biogenesis of its unique macrocyclic carbonate moiety. Its formation is catalyzed by CcsB, a Baeyer-Villigerase encoded in the gene cluster for cytochalasin E in *Aspergillus clavatus*. CcsB was heterologously expressed, purified and assayed *in vitro* using chemically synthesized substrates. CcsB formally catalyzes a double Baeyer-Villiger reaction and its mechanism was investigated using isotope labeling. Formation of cytochalasin E's carbon backbone was investigated by expressing CcsA *in vitro*. Attempts towards the synthesis of a late-stage, fully

functionalized PKS intermediate are detailed. The unusual activity and role of the reductase domain (R) of the NRPS region of CcsB was examined as well.

The programming of lovastatin biosynthesis was studied by focusing on the activity of one domain of the PKS-NRPS, namely the methyltransferase domain (MT). The MT domain of LovB is active during one single round of chain elongation in the process of lovastatin biosynthesis. This activity was explored by expressing the megasynthase LovB *in vitro* and assaying the methylation activity using synthetic intermediates. Results indicate that the selection is at the substrate level and may be kinetically controlled.

Acknowledgements

I would like to acknowledge my supervisor Prof. John Vederas for his enduring support and guidance during my PhD studies at the University of Alberta. He gave this keen, naive student a chance at research and I'll always be grateful. I would also like to thank my collaborators at the UCLA, Prof. Yi Tang and his coworkers Ralph A. Cacho, Bo Wang, Dr. Kangjian Qiao, Jingjing Wang and Dr. Youcai Hu for all of the support and answering my numerous queries on various aspects of their work. I would also like to thank Shaun McKinnie and Stephen and Rachel Cochrane for their support during my PhD. Especially Shaun for his company during weekends and late evenings. Our camaraderie and mutual work schedules made lab work bearable for me. I would also like to thank Dr. Brandon Findley for his prompt edits of this thesis.

I would like to genuinely thank Dr. David Dietrich for his contributions to my PhD studies. I feel a debt of gratitude that I'm afraid will never be fully paid. Not only did he inspire me to switch into the doctoral program, but his encouragement and support during times when I truly needed it have affected me in ways that I cannot describe. He is a role model for all scientists because he inspires people to think creatively while also leading by example with his work ethic. He's never selfish with his time and I never felt guilty for asking for his help. The next round's on me, Dave.

I would be remiss if I didn't mention the amazing support staff in the chemistry department including, but not limited to, Dr. Randy Wittal, Jing Zheng, Dr. Angie Morales, Dr. Wayne Moffatt, Mark Miskolzie, Dr. Ryan McKay, Bernie Hippel, Matt Kingston and Andrew Yeung. Your collective fingerprints are all over this PhD and none of this work would be

possible without your tireless dedication to the students in the Chemistry department. Special shout-out to Jill Bagwe for her support in my extracurricular volunteering in the department.

I would also like to thank my parents, Tony and Karen Thuss, and Tessa Margetts for their roles in maintaining my sanity through my PhD. Especially Tessa's unwavering patience through the writing process of this document. In that vein, I would also like to thank actor, governor, philanthropist Arnold Schwarzengger for being the embodiment of excellence and achievement as well as a constant source of quotable lines and puns.

Preface

Some of the work presented in this thesis was done in collaboration with Prof. Yi Tang's lab at the UCLA. The coworkers in Prof. Tang's lab were responsible for the molecular biology components of this thesis as well as some of the *in vitro* testing. All specific contributions are marked in detail by footnotes in the main body. Part of chapter 2 has been published: Hu, Y.; Dietrich, D.; Xu, W.; Patel, A.; Thuss J. A. J.; Wang, J.; Yin, W.-B.; Qiao, K.; Houk, K. N.; Vederas J. C.; Tang, Y. *Nat Chem Biol* **2014**, *10*, 552. My contributions included the synthesis of enzymatic substrates and proposal of the enzymatic mechanism. The manuscript was prepared by the lead author, and Profs Vederas and Tang. The rest of the work presented in this thesis is unpublished at the time of writing.

Table of contents

List of Figures

List of schemes

List of tables

Abbreviation list

[α]	specific rotation
6-MSA	6-methylsalicylic acid
A	adenylation domain
Å	angstrom
ACP	acyl carrier protein
AT	acyl transferase
n-BuLi	*n*-butyl lithium
BVMO	Baeyer-Villiger monooxygenase
c	concentration in g/ml (for optical rotation)
C	condensation domain
CHMO	cyclohexanone monooxygenase
CHS	chalcone synthase
CLF	chain length factor
CoA	coenzyme A
δ	chemical shift in ppm
d	doublet
6-DEB	6-deoxyerythronolide
DEBS	6-deoxyerythronolide synthase
DH	dehydratase
DIPEA	*N,N*-diisopropylethylamine
DKC	Dieckmann cyclase domain

DMAP	4-(dimethylamino)pyridine
DMB	desmethylbassinin
DMBS	desmethylbassinin synthase
DML	dihydromonacolin L
DMP	Dess-Martin periodinane
DMSO	dimethyl sulfoxide
EDC	1-ethyl-3-(3-dimethylaminopropyl)carbodiimide
Eq	equivalents
ER	enoyl reductase
EtOAc	ethyl acetate
$FADH_2$	flavin adenine dinucleotide (reduced)
FAS	fatty acid synthase
FDA	Food and Drug Agency (USA)
FUSS	fusarin synthase
GC-MS	gas chromatography coupled mass spectrometry
HMG-CoA	3-hydroxy-3-methylglutaryl-coenzyme A
HR-EI	high-resolution electron impact
HR-ES	high-resolution electrospray
HR-PKS	highly reducing polyketide synthase
HWE	Horner-Wadsworth Emmons
IR	infrared
J	coupling constant in hertz
kDa	kilo Daltons

KR	ketoreductase
KS	ketosynthase
LC-MS	liquid chromatography-coupled mass spectrometry
m	multiplet
m/z	mass to charge ratio
MAT	malonyl:acyl transferase
Me	methyl
MeOH	methanol
MSAS	6-methylsalicylic acid synthase
MT	methyltransferase domain
NADPH	β-nicotinamide adenine dinucleotide phosphate
NaHMDS	sodium hexamethyldisilazide
NCE	new chemical entity
NMR	nuclear magnetic resonance
NP	natural product
NR-PKS	non-reducing polyketide synthase
NRPS	non-ribosomal peptide synthetase
PD	potato dextrose
Ph	phenyl
PKS	polyketide synthase
PKS-NRPS	polyketide synthase-non ribosomal peptide synthetase
Ppant	phosphopantetheine
Ppm	parts per million

pptase	phosphopantetheinyl transferase
PR-PKS	partially reducing polyketide synthase
PT	product template domain
q	quartet
quant.	quantitative yield
R	reductase domain
RAL	resorcylic acid lactone
SAM	*S*-adenosyl methionine
SAT	starter acyl transferase
SNAC	*N*-acetyl-cysteamine
T	thiolation domain
TBAF	tetrabutylammonium fluoride
TBS	*tert*-butyldimethylsilyl
TE	thioesterase domain
TENS	tenellin synthase
TLC	thin layer chromatography
UV	ultraviolet spectroscopy

1 Introduction

Natural products (NPs) can be broadly defined as biologically active secondary metabolites derived from natural sources, such as plants, bacteria or fungi[1]. Natural products are of high interest to synthetic and biological chemists alike, as they provide challenging targets for total synthesis or thought-provoking biosynthetic puzzles. They are also of interest to medicinal chemists, with 64% of all FDA-approved drugs from 1981-2010 being NPs, semi-synthetic NPs or NP inspired.[2,3] NPs provide medicinal chemists with pharmacologically active cores (termed pharmacophores) from which they can draw inspiration or derive new chemical entities (NCEs). The current paradigm for drug discovery is challenged by the rise of generic drug companies and the shrinking of R&D expenditure from the pharmaceutical industry.[4] These factors have contributed to a steady decrease in the amount of NCEs in clinical trials.[3] It is not difficult to understand why big pharmaceutical companies have veered away from the development of NCEs when the financial cost is considered. This is perhaps best exemplified in the recent exhaustive review from Hay and co-workers in 2014 of the FDA approval of drugs for over 800 drug developers over the course of 2003-2011.[5] They concluded that new drug candidates going through clinical trials have only a ten percent likelihood for FDA approval. Combined with the fact that the latest estimate of bringing a drug through clinical development is almost $2.6 billion US, developing new chemical entities is an extremely expensive endevour.[6] Drug manufacturers have previously relied on the development of so called “blockbuster drugs” but this business model is no longer sustainable.[4] Unfortunately, this problem becomes more complicated with the urgent need for new antibiotics and the growing concern over antimicrobial resistance with some

referring to this as the "post-antibiotic era".[7] The key to this problem may very well lie in the vastly untapped potential of natural products and their biosynthesis.

If we can understand how natural products are assembled by nature, not only do we gain a deeper knowledge of functional enzymology, but we may also unlock the potential to engineer biosynthetic enzymes to create hybrid, novel natural products. The ultimate goal would be to use these enzymes in a combinatorial fashion to create NP-centric drug screening libraries to screen against any medical condition with an appropriate assay, including antimicrobial resistance. Before this dream can be realized, the scientific community needs an understanding of how these molecules are assembled enzymatically.

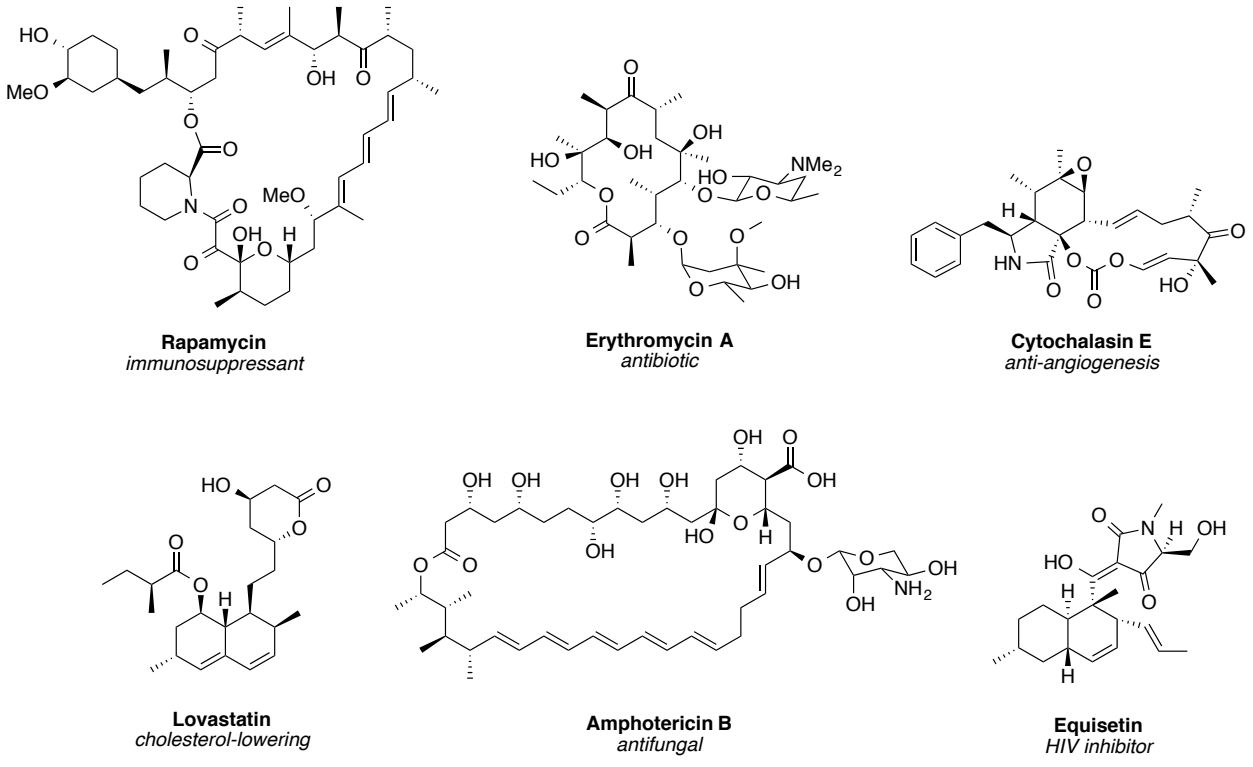

Figure 1-1. Examples of polyketide natural products, demonstrating the chemical diversity of polyketide structures and bioactivities.

Polyketides represent a subset of natural products that contain complex carbon backbones.[8-10] The structural diversity of polyketides leads to a suite of bioactive properties such as immunosuppressive[11], antiviral[12], antibacterial[13], anti-tumor[14] and cholesterol-lowering[15] activity (Figure 1-1). Interestingly, these complex carbon skeletons are predominantly assembled from nature's simplest building blocks: acetic acid and/or propionic acid. This discovery was originally called the "Collie-Birch hypothesis" named after John Norman Collie and Arthur Birch for their early elucidations of the assembly of aromatic polyketides like 6-methylsalicylic acid (6-MSA)[16] and orcinol.[17] In 1893, James Collie performed degradation studies to determine the structure of dehydroacetic acid by boiling it in barium hydroxide and working up with acid. He determined that it formed orcinol and proposed a triketone intermediate, the first suggestion of a poly-ketone precursor to what would later be called a polyketide (Scheme 1-1).[18] The theory of biogenesis of polyketides from repeating acetate units didn't gain traction until a pioneering study by Arthur Birch and the incorporation of ^{14}C-labeled acetic acid into 6-MSA by *Penicillium griseofulvum* (Scheme 1-2).[19] This led to the widespread acceptance of the biological origin of this new class of natural products as polymerized acetic acid C_2 units that could then be aromatized, as is the case with 6-MSA and orcinol. With this came a veritable explosion of study into polyketide and fatty acid biosynthesis, which was independently discovered to also be made from repeating C_2 units.[20,21]

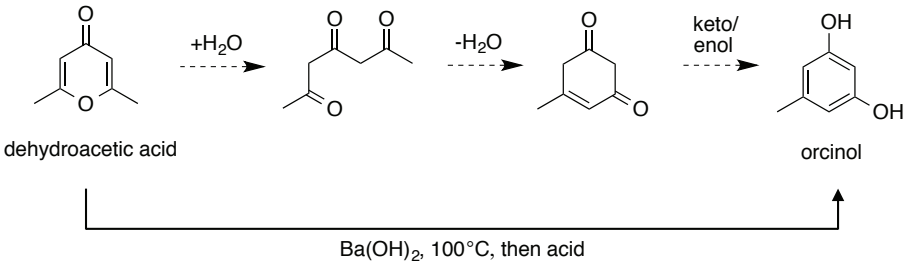

Scheme 1-1. Synthesis of orcinol by Collie and proposal of polyketide intermediate.

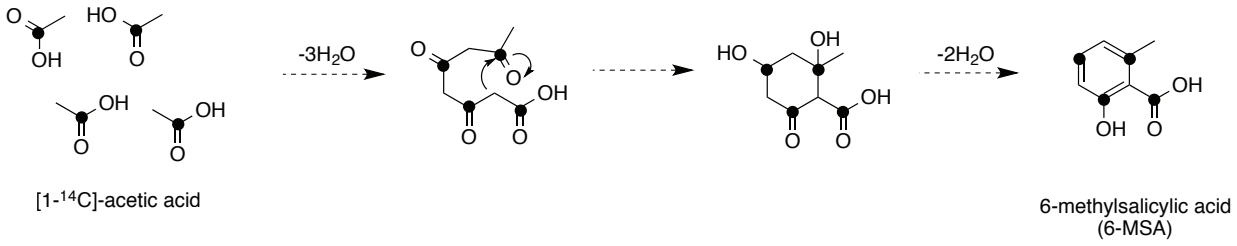

Scheme 1-2. Proposed biosynthesis by Birch to explain ^{14}C-labelling of 6-MSA in *P. griseofulvum*. Modified from a review by Staunton *et al*.[8]

The genetic basis for fatty acid and polyketide biosynthesis was arguably the next major milestone in natural product biochemistry. Decades of research from many academic groups culminated in the elucidation of the genes responsible for fatty acid biosynthesis. In 1964 Konrad Bloch and Feodor Lymen were awarded the Nobel Prize in Medicine, for "The Biosynthesis of Fatty Acids and Cholesterol".[22] In the PKS discipline, the credit for genetic determination of PKS biosynthesis often goes to David Hopwood for his work on genetic manipulation of actinorhodin biosynthesis in *Streptomyces sp.*[23] and Leonard Katz and Peter Leadley for erythromycin biosynthesis in *Saccharopolyspora erythraea*.[24,25] This work was expanded by the efforts of Cane[26], Khosla[27], Walsh[28] and others to gain insight into the mechanism of how these giant, multidomain megasynthases operate. The next few sections of this chapter will delve into

the state of the art of PKS enzymes, spanning from the fatty acid synthase (FAS) and modular PKSs commonly found in bacteria to the fungal iterative PKSs, the main focus of this thesis. Understanding the "programming" of these molecular machines and the nuances of their function will improve our ability to engineer functional, rationally designed PKSs.

1.1 General biosynthesis of fatty acids and polyketides

Fatty acids are assembled in a head-to-tail fashion from acetate units (C_2) by fatty acid synthase (FAS), a large multimodular enzyme.[8,22] FAS uses its seven catalytic domains in an iterative fashion to yield long, saturated carbon chains. The order of domain reactivity is shown in Figure 1-2. Although fatty acids are largely devoid of functional groups, it requires an impressive number of steps and co-factors to synthesize them. To form palmitic acid (a C_{16} fatty acid), FAS catalyzes 7 condensation reactions and over 21 β-carbon processing reactions in less than one second.[22] It is important to understand how FASs assemble fatty acids because the domains in polyketide synthases (PKSs) assemble polyketides in an analogous fashion.

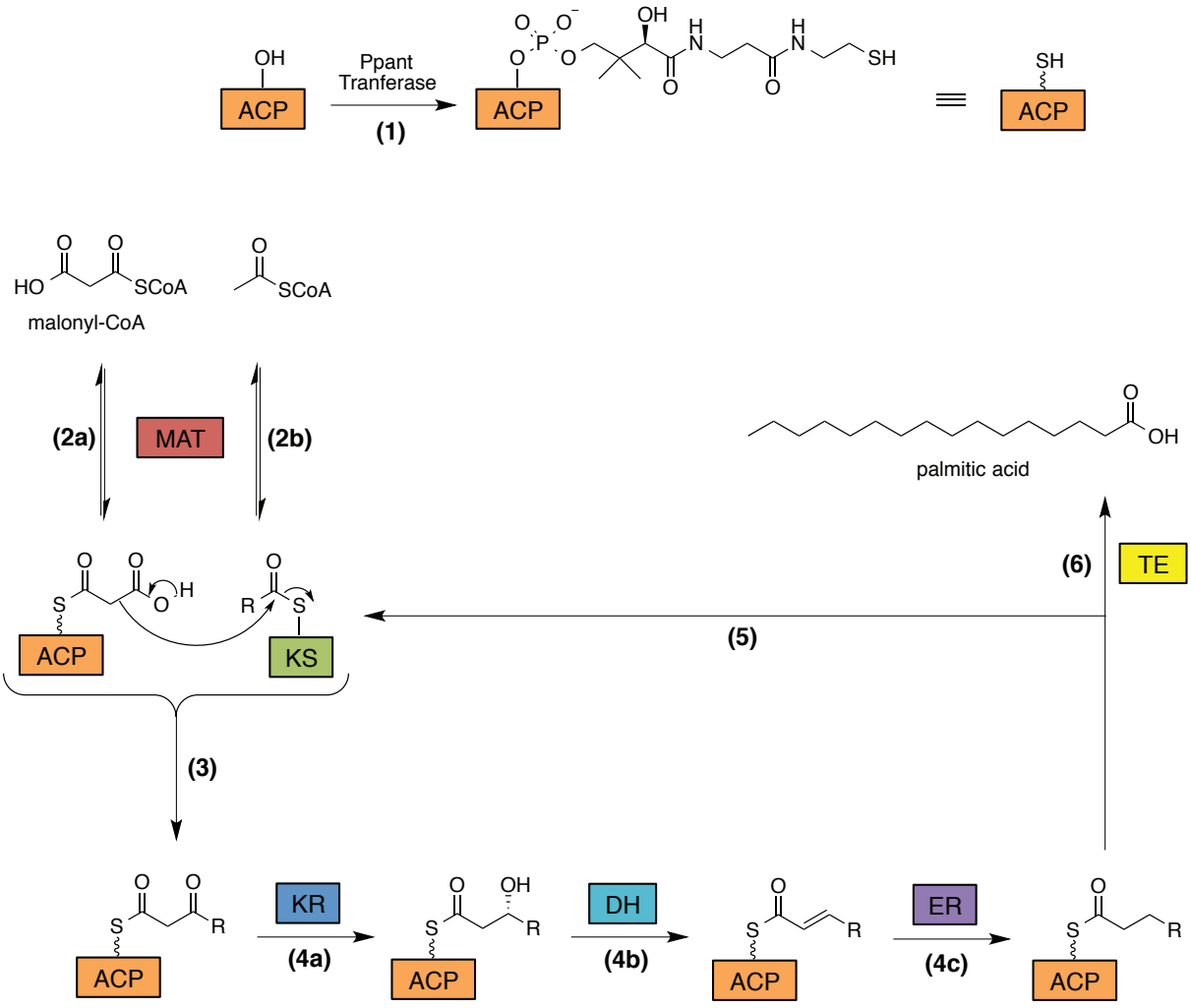

Figure 1-2. General biosynthesis of palmitic acid by FAS. ACP = acyl carrier protein, MAT = malonyl CoA:acyl transferase, KS = ketosynthase, KR = ketoreductase, DH = dehydratase, ER = enoyl reductase, TE = thioesterase. Step numbers are bolded and in parentheses.

First, the acyl carrier protein (ACP) domain of FAS has to be modified with phosphopantetheine to convert the enzyme from its *apo* to *holo* form (Figure 1-2, step 1).[29] This approximately 18Å-long prosthetic group is donated from coenzyme A and is transferred to a serine residue on ACP by a phosphopantetheinyl transferase. Once ACP has been modified, it can facilitate the growing acyl chain inside the active site of FAS and bring the chain into proximity of the other domains. With the FAS in its *holo* form, it can be loaded with both a

'starter' unit (acetyl-CoA) and 'extender' unit (malonyl-CoA). Both acyl transfers are facilitated by the malonyl CoA:acyltransferase (MAT) domain (step 2a/b). The MAT domain has the dual responsibility of loading both acetyl-CoA and malonyl-CoA and therefore both substrates are competitive inhibitors of each other. The MAT compensates by having both acyl groups in a fast equilibrium between their CoA and protein-bound forms to prevent this step from becoming rate limiting.[30,31]

Once the ketosynthase (KS) domain active site cysteine residue is loaded with the starter unit (step 2a) and the ACP domain is loaded with the extender unit (step 2b), fatty acid synthesis can begin. The KS domain catalyzes a decarboxylative Claisen condensation that results in loss of CO_2 from malonyl-CoA and generation of a nucleophilic enolate that can attack the acyl group on the KS, creating a new C-C bond and transferring the acyl group onto the ACP domain (step 3). This step is referred to as the 'chain extension' step as it results in the elongation of the growing acyl chain by one ketide unit (-C(O)CH_3). After the new C-C bond is formed, the newly formed β-carbonyl is reduced in a series of reactions referred to as the 'tailoring steps' (step 4). These include reduction of the ketone to a "3*R*" hydroxyl[22] by the NADPH-dependent ketoreductase (KR; step 4a), *syn*-elimination of the hydroxyl to a trans double bond by the dehydratase domain (DH; step 4b) and reduction of the trans double bond to the saturated carbon chain by the enoyl reductase using one molecule of NADPH (ER; step 4c). Interestingly, the reduction of the enoyl group proceeds by a "syn" addition of the NADPH-derived hydride and proton (from water) in mammalian and prokaryotic FAS but yeast FAS occurs by an "anti" addition.[22] These tailoring steps all occur on the growing acyl chain attached to the ACP domain. For this reason, the ACP is often thought of as a 'polyketide shuttle' that moves the growing acyl chain from domain to domain in an 'assembly line' fashion.[29]

After the tailoring steps are complete, the reduced acyl chain has two possible fates: either the chain is transferred back to the KS domain for another round of chain extension and reductions (step 5), or it is released by the thioesterase (TE) domain as a carboxylic acid (step 6). In the biosynthesis of palmitic acid, the iterative processing occurs six more times to synthesize a C_{16} fatty acid, using one molecule of acetyl-CoA (only one starter unit is needed per product) and seven molecules of malonyl-CoA. The ACP-bound C_{16} acyl chain is then released from the enzyme by the TE domain as a carboxylic acid.

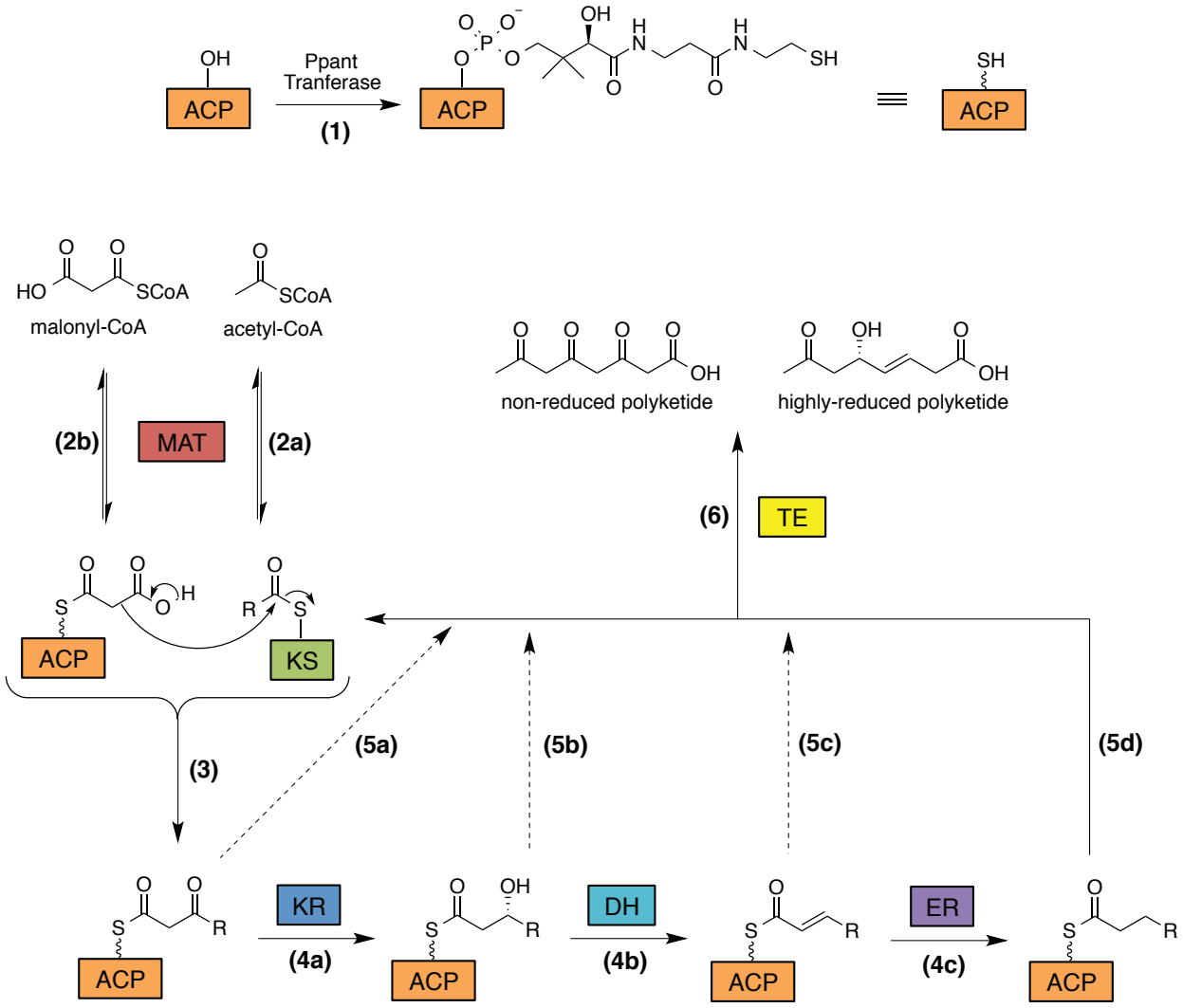

Figure 1-3. Generic representation of biosynthesis of non-reduced or semi-reduced polyketides.

Polyketide biosynthesis occurs in a similar fashion to fatty acid biosynthesis with a few distinct differences (Figure 1-3). PKS enzymes still gain a phosphopantetheinyl arm via post-translational modification and loading of the starter and extender units occurs by the same domains and mechanisms (steps 1 and 2). The mechanism of chain extension is also similar, but the divergence in biosynthetic logic is ultimately in the tailoring steps (steps 5a-d). PKS enzymes can 'interrupt' the full reduction of the new ketide unit either partially (resulting in either a

hydroxyl group or trans double bond) or completely (to keep the ketide intact) before starting the cycle over. This unique "programming" of the PKS enzyme allows for the biosynthesis of functionalized carbon chains that contain more functional groups than just a saturated C_2 unit. The functionalized chains can then be released from the ACP by the action of a TE domain (step 6). Several different types of chain release have been documented, including cyclization reactions such as lactonization[32-34], pyrone formation[10], or hydrolysis by a molecule of water to make a carboxylic acid.[35] Release of the linear or cyclic polyketide product can be followed by additional diversification by reactions including but not limited to: glycosylation[36], additional cyclizations[37], oxidation[38] or skeletal rearrangements.[39,40]

PKS enzymes are divided into several different types and subtypes, determined by their architecture and if the domains are used iteratively or in a modular fashion (Table 1-1). Modular PKS enzymes contain many copies of the same domains, where iterative PKS only contain one functional copy, similar to FAS. Interestingly, modular PKS systems obey the rule of "co-linearity" where the presence and order of domains confers knowledge of its polyketide product. This will be explained in further detail in section 1.2.1. The PKS types are divided by their overall architecture (Figure 1-4). PKS type I enzymes have all the domains fused as one polypeptide and act in *cis* while type II domains are separate proteins that act in *trans* to assemble polyketides. Type III domains also act in *trans* but are unique because they do not require an ACP, opting instead to use acyl-CoA building blocks that are extended to form larger polyketides. The biosynthetic logic and programming will be discussed in the next chapter sections. Fungal iterative PKSs will be discussed in greater detail than the bacterial type I, II and type III systems with special emphasis on the PKS-NRPSs (the focus of this thesis).

PKS Type	Subtype	Organism
I	Modular	Bacteria, some protists
	Iterative	Fungi, some bacteria
II	Iterative	Bacteria only
III	Iterative	Mostly plants, some bacteria and fungi
PKS-NRPS	Modular	Bacteria
	Iterative	Fungi and bacteria

Table 1-1. Types of PKSs. Modified from a review by C. Hertweck[10]

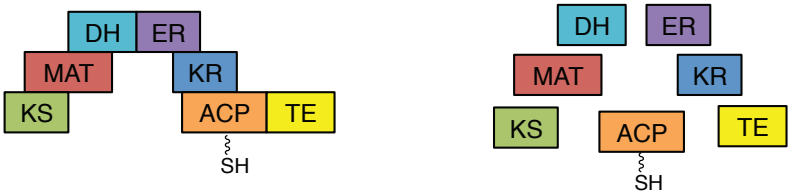

Figure 1-4. Overall architecture of PKS types I (*cis*) and II (*trans*).

1.2 Type I PKS

1.2.1 Modular type I PKS enzymes

Modular type I PKSs are typically found in bacteria with a small number discovered in protists.[41] Modular PKS enzymes are defined by having multiple copies of the same domains that are divided into 'modules' that are each responsible for the installation and tailoring of one polyketide unit. The programming rules for modular PKS often follow a rule of "co-linearity" meaning that the polyketide product size matches the number of modules and the functionality matches the order of those domains in a linear fashion. An illustrative (and incredibly well

studied) example is the biosynthesis of 6-deoxyerythonolide B (6-DEB) by DEBS (deoxyerythronolide B synthase).[26] DEBS is a large (2 MDa), multimodular protein produced by *S. erythraea* that is encoded over 3 genes and catalyzes a plethora of chemical reactions to generate the macrolide precursor to erythromycin A, 6-DEB (Figure 1-5). According to the rule of co-linearity, the number of modules correlates to the number of ketide units in the final product. DEBS follows this rule with seven modules catalyzing 6 condensation reactions to make a highly methylated heptaketide.

Each module contains a set of core domains (ACP, AT, KS) that are responsible for chain extension and consequentially, ketide production. Interestingly, the AT domain can select a wider variety of acyl CoAs then have been observed for FAS. In the case of DEBS, methylmalonyl-CoA (MeMal-CoA) is used as the extending unit at each ketide stage, resulting in a highly methylated product. The presence of active tailoring domains in each module determines the final functionality of that ketide unit. For example, in DEBS module 2, only the KR domain is present (outside the core domains), so the β-ketone is reduced to a hydroxyl and full reduction to the methylene does not occur. In contrast, module 4 possesses all tailoring domains so the β-ketone is reduced fully to the methylene. DEBS has been the subject of intense research, with almost all of its domains and functions mapped. Recently, the catalytically inactive KR domain in module 3 was determined to have epimerization activity, specifically epimerizing the α-methyl of the tetraketide from (*S*) to (*R*).[42] The next frontier for DEBS research is solving the full 3D structure to understand more of the mechanism and domain interplay.

Unfortunately, the simplicity of co-linearity doesn't apply to all modular PKS type I systems. The well-documented phenomena of module skipping or stuttering (iterative use of the

same module) and trans-acting domains provide an imperfect view of how these molecular machines operate.[43] Although these issues muddle our understanding of the programming of modular type I PKS systems, we have an even murkier view of how iterative type I PKS work.

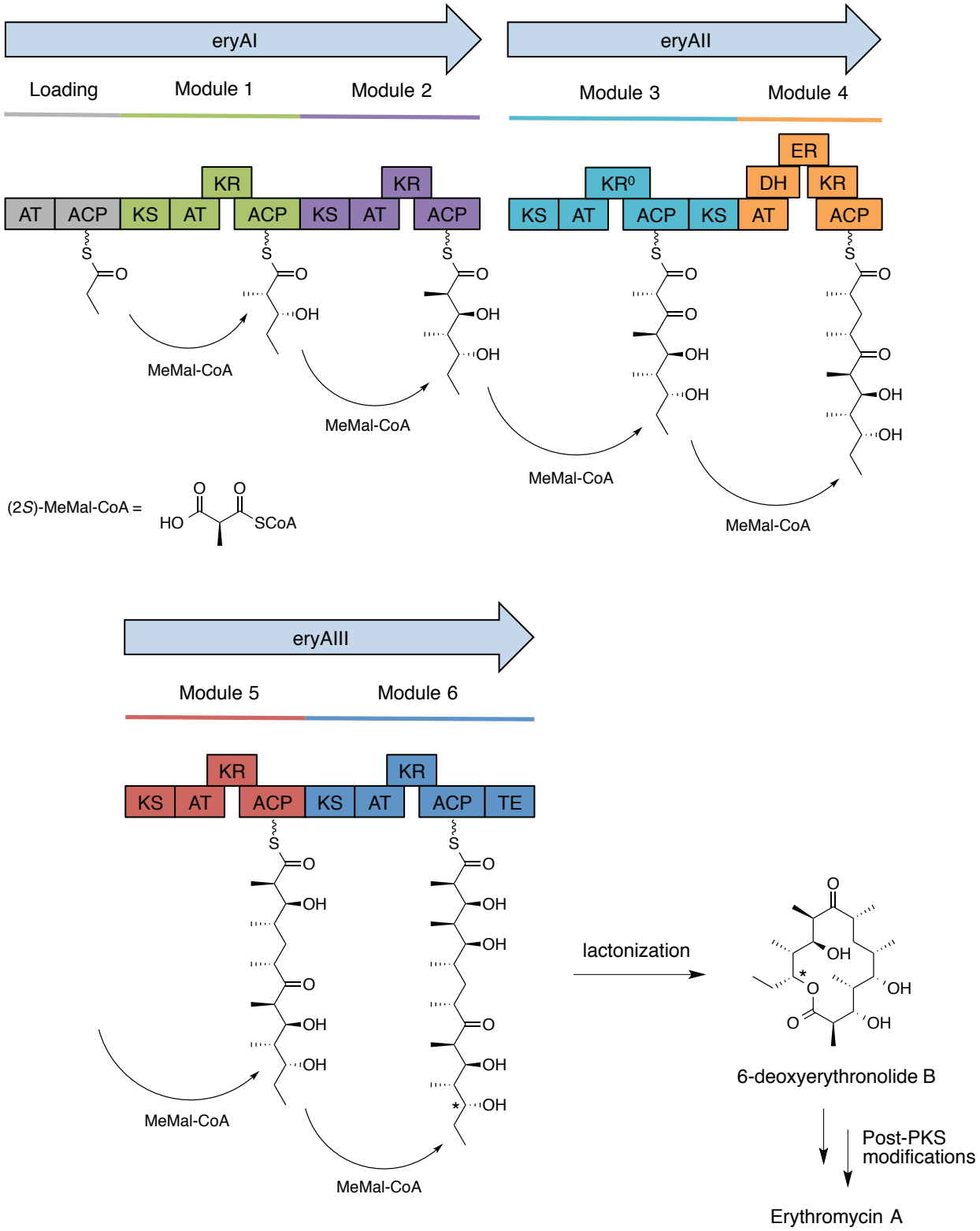

Figure 1-5. Biosynthesis of 6-deoxyerythronolide B by deoxyerythronolide B synthase (DEBS), a type I modular PKS. Asterisk indicates point of cyclization by TE domain.

1.2.2 Iterative type I PKS enzymes

Iterative type I PKS systems closely resemble FAS in their architecture and function. Similar to FASs, iterative PKS enzymes possess a single functional copy of all necessary domains fused as a single polypeptide.[44,45] The divergence is in the selective activity of the tailoring domains. As shown in Figure 1-3, PKS enzymes can prevent full reduction at certain ketides, resulting in either a highly reduced (HR-PK), partially reduced (PR-PK) or a non-reduced polyketide (NR-PK). This designation is used for the synthases as well and are generally split into 4 groupings: NR-PKS, PR-PKS & HR-PKS (section 1.2.2.1), and PKS-NRPS enzymes (section 1.5).[46] Unfortunately, the rule of co-linearity does not apply to the iterative PKSs and the basis for selectivity and timing of the tailoring domains is poorly understood.

1.2.2.1 NR-, PR-, & HR-PKS enzymes

Iterative PKS enzymes are categorized by their gene sequence and the presence or lack of tailoring domains (KS, DH, ER). In addition to the tailoring domains, there are a few domains that are unique to each grouping. NR-PKSs are defined by possessing the necessary core domains for chain extension (ACP, KS, AT) and a lack of functional tailoring domains (Figure 1-6A). Typically, NR-PKS enzymes synthesize long unreduced polyketide chains that cyclize in a series of Dieckmann-like condensation reactions to form polyaromatic compounds. The first step in the biosynthesis of norsolorinic acid, a precursor *en route* to aflatoxin B1, by a NR-PKS named PksA is the recruitment of a hexanoyl starter unit by the starter acyl transferase (SAT) domain. The SAT domain is responsible for recognition and priming of 'unusual' starter units, including hexanoyl-CoA. PksA then extends the hexanoyl group by seven ketides derived from seven malonyl-CoAs through the iterative action of the KS and MAT (malonyl acyl transferase)

domains. The octaketide is then cyclized through three Claisen cyclizations catalyzed by the product template domain (PT) and the TE domain to release norsolorinic acid as a fused aromatic compound. The PT domain is unique to NR-PKS enzymes and determines the folding pattern of the polyketide before cyclization.[47] Recent studies have shown that PT domains can be rationally reprogrammed to give new cyclized products through site-directed mutagenesis.[48] A remarkable amount of information about the structure and function of PksA has been elucidated over the past five years.[47,49] The SAT domain of PksA has also been shown to have flexible substrate recognition, allowing for the incorporation of many unnatural acyl substrate analogues (SNAC esters, discussed in greater detail in chapter 2) of varied length and functionality into the final product.[49] The PT domain has been crystalized as a dissected monodomain with palmitic acid bound in the active site[50] and the natural substrate has been mapped into it using molecular modeling to find the active site residues responsible for cyclization.[51]

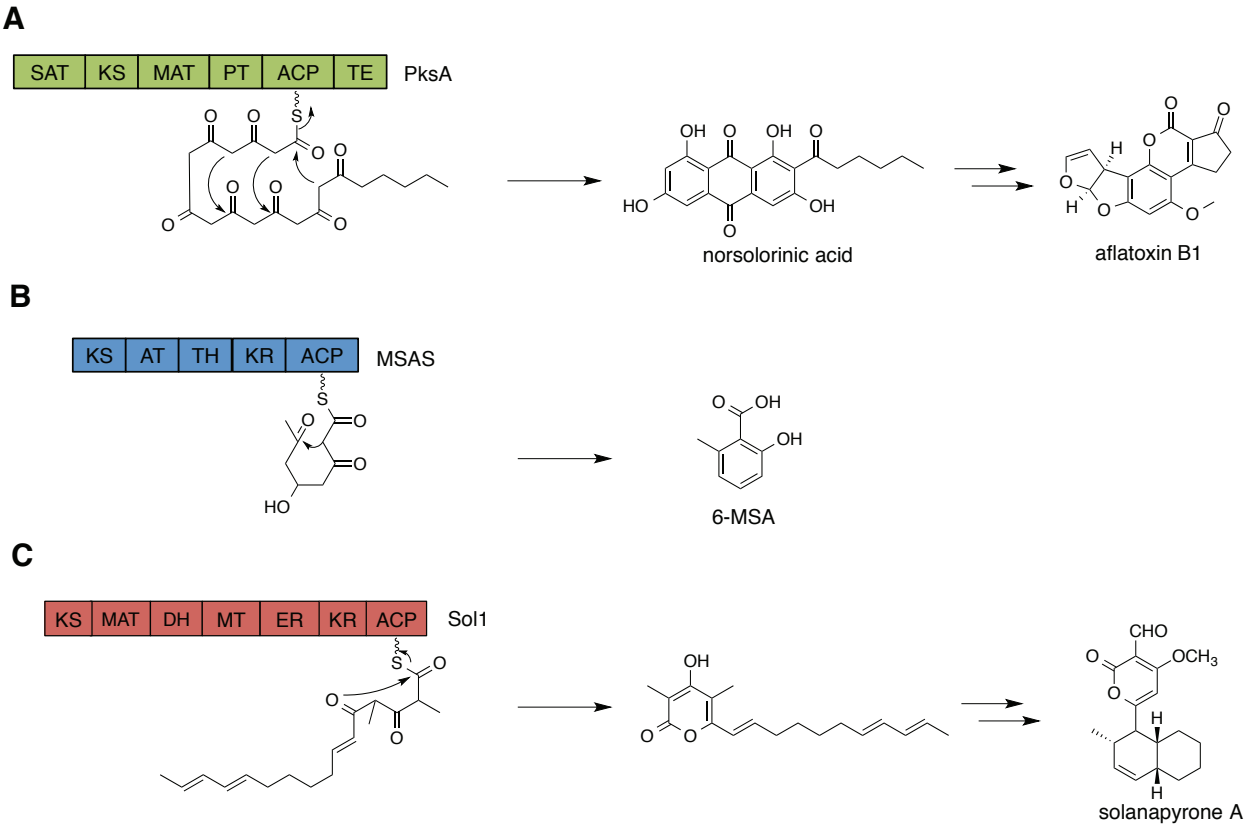

Figure 1-6. Biosynthesis of norsolorinic acid, 6-MSA and solanapyrone by a NR-, PR- and HR-PKS. A) Biosynthesis of norsolorinic acid by PksA, a NR-PKS from *Aspergillus parasiticus*; B) Biosynthesis of 6-MSA by MSAS (6-methylsalicylic acid synthase), a PR-PKS from *P. patulum*; C) Biosynthesis of a precursor to solanapyrone A by Sol1, a HR-PKS from *Alternaria solani*.

PR-PKS enzymes are classified as having the core domains and a limited number of tailoring domains. Fifteen years after Birch's research into the biogenesis of 6-MSA, MSAS (6-methylsalicylic acid synthase) was discovered.[52] This relatively small PR-PKS enzyme is responsible for 6-MSA biosynthesis. The authors were able to detect the activity of MSAS in cell-free extracts of *Penicillium patulum* and partially purified active enzyme, marking it as the first (mostly) isolated PKS.[53] MSAS synthesizes an ACP-bound triketide using its KS, AT and a KR that is only used once at the diketide stage. Interestingly, an NADPH-dependent DH domain cleaves the thioester bond instead of catalyzing the typical elimination reaction. This domain was

renamed thioester hydrolase (TH) to reflect its unusual activity.[54] TH domains have been found in other PR-PKS enzymes, such as those responsible for micacocidin[55] and (*R*)-mellein[56] biosynthesis, suggesting the domain may be more ubiquitous than previously thought.

Finally, HR-PKS enzymes are categorized by possessing all tailoring domains necessary to perform a full ketide reduction. In this way, they are the most similar to FAS. Solanapyrone A is a pyrone-containing natural product that is assembled by *Alternaria solani* through a HR-PKS named Sol1 and several post-PKS enzymes.[57] Sol1 builds an octaketide with seven condensation reactions connecting a molecule of acetyl-CoA to seven malonyl-CoAs. The octaketide is highly functionalized with three trans-double bonds, a few saturated carbons and two methyl groups, the latter installed by the methyltransferase domain (MT). Methyltransferase domains will be discussed in greater detail in Chapter 3. In some organisms, HR-PKS enzymes work in tandem with NR-PKS enzymes to assemble highly functionalized macrocyclic rings fused with one or more aromatic rings.[46] Resorcylic acid lactone (RAL) biosynthesis is an example of this enzymatic co-operation.[58]

1.3 Type II PKS

As discussed earlier, type II PKS enzymes are comprised of small, *trans*-acting domains that closely resemble plant and bacterial type II FAS.[59] Typically comprised of a tightly bound minimal PKS complex, type II PKSs have only been found in terrestrial and marine *Actinomycetes sp*. and produce clinically important aromatic polyketides.[59] Tetracyclines are a class of broad-spectrum antibiotics produced by type II PKS enzymes and have seen wide clinical application for decades but rapid resistance has led to a decrease in use.[60,61] The biosynthesis of oxytetracycline, one of the first tetracycline antibiotics to be discovered, is a

concerted effort of over 13 enzymes. The carbon skeleton is assembled by three PKS domains named OxyA, OxyB, and OxyC, while OxyD synthesizes and primes the starter unit (Figure 1-7). The three core domains comprise the minimal PKS complex and consist of an ACP and two KS domains (often termed as KS_α and KS_β). The KS_β domain is sometimes denominated as a chain length factor (CLF) domain as its active site cysteine has been mutated to a glutamine, rendering it catalytically inactive.[62] Co-crystal structures of the KS and CLF together have shown that they heterodimerize to form a 'hydrophobic tunnel' where chain elongation occurs.[63] The CLF controls the chain length by permitting elongation until the chain hits a gatekeeping residue that prevents further condensation reactions. The chain is then off-loaded and cyclized.[64] The KS and ACP domains catalyze chain elongation by self-loading malonyl-CoA, facilitating the Claisen condensation and acyl transfer reaction without an AT domain.[27] After eight rounds of iterative chain elongation, the enzyme bound nonaketide is cyclized and released by additional biosynthetic enzymes.[61]

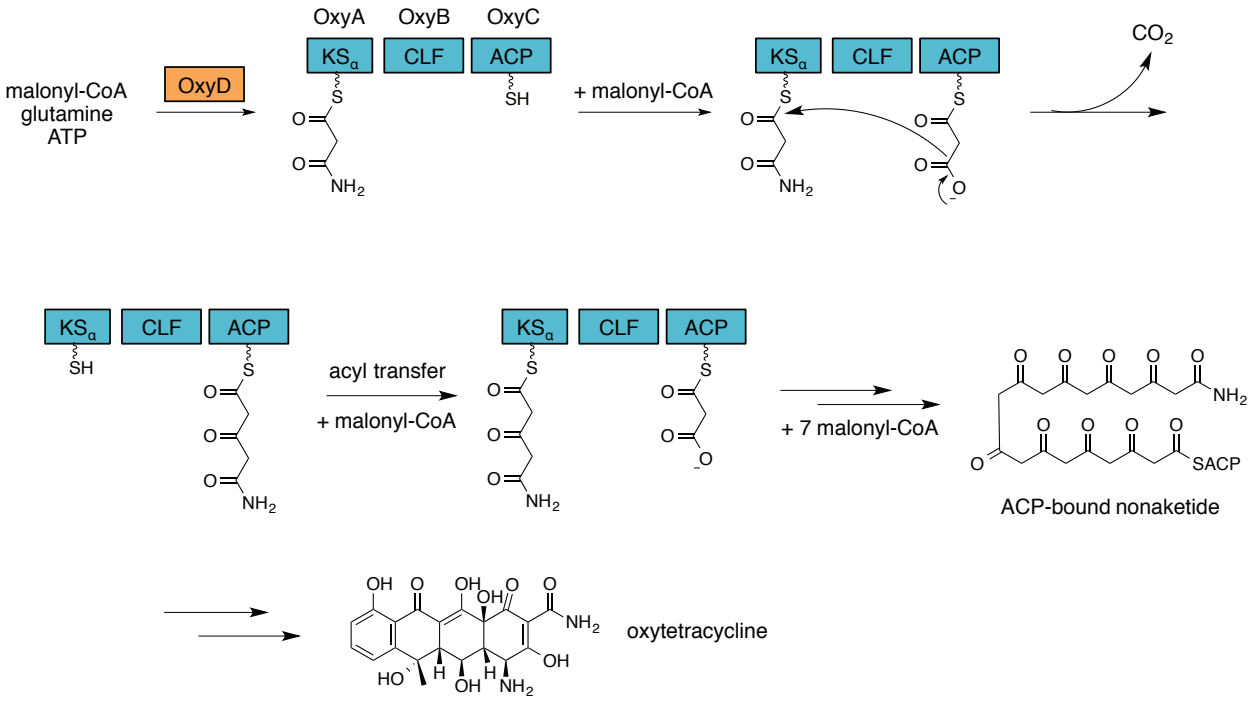

Figure 1-7. Biosynthesis of a nonaketide intermediate of oxytetracycline by a type II PKS, OxyABC. CLF = chain length factor; OxyD is an amidotransferase that prepares the unusual starter unit.

1.4 Type III PKS

Sometimes referred to as the chalcone synthase (CHS) superfamily, Type III PKS enzymes are mechanistically and structurally simpler than their iterative type I and II counterparts. Typically found in plants but also some bacteria[65], type III PKSs are unusual because they are ACP-free, opting instead to use the CoA building blocks directly.[66] Surprisingly, these synthases use a single active site for all iterative processing, including decarboxylation, condensation and cyclization.[67] Even more surprising is that most of the activity has been attributed to just three catalytic residues in the active site (Cys-His-Asn).[68] The mechanism for naringenin chalcone synthesis by *Huperzia serrata* is detailed in Figure 1-8. The

first step is loading of the coumaroyl-CoA starter unit by the CHS (named Pks1). A malonyl-CoA then condenses to the coumaroyl starter unit, releasing the latter from the cysteine. Following a decarboxylative Claisen condensation the coumaroyl group has been extended by one ketide. This iterative process occurs twice more to furnish the enzyme bound linear precursor, which is cyclized to the chalcone by Pks1.

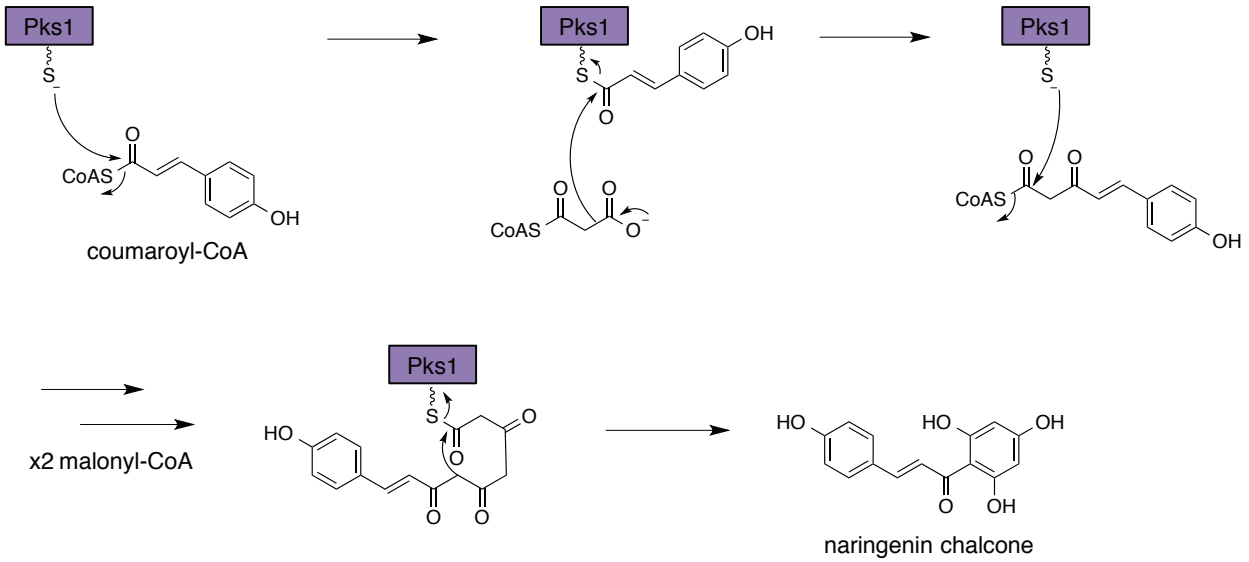

Figure 1-8. Biosynthesis of naringenin chalcone by Pks1, a type III PKS from *H. serrata*.

As of 2010, more than 900 PKS type III genes have been reported and over 20 have been cloned, purified and characterized.[69] Despite their simplicity, CHS enzymes can synthesize a surprising variety of chemical structures. The diversity arises from the number of chain extensions, selection of the starting unit and different modes of cyclization. The dramatic reduction in mechanistic complexity has made type III PKSs the perfect candidate for genetic engineering and rational redesign. Some examples include changes in cyclization selectivity[70], expanding starting unit specificity[66] and catalyzing C-N bond formation to synthesize tetramic acids.[66]

1.5 PKS-NRPS

PKS-NRPS hybrids produce a large number of polyketide natural products with rapamycin, epothiolone, and yersinibactin being some of the most well known. The architecture of PKS-NRPS hybrid enzymes are distinct from types I, II, III because they contain non-ribosomal peptide synthetase (NRPS) domains. These domains can select and incorporate an amino acid into the growing polyketide chain, increasing their chemical diversity. Some PKS-NRPS enzymes are sometimes categorized as type I HR-PKS enzymes because they typically contain all tailoring domains and contain similar architecture to FAS. These hybrid enzymes have been found in both fungi and bacteria, with the fungal enzymes being primarily iterative (and most similar to FAS) and the bacterial enzymes both iterative (dihydromaltophilin[71]) and modular (bacillaene[72]). Pre-tenellin A is a product of a fungal, iterative PKS-NRPS and is a biological precursor to tenellin, a cytotoxic metabolite of *Beauveria bassiana*.[73] Although its erythrocyte toxicity has been known for years[74], recent research suggests it plays a role in iron uptake in iron-deficient environments as well.[75] The biosynthesis of tenellin by TENS (tenellin synthase) and TenC (trans-ER) is detailed in Figure 1-9.

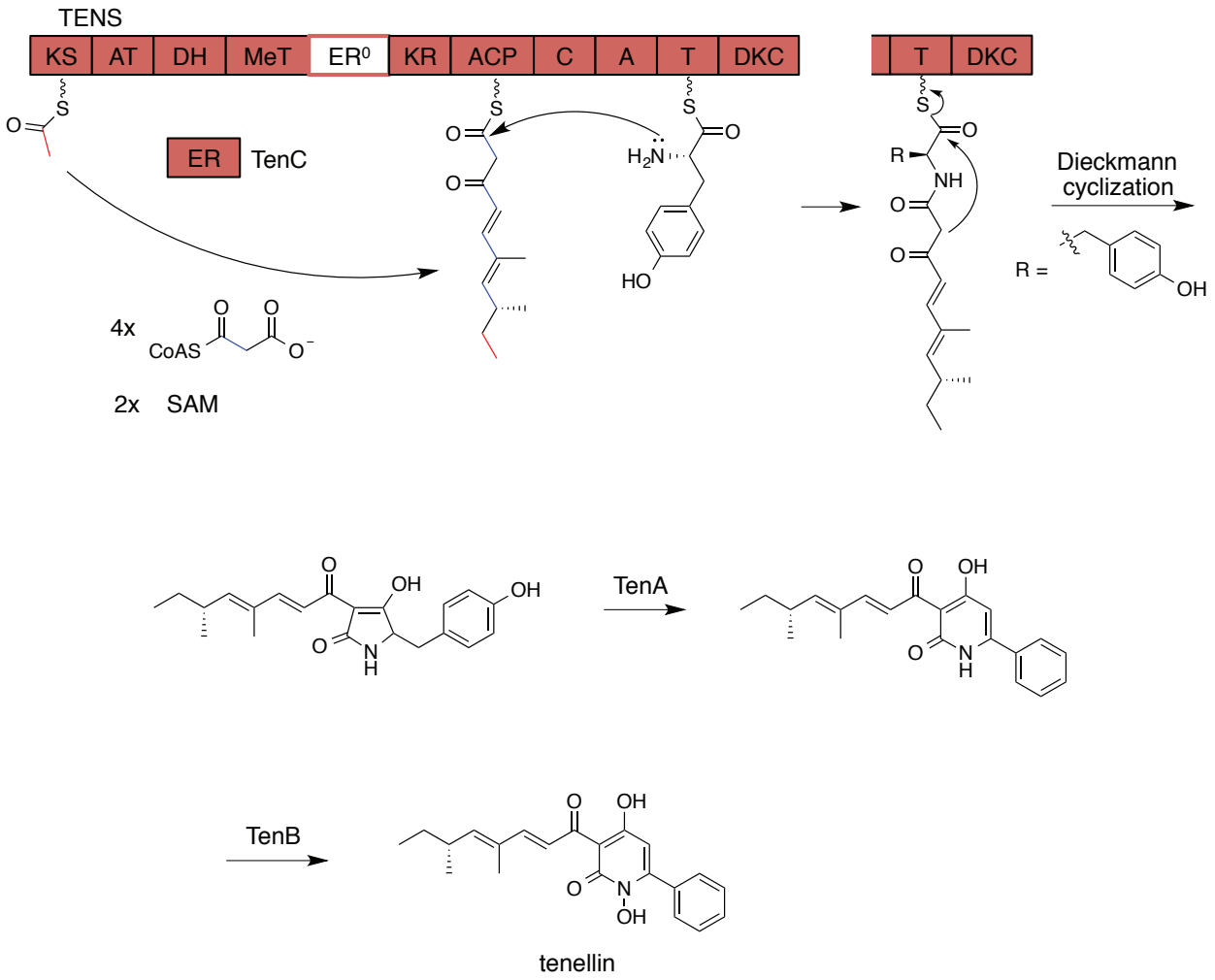

Figure 1-9. Biosynthesis of tenellin by TENS and TenA, B & C.

The PKS modules of TENS (KS, AT, ACP, DH, KR, MT and catalytically inactive ER^0) and TenC assemble the ACP-bound pentaketide.[73] The MT domain and two molecules of *S*-adenosylmethionine (SAM) methylate the pentaketide at the di- and tri-ketide stages. After the acyl chain is assembled, the adenylation (A) domain of the NRPS portion of TenS adenylates tyrosine, activating it for thioester formation by the thiolation (T) domain. The thiolation domain is analogous to the ACP domain of PKS systems. It is phosphopantethienylated by a PPTase and carries the growing peptide-acyl chain to the appropriate domains.[28] The condensation (C)

domain catalyzes the amide bond formation, transferring the polyketide from the ACP to the T domain. The final product is released by the reductase (R), which typically reduces the thioester bond by cyclizing it to a tetramic acid (second reaction arrow in Figure 1-9). The R domain in TENS is sometimes referred to as a Dieckmann cyclase (DKC) because it cyclizes the aminoacyl chain in a Dieckmann condensation fashion, releasing it as a tetramic acid. Pretenellin A is then transformed by ring expansion and hydroxylation to furnish tenellin. Interestingly, the inactivated ER domain appears to be a common trait of fungal PKS-NRPS hybrids. With the exception of fusarin synthase (FUSS)[76], the missing activity is typically complimented by a trans-acting ER domain.[77]

Domain swapping experiments have been used to investigate the programming of PKS and NRPS domains of TENS. A series of chimeric PKS-NRPS enzymes were made with domain(s) swapped with desmethylbassinin synthase (DMBS), a related PKS-NRPS enzyme from *B. bassiana* (Figure 1-10).[44] Swapping domains with DMBS produced functional chimeric proteins due to their high similarity (up to 97% sequence similarity in the domain regions). Notable differences between DMB and tenellin biosynthesis are an extra acetate unit incorporated by the AT-KS-DH and one less methyl group used in DMB synthesis. Swapping domains between these highly similar synthases provides insight into their individual role in programming of chain length or methylation. It is important to note that the chimeric proteins saw no significant change in titre compared to the wild type. Initial tests with swapping the *trans*-ER proteins showed no change in products or titre. This differed from previous results by the Tang and Vederas labs that saw a change in methylation pattern when the lovastatin LovC *trans*-ER was swapped with equisetin (more in Chapter 3).[78] Swapping the NRPS regions between the synthases saw no change in the product formed, indicating that the PKS regions

were solely responsible for acyl chain production (Figure 1-10B and C). Swapping the core domains (KS-AT) and DH was also a conservative trade, as no change in product length or methylation was found.[79] A change in methylation did occur when either the KS-AT-DH-MT was swapped or just the MT alone. The DMBS MT only methylates once in the TENS system, which is the expected result as DMB only has one methyl group. Interestingly, the switch in programming of the PKS genes only occurred when the domains are swapped up to the KR (Figure 1-10G), suggesting its role in chain length regulation. When the KR domain alone was changed to the DMBS KR, four different products were obtained with differing methylation and chain lengths.

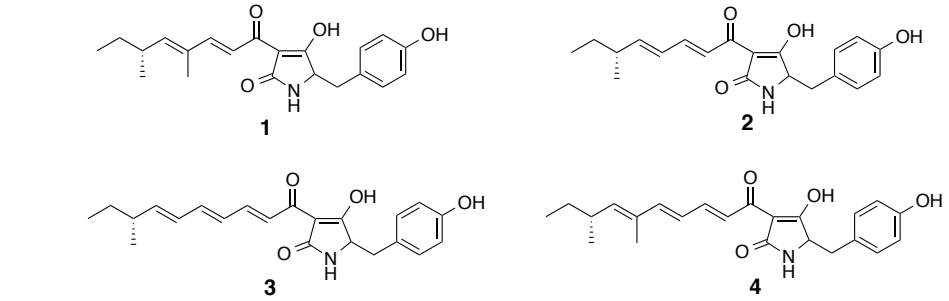

Figure 1-10. Chimeric PK-NRPS proteins synthesized by heterologous recombination and expressed in *Aspergillus oryzae*. All enzyme assays were conducted with the necessary cofactors for polyketide production. Red domains = TENS; Green domains = DMBS.

In 2010, Tang and co-workers studied the biosynthesis of aspyridone by ApdA, a fungal iterative PKS-NRPS from *Aspergillus nidulans*.[80] The authors severed the NRPS modules from the PKS modules in ApdA and evaluated their activity for preaspyridone synthesis *in vitro*. Surprisingly, the disconnection was well tolerated and the equimolar amounts of ApdA NRPS

and PKS *trans* modules synthesized the correct product in comparable yield. Even more impressive was that the swapping the *trans*-acting NRPS modules from the native system with the NRPS of CpdA (cyclopiazonic acid PKS-NRPS) produced a new tryptophan containing aspyridone in low yield. This result demonstrates that the PKS domains and NRPS domains must operate independently, as otherwise their activity would change when they were separated. This result collaborates well with the well-conserved NRPS domain swap between TENS and DMBS.[44]

1.6 Conclusion

Although great strides have been made in elucidating the cryptic programming of PKS-NRPS enzymes, we are still far away from truly understanding how they function. Poor expression levels in bacterial heterologous hosts, such as *Escherichia coli*, hampered progress. The recent development of engineered eukaryotic expression hosts such as *Saccaromyces cerevisiae*[78] or *A. oryzae* have dramatically improved expression levels of fungal PKSs.[81,82] These engineered strains have provided researchers with enough soluble, active PKS material to start reconstituting biosynthetic pathways and testing the enzymatic function *in vitro*.[78] Unfortunately, the size and mobility of these enzymes precludes them from traditional protein crystallography. Data on 3D shape of modular PKSs have been obtained for mono- or didomains by NMR studies or X-ray crystallography[83,84], but without the other domains present it is far from certain that these structures are relevant to the whole synthase. There has been some recent success with cryo-EM imaging of an intact, modular PKS enzyme from the pikromycin system but this data conflicts with previous data and has been deemed controversial.[85,86]

The vast majority of the information about PKS biosynthesis is limited to the bacterial, type I PKS systems.[77] There is a large gap of knowledge in our understanding of how the iterative domains function, not only in chain length determination (number of iterations) but in the selective activity of the tailoring domains as well (referred to as 'programming'). This cryptic activity is a long-standing problem in the field of natural product biochemistry and is notoriously difficult to address with iterative PKSs often being referred to as a 'black box'. Fortunately, some recent breakthroughs have provided us with tools to help illuminate the cryptic programming of iterative PKSs. These tools have grown from isotopically labeled small building blocks to using chemical synthesis to assemble advanced labeled intermediates and screening

them for recognition and transformation by the iterative PKS.[87] If these synthetic compounds are recognized and transformed by the synthase, it provides very convincing evidence that it is similar to the true enzyme-bound intermediate. Our lab in collaboration with the molecular biologists in the Yi Tang lab at the UCLA studied the mechanism of iterative PKS enzymes by assembling hypothetical intermediates and screening for incorporation into the final product. Chemical synthesis is an extremely valuable tool because we can assemble intermediates with missing functionality or unnatural stereochemistry to elucidate the basis for recognition by the domains. This thesis will explore the application of chemical synthesized intermediates to PKS-NRPS biosynthesis, which at the time of writing has not yet been reported.

This thesis will explore some unanswered questions about two PKS-NRPS enzymes, LovB and CcsA, from lovastatin and cytochalasin E biosynthesis, respectively. Using synthetic intermediates and purified enzymes, we will explore the mechanism of off-loading and cyclization by CcsA and the timing of methylation by the MT domain of LovB. This thesis will also examine the mechanism and substrate for a post-PKS enzyme in cytochalasin E biosynthesis, CcsB, which is a putative 'double' Baeyer-Villigerase.

2 Probing Cytochalasin E Biosynthesis: Labeling studies, synthesis of proposed intermediates and investigation into carbonate formation

2.1 Introduction to cytochalasin E: discovery, bioactivity, structure

Cytochalasin E (**5)** was originally discovered by Aldridge and co-workers in 1972[88] as a metabolite of *Rosellinia necatrix,* a pathogenic plant fungus,[89] and was independently discovered as a toxic metabolite of *Aspergillus clavatus* in 1973 by the Büchi group.[90] *Aspergillus clavatus* was first isolated from mold-damaged rice in a Thai home after the unfortunate death of a young boy by a then-unknown toxicosis. The Büchi lab and co-workers were pursuing the toxic metabolite profile of *A. clavatus* and determined the first unambiguous structure of **5**, using NMR, IR and X-ray crystallography. Since these findings, **5** has been discovered to be produced by a number of fungal hosts isolated from various sources, such as infected grains (*A. clavatus* and *Aspergillus terreus*), soil (*Mycotypha sp.*) and the marine environment (*Spicaria elegans*).[91] Although there are many organisms that produce this metabolite, *A. clavatus* is considered to be the model organism for the study of cytochalasin E production and biosynthesis.

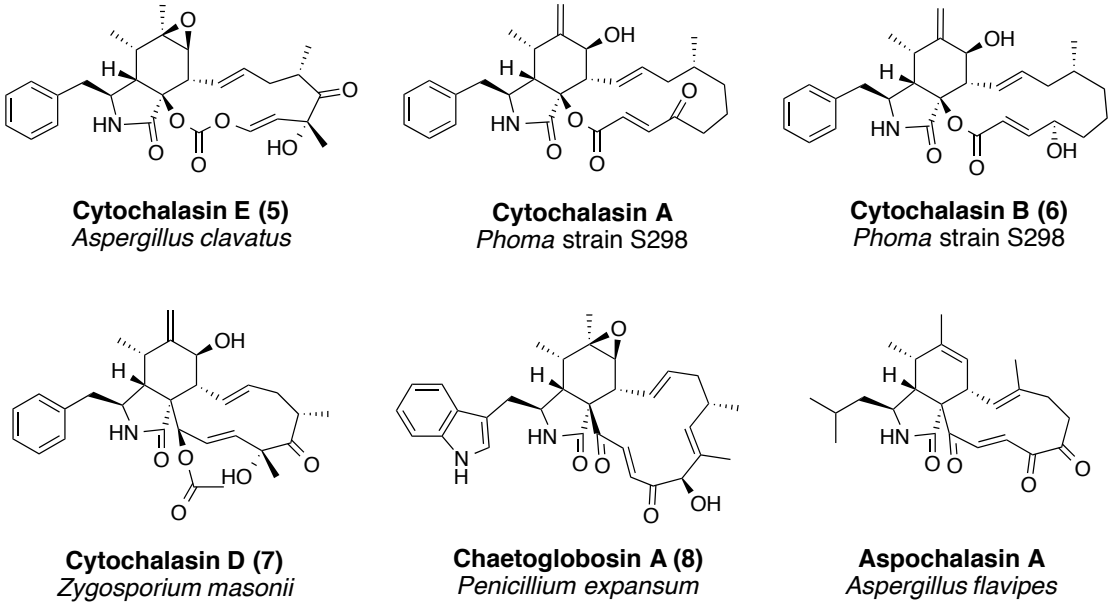

Figure 2-1. Structures of select cytochalasins, and their producing organism

Cytochalasin E is a member of the cytochalasin family of natural products, in which there are over 100 examples with diverse functionality and bioactivity.[92] Cytochalasins are typically characterized by the presence of a macrolide fused to a perhydro-isoindolone derived in part, from an amino acid. A few representative examples of this class are found in Figure 2-1. Similar to cytochalasins A, B, D, and F, **5** exhibits activity against cell proliferation by preventing actin polymerization.[93] It blocks proliferation of bovine endothelial cells, preventing angiogenesis.[94] This anti-proliferative activity combined with its low cytotoxicity is why **5** has seen extensive use as an angiogenesis inhibitor in cellular assays. Interestingly, rearrangement of the epoxide moiety to an allylic alcohol by treatment with non-aqueous acid abolishes the anti-angiogenesis activity.[94]

Although cytochalasin E has been studied for more than 40 years and is the topic of over 350 publications, very little is known about how it is assembled in nature. Particularly interesting is the biogenesis of the in-line carbonate moiety, which is an unusual functional group in natural

product chemistry. If the complete biosynthesis of this metabolite is elucidated, then it could be possible to engineer new cytochalasins that are more stable, or more biologically active.

2.1.1 Previous results for cytochalasin biosynthesis

In 1974, Tamm and co-workers identified the biogenesis of the atoms in cytochalasin B (**6**).[95] This was achieved by adding sodium [2-^{13}C] acetate to the growth medium of *Phoma sp.* S. 298, fermenting the fungus for 12 days, and then extracting **6** from the culture supernatant. The authors were able to track which carbon atoms were derived from acetate using ^{13}C-NMR (Figure 2-2). These results are in agreement with their earlier publication, where they observed incomplete incorporation of [2-^{14}C]-sodium acetate, [^{14}C-Me]-S-adenosylmethionine (SAM) and [U-^{14}C]-L-phenylalanine[96,97] into cytochalasin B. Combined, these results allowed them to map the origin of nearly every atom in **6**. These results marked the first conclusive evidence for the polyketide and non-ribosomal peptide origins for cytochalasin biosynthesis. Still unknown was the origin of the oxygen atoms. In 1975, Robert and Tamm suggested that based on the acetate labeling pattern, a Baeyer-Villiger monooxygenase (BVMO) must install the the macrocyclic ester in **6**.[98] Following from this, the carbonate moiety in cytochalasin E may stem from two Baeyer-Villiger-type (BV) oxygen insertion reactions.

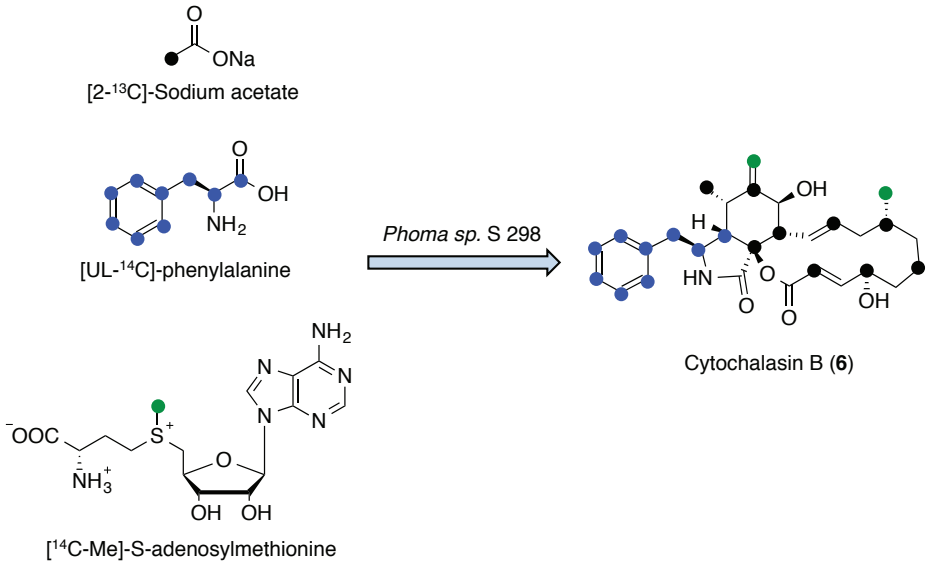

Figure 2-2. Summary of cytochalasin B labelling studies by Tamm and co-workers.

Although the biogenesis of the carbon skeleton of cytochalasin was elucidated and a plausible biosynthetic pathway was proposed, little was known about the genes responsible for its assembly for nearly 40 years. In 2007, research in the Hertweck group identified the biosynthetic gene cluster responsible for the production of chaetoglobosin A (**8**) in *Penicillium expansum*.[99] The authors used RNA silencing to knock down a PKS-NRPS gene (CheA), which decreased the titre of **8.** They were able to expand their analysis to discover the gene cluster and propose a biosynthetic route for **8.** By extension, this was the first evidence for the genetic determinants for cytochalasin E biosynthesis. More specifically, it identified that an iterative highly-reducing PKS-NRPS hybrid enzyme was involved in the production of cytochalasin E.

2.1.2 Genetic determinants of cytochalasin E production

Recently, Qiao *et al*. published the sequence of the gene cluster responsible for cytochalasin E biosynthesis in *A. clavatus*.[100] Armed with the knowledge that a PKS enzyme was responsible, the authors used the genome sequence of *A. clavatus* and the sequence of CheA as a search query to target the gene cluster of **5** (Figure 2-3). The presence of a putative Baeyer-Villiger monooxygenase (BVMO) in the gene cluster supported their hypothesis. This enzymatic reaction will be discussed in more detail in Section 2.2.2. The authors confirmed the function of this gene cluster with a gene disruption experiment, where they integrated a resistance cassette into the putative PKS-NRPS gene CcsA, which abolished cytochalasin E production. The authors were also able to increase the expression of CcsR (a putative TetR-like regulation gene) and subsequently increase the titre of cytochalasin E up to seven-fold, suggesting its role as a pathway specific regulator.[100]

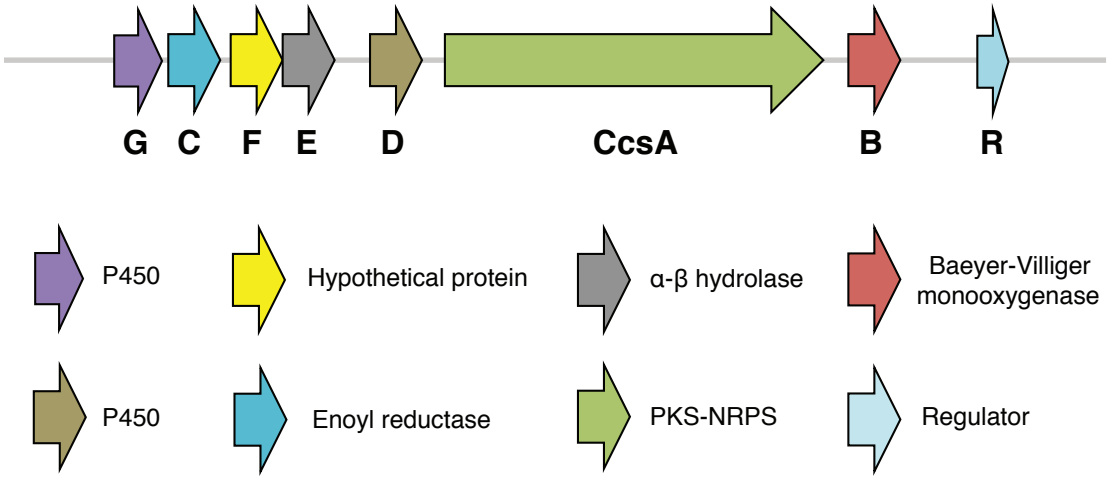

Figure 2-3. Cartoon representation of cytochalasin E gene cluster in *A. clavatus* and assigned function, based on BLAST analysis.

2.1.3 Proposed biosynthesis of cytochalasin E (5)

With the gene cluster for **5** elucidated, Tang and coworkers proposed the enzymatic sequence and intermediates *en route* to its production (Figure 2-4).[100] The authors used the previously proposed chaetoglobosin (**8**) biosynthesis as a guide and assigned roles for the genes found in the *A. clavatus* gene cluster. Their proposal started with production of an ACP tethered highly reduced polyketide chain, generated by the iterative incorporation of eight acetate moieties by a PKS-NRPS hybrid enzyme named CcsA. Bioinformatic analysis showed that CcsA possessed all the domains expected for a PKS-NRPS enzyme, including an inactivated ER domain, whose activity could be complemented by a trans-acting ER, CcsC, also found in the gene cluster. A phenylalanine residue is proposed to extend the acyl-bound polyketide chain **9** by NRPS C domain-mediated amide bond formation. The R domain of CcsA contains an NADPH-binding domain, and was hypothesized to facilitate chain release by reducing the ACP-bound thioester to transient aldehyde **11**. This type of reductase has been seen in other fungal natural products such as thiopyrazine biosynthesis.[101] After chain release, the β-keto amide is thought to react in a Knoevenagel-type condensation to synthesize deoxy-tetramic acid **12**, which is perfectly set up for an intramolecular Diels-Alder reaction to create the fused isoindolone moiety **13**. These reactions closely match the proposal for chaetoglobosin biosynthesis. It is plausible that either or both of these reactions could be spontaneous or enzyme catalyzed. After Diels-Alder cyclization, the authors proposed a pair of P450 monooxygenases, CcsG and CcsD, install the ketone, hydroxyl and epoxide moieties (**15** and **16**). A recent review has detailed the precedent for multiple oxidations by a single oxygenase.[38] Finally, a late stage sequential set of

Baeyer-Villiger reactions catalyzed by a flavin-containing BVMO, CcsB, was proposed to install the labile carbonate and furnish the final structure **5**.[100]

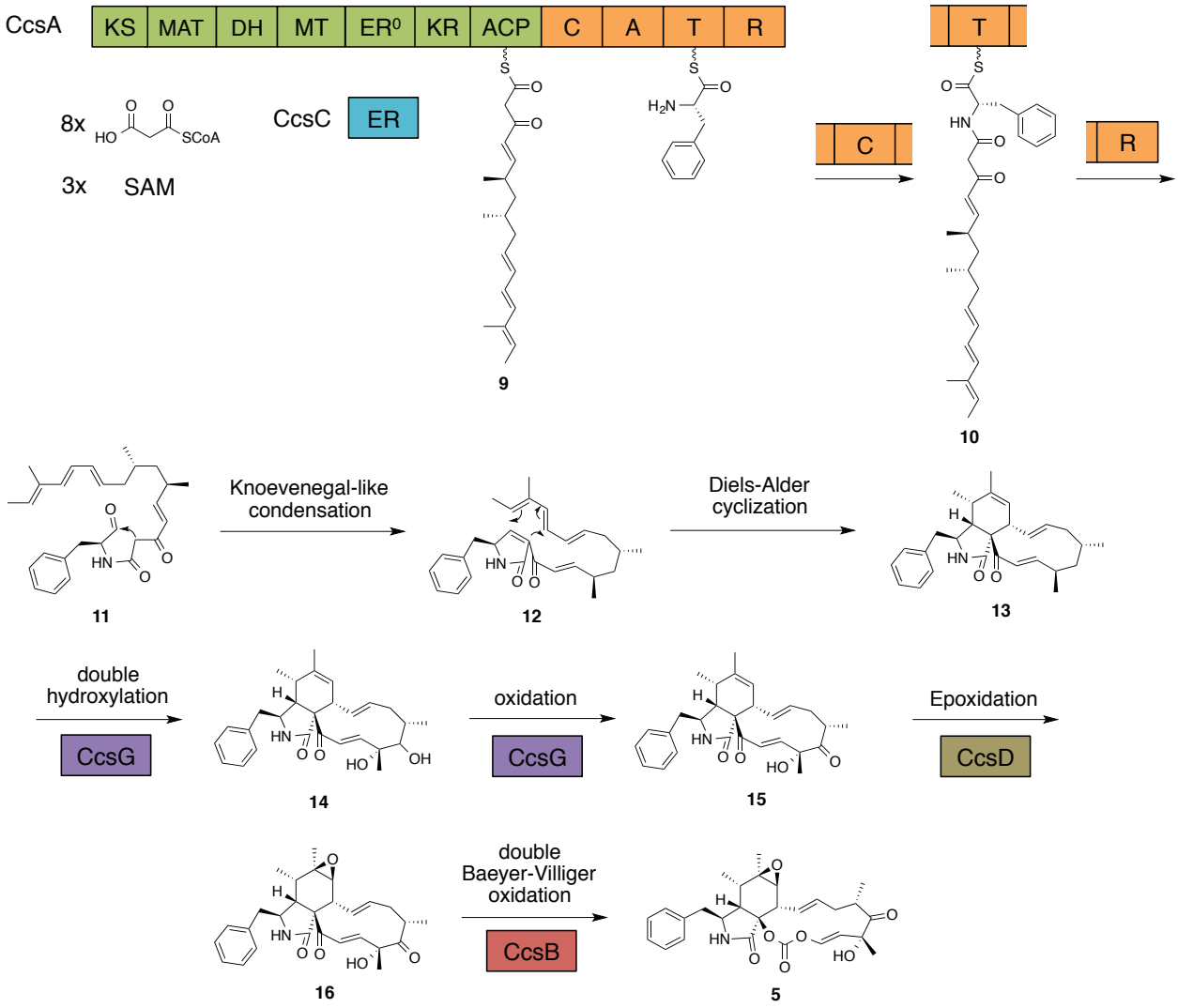

Figure 2-4. Proposed biosynthesis of cytochalasin E by Qiao *et al.* in 2011[100].

Although this proposal is an agreement with the knowledge gained from chaetoglobosin biosynthetic studies, gene cluster mapping and the original labeling studies, many questions remain. What portions of cytochalasin E are derived from the PKS-NRPS enzyme CcsA and

what are added post-PKS? Specifically, the ketone at position 17 could be plausibly introduced by an acetate precursor or alternatively through the action of a post-PKS oxygenase. Can one introduce advanced intermediates into the catalytic cycle of CcsA, similar to work with the HR-PKS and NR-PKS systems in dehydrozearalenol biosynthesis?[87] Are the oxygen atoms in the carbonate group derived from acetate or introduced aerobically as the proposal by Tamm and coworkers suggests? Can one reconstitute carbonate synthesis with CcsB? This chapter aims to address these questions through labeling and reconstitution assays and chemical synthesis.

2.1.4 Project objectives

This chapter will seek to answer the questions posed above. In order to fully understand how cytochalasin E is assembled, a combination of organic chemistry and molecular biology techniques will be used. The biological origins of the carbon and oxygen atoms can be detailed through isotope feeding experiments. Once the biogenesis is determined, the activity of CcsB, a post-PKS putative "double" Baeyer-Villigerase, can also be investigated as the catalyst for carbonate formation. Proposed mechanisms can be investigated through *in vitro* assays and isotopic labeling. Attempts towards synthesis of the possible enzyme bound polyketide chain and product of CcsA, will be outlined. The structure of the offloaded product and existence of a possible Diels-Alderase could also be investigated.

2.2 Results and discussion

2.2.1 Isotopic labeling studies for cytochalasin E production in *A. clavatus*[*]

We first set out to determine the origin of the oxygen atoms in **5.** We devised two labeling experiments, partially to confirm that the carbon labeling patterns observed in **6** are the same for **5**, and to determine which oxygen atoms were derived from molecular oxygen. If the flanking oxygen atoms in the carbonate were derived from oxygen, this would provide strong evidence for the BV oxidation hypothesis by Tamm and Binder in 1975[98] and would warrant enzymatic investigation.

Both experiments involve the growth of *A. clavatus* in potato dextrose broth in a standing culture for 4 days at 30°C. In one experiment doubly labeled acetate (1-^{13}C, 1-$^{18}O_2$) was added to the culture broth in a normal aerobic atmosphere, and in the other experiment the fungus was grown in an $^{18}O_2$ atmosphere. Following extraction and purification of cytochalasin E, NMR analysis was used to identify carbon and oxygen labeling patterns. Atoms labeled after [1-^{13}C, 1-$^{18}O_2$]-acetate addition suggests incorporation by the polyketide synthase, CcsA. Oxygen atoms labeled in the presence of $^{18}O_2$ (which is visualized indirectly through their effect on ^{13}C shifts in NMR)[102], suggests that they are added aerobically following the action of CcsA, by oxygenases such as CcsF, CcsG or CcsB. The first experiment was conducted under standard fermentation conditions, while the second experiment required a specially designed apparatus as illustrated in Figure 2-5. In the $^{18}O_2$ experiment, a series of fermentation flasks inoculated with *A. clavatus* were placed in an incubator in a closed loop, and grown in a controlled oxygen environment. The

[*] This work was done by Dr. David Dietrich, a former post-doctoral fellow in the Vederas group

flasks were connected via Tygon tubing to a water trap (to remove excess condensation) and a KOH trap (to remove excess CO_2). A hermetically sealed aquarium pump was then connected to keep the airflow constant. A 3-way valve is used to introduce either $^{16}O_2$ or $^{18}O_2$ into the system. A pressure-equalizing buret containing aqueous $CuSO_4$ (as an antimicrobial agent) was used to measure oxygen gas consumption and keep a slightly positive pressure in the system. This allowed for the fungus to grow in an isotopically enriched atmosphere for several days, all while inside an incubator.

After four days of growth, the cultures were extracted with EtOAc and labeled **5** was then purified by flash column chromatography. The labeling pattern was determined by ^{13}C-NMR spectroscopy. Comparing the peak heights of carbon resonances of an unlabeled standard of cytochalasin E to the sample extracted in the presence of doubly labeled acetate identified carbon atoms containing ^{13}C beyond natural abundance levels. Furthermore, these were compared to published chemical shifts to confirm previous labeling studies.

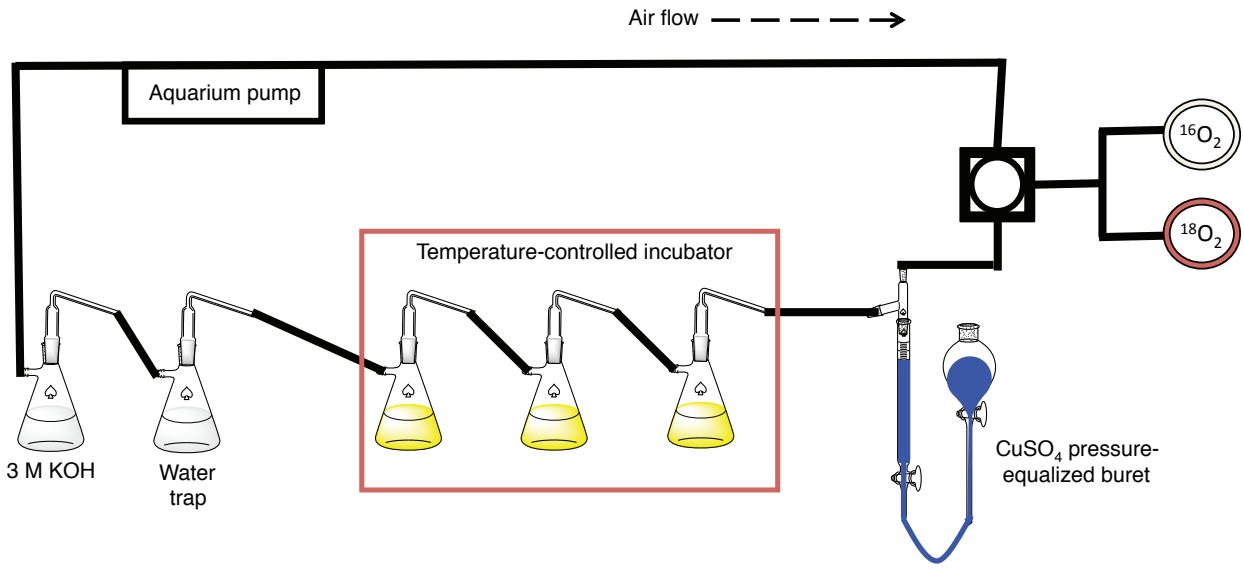

Figure 2-5. Whole cell isotopic atmospheric labelling apparatus schematic

Importantly, the presence of an ^{18}O isotope was evaluated by the change in chemical shift ($\Delta\delta$) of the carbon signal adjacent to the oxygen, a phenomenon documented by Vederas and Nakashima in 1980 in the biosynthesis of averufin by *Aspergillus parasiticus*.[102,103] The heavy isotope of oxygen causes small changes to the adjacent carbon chemical shift, on the order of 0.01 – 0.05 ppm for either a hydroxyl or ketone. Using ^{13}C-NMR, one can determine ^{18}O incorporation by the appearance of additional carbon resonances from incomplete incorporation at that carbon (Figure 2-6). The ^{13}C-NMR spectrum of **5** after labeled acetate feeding experiment revealed that two oxygen atoms were derived from acetate, at positions C1 and C22. The $^{18}O_2$ feeding experiment mapped the rest of the oxygen atoms, at positions C6 and C7, C17, C18 and most interestingly, the flanking oxygen atoms in the carbonate. This marked the first definitive evidence for oxygenase-mediated carbonate formation and more importantly, gave credence to the hypothesis of a double Baeyer-Villigerase. Summaries of the results from the isotope feeding studies are found in Figure 2-7 and Table 2-1.

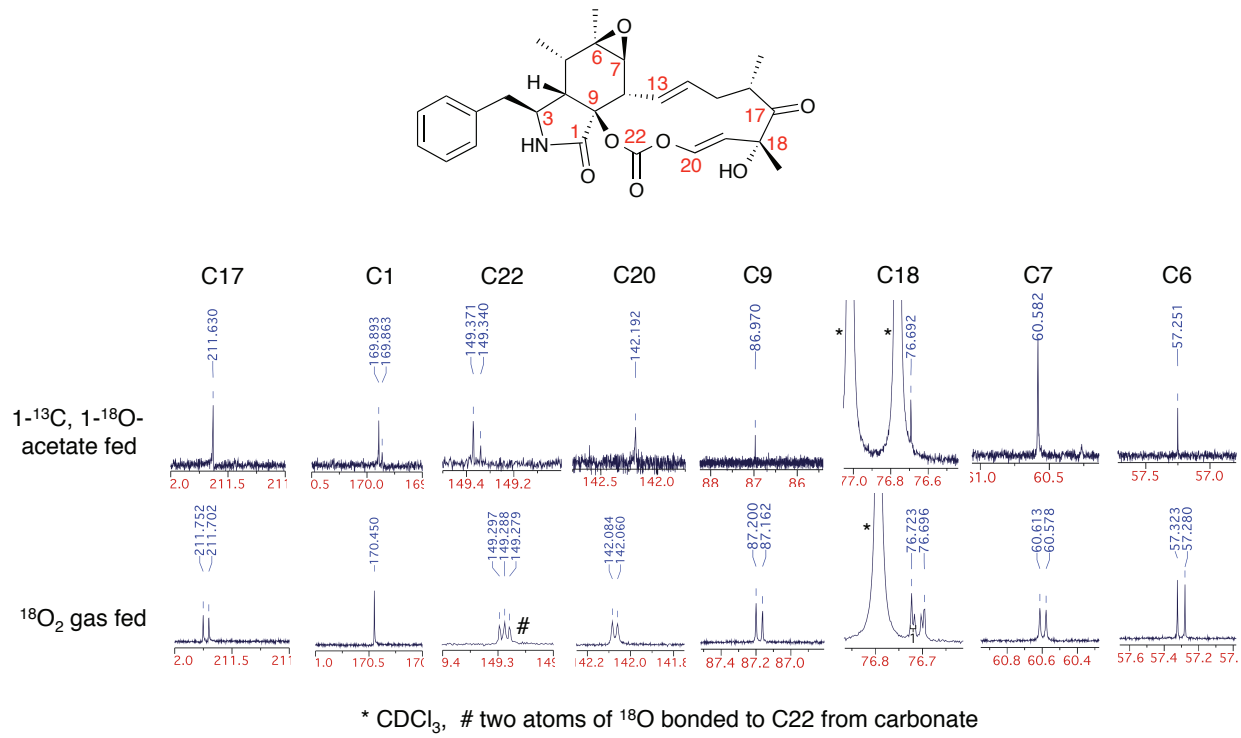

Figure 2-6. ^{13}C-NMR of select resonances of cytochalasin E after isotope feeding experiments in *A. clavatus*.

	1-^{13}C, 1-$^{18}O_2$ acetate labeled			$^{18}O_2$ labeled		
Carbon	**^{13}C ppm**	**Isotope shifted**	**Δ ppm**	**^{13}C ppm**	**Isotope shifted**	**Δ ppm**
C17	211.630	-	-	211.752	211.702	0.05
C1	169.893	169.683	0.030	170.450	-	
C22	149.371	149.340	0.031	149.297	149.288, 149.279	0.009, 0.018
C20	142.192	-	-	142.084	142.060	0.024
C9	86.970	-	-	87.200	87.162	0.038
C18	76.692	-	-	76.723	76.696	0.027
C7	60.582	-	-	60.613	60.578	0.035
C6	57.251	-	-	57.323	57.280	0.043

Table 2-1. Results of cytochalasin E labeling in *Aspergillus clavatus*

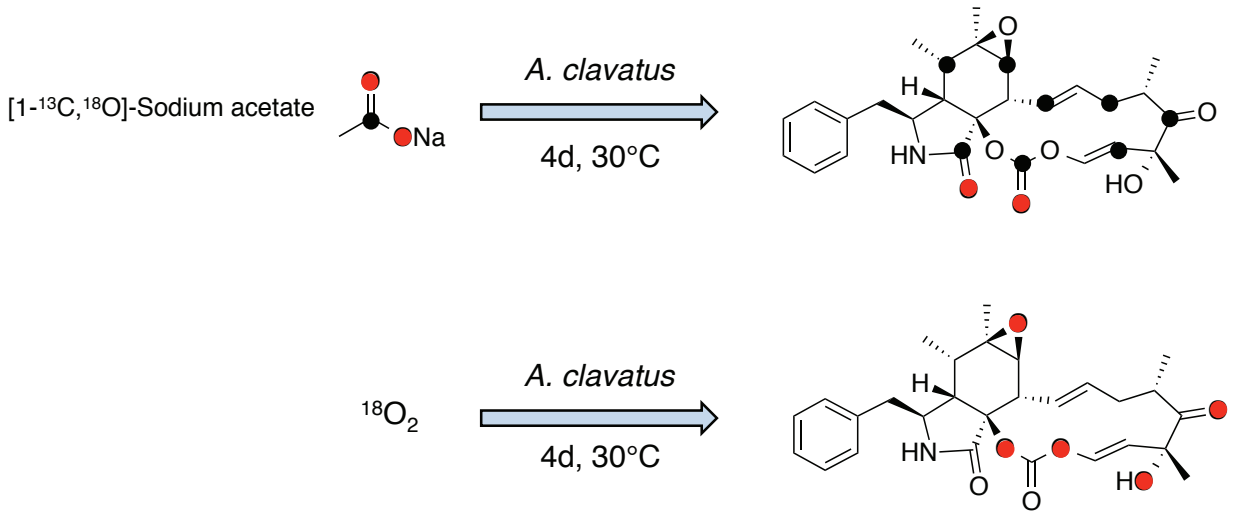

Figure 2-7. Summary of results from isotope feeding experiments in *A. clavatus*.

2.2.2 Characterization of CcsB, a carbonate-forming Baeyer-Villigerase[†]

With the isotope feeding experiments in agreement with the double Baeyer-Villigerase hypothesis, our lab in collaboration with Prof. Yi Tang's lab at UCLA, set out to determine the enzymatic basis for formation of the carbonate moiety in **5**. The conversion of an α-β unsaturated ketone to a vinyl carbonate is intriguing from the perspective of both synthetic and biological chemists. Not only has the biosynthesis of in-line carbonates not been previously reported, but there are also very few examples of this transformation in synthetic literature and none of these are adjacent to a double bond.[104,105] As an apt illustration, there have been a few syntheses of cytochalasin structures[106-109] but the total synthesis of **5** has not yet been reported, presumably because of the challenging carbonate group. If the biosynthesis of this moiety can be elucidated,

[†] This work was done in collaboration with Dr. David Dietrich and the Yi Tang lab in UCLA

it might shed light into how inline carbonates are constructed enzymatically, which could possibly lead to new synthetic or chemoenzymatic transformations.

The division of labor was as follows: the Tang lab was responsible for expression and purification of CcsB, and metabolite isolation of mutants, and our lab was responsible for synthesis of hypothesized substrates. Synthesis of the proposed substrate **16** presented a challenge, as it is a highly functionalized late stage intermediate with ten stereogenically defined carbon atoms. Instead of a total synthesis approach a shorter semi-synthetic approach was devised, starting from a related metabolite, cytochalasin D (**7**) (Figure 2-8). Although **7** (also known as zygosporin D) is relatively expensive ($100/mg, Enzo Life Sciences), isolating it from its producing organism is much more cost-effective. Once the substrate mimic is synthesized, the activity of purified CcsB can be evaluated through an enzymatic assay, in which the proper co-factors (FADH, NADPH), are added. The resulting product **20** can then be analyzed by LC-MS and NMR to observe this proposed carbonate formation.

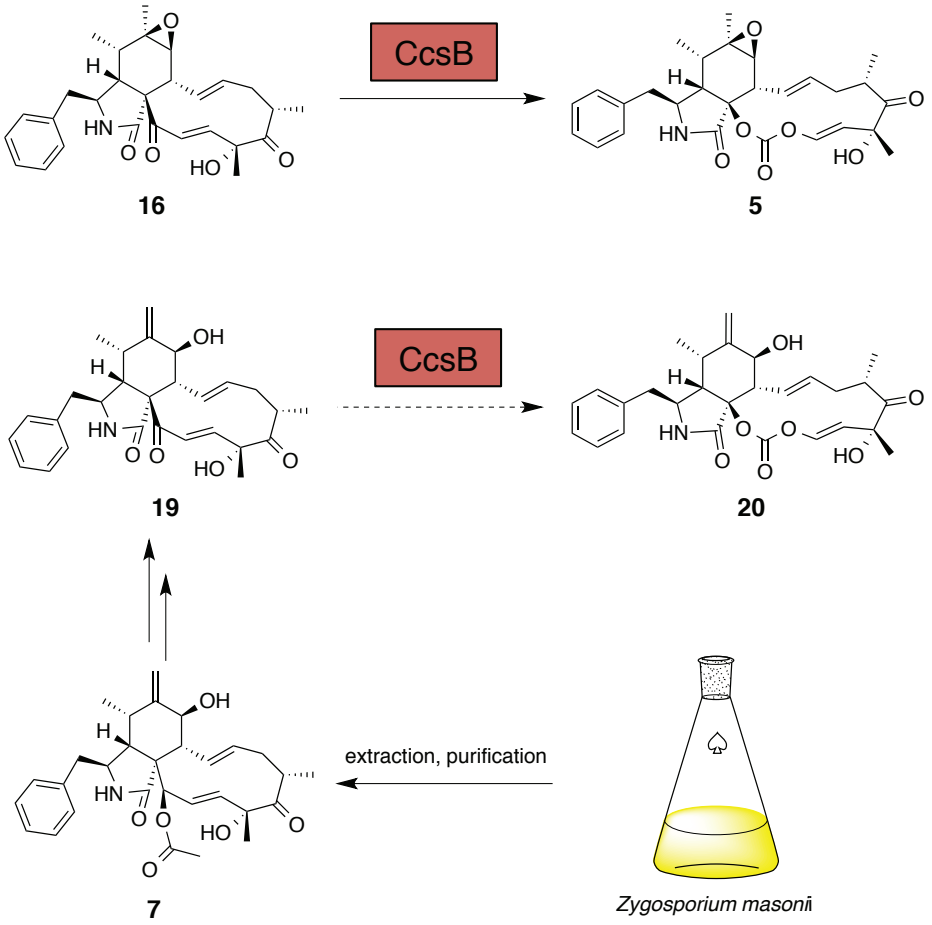

Figure 2-8. Outline for initial CcsB assay with substrate mimic **16**. Top reaction is the proposed biosynthetic step. The bottom reactions are our proposed model system to study CcsB.

2.2.2.1 Synthesis of proposed CcsB substrate analogue 19

Zygosporium masonii, a sporulating fungus, was grown in potato dextrose (PD) medium for 3 days, after which off-white spheres of mycelial growth were visible. The fungal growth was filtered aseptically and transferred to freshly autoclaved minimal media. After 1 day at 30°C, the mycelium were filtered, blended in a Waring blender and returned to the liquid broth before extraction with EtOAc. Purification by flash silica chromatography yielded pure **7** as a white powder in a yield of 30-40 mg/L. The semi-synthetic scheme that was used to transform

cytochalasin D (**7**) to **22** can be found in Scheme 2-1. Cytochalasin D (**7**) was dissolved in dry MeOH and a 1M solution of freshly prepared NaOMe solution in MeOH was used to cleave the acetate moiety. The resulting allylic alcohol **21** was selectively oxidized to ketone **19** by adding small aliquots of Dess-Martin periodinane (DMP) and monitoring the reaction by ^{1}H-NMR analysis. Addition of more than approximately 0.5 equivalents of DMP resulted in the oxidation of the other allylic alcohol, producing a doubly oxidized product that was difficult to separate. This regioselectivity can be attributed to the shape of cytochalasin D and the orientation of the hydroxyl groups. The crystal structure of **7** was published in 2003 and gives us a glimpse of the hydroxyl groups in three-dimensional space (Figure 2-9).[110] Assuming the stereochemistry of the macrocyclic alcohol doesn't change during conversion of **7** to **21**, it would remain in an axial orientation (orange arrow, Figure 2-9). Oxidation to the ketone would alleviate the axial strain while oxidation of the equatorial alcohol would leave the destabilizing axial hydroxyl intact. This kinetic effect has been well documented by Eschenmoser, Winstein and others.[111,112] The selective oxidation of the axial allylic alcohol allowed for the protecting group-free synthesis of **19** in good overall yield.

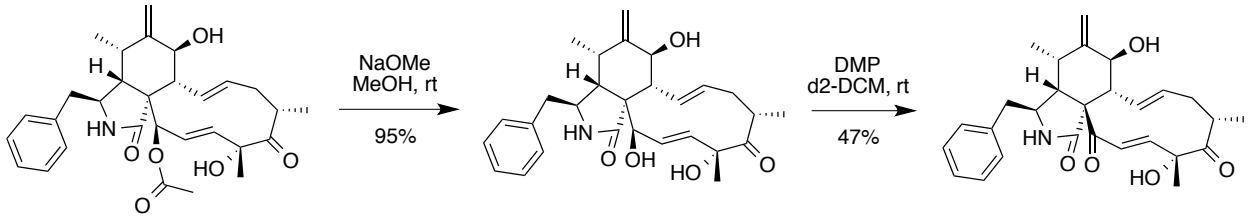

Scheme 2-1. Conversion of cytochalasin D (**7**) to substrate analogue **19**.

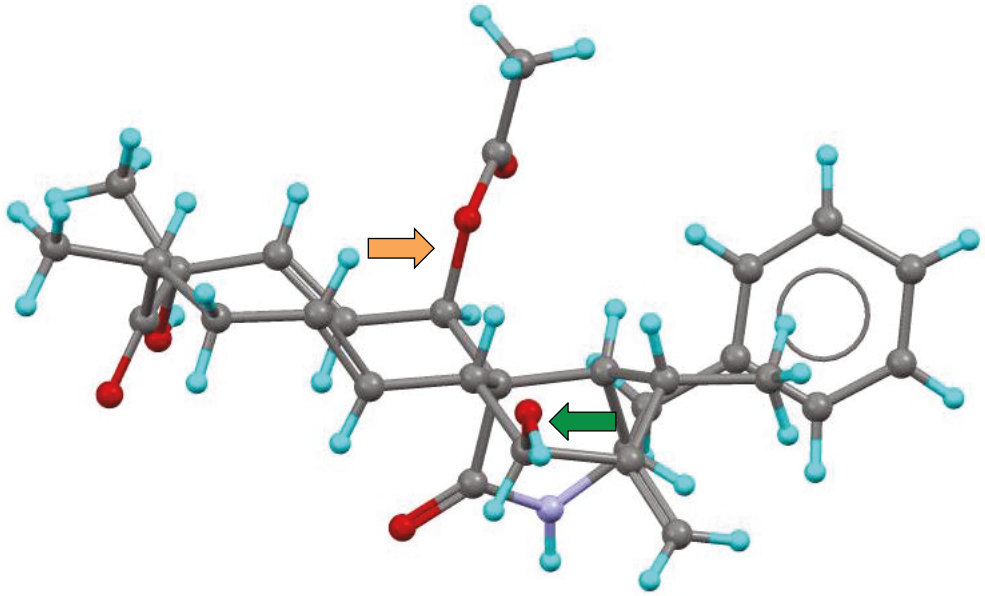

Figure 2-9. Crystal structure of cytochalasin D (**7**).[110] The orange arrow indicates the axial acetyl group and the green arrow indicates the equatorial hydroxyl. DMSO co-crystal not pictured.

2.2.2.2 Testing of ketocytochalasin D and activity of CcsB[‡]

Compound **19** was sent to our collaborators at UCLA and was tested as a substrate for carbonate formation by CcsB. The assays were performed in an aqueous buffer in the presence of the test substrate, NADPH, $FADH_2$ and SsuE, an FAD^+ reductase. Cytochalasin B (**6**) and rosellichalasin (**18**) were also tested as ester-containing metabolites to test if CcsB recognized esters or ketones. Cytochalasin B was used to see if ring size was a factor for recognition. Somewhat surprisingly, CcsB was not able to transform any of the initial test substrates (Figure 2-10). Since the substrate selectivity of CcsB seemed to be quite high, a new strategy was devised, where the natural substrate of CcsB would be prepared.

[‡] The majority of this work is published: Hu, Y.; Dietrich, D.; Xu, W.; Patel, A.; Thuss J. A. J.; Wang, J.; Yin, W.-B.; Qiao, K.; Houk, K. N.; Vederas J. C.; Tang, Y. *Nat Chem Biol* **2014**, *10*, 552.

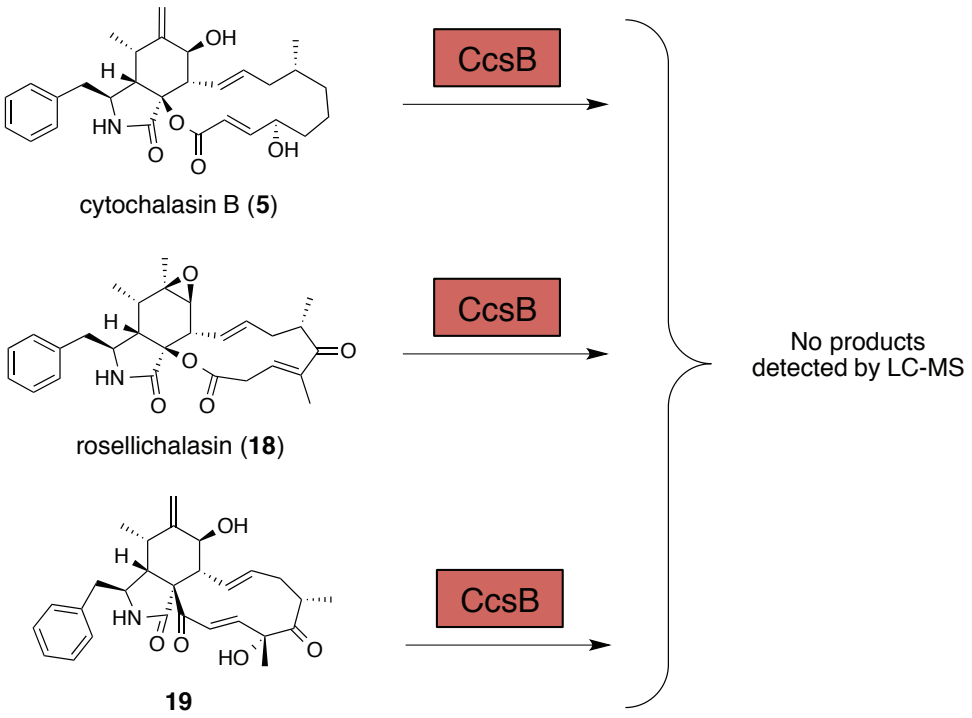

Figure 2-10. Initial CcsB enzymatic assay results. All in vitro assays pictured contained NADPH, $FADH_2$, SsuE (flavin reductase) and were buffered at pH 7.

A ΔCcsB knockout strain of *A. clavatus* was made using a double-recombination strategy where a resistance gene (glufosinate) was exchanged with the CcsB gene, generating a knockout mutant. After confirmation of the recombination by PCR analysis, our collaborators grew *A. clavatus* ΔCcsB in PD broth as a standing surface culture and extracted metabolites using EtOAc. Using LC-MS to analyze the new metabolite profile, the abolition of **5** and the commonly isolated side product rosellichalasin (**18**) was observed. Furthermore, the production of a new 1,5-diketone **23** (Figure 2-11) was also noted. The structure of **23** was determined through MS, NMR and X-ray crystallography. The accumulation of this new metabolite prompted the hypothesis that it might be the natural substrate for CcsB. A buffered enzymatic assay with purified, heterologously expressed CcsB in the presence of $FADH_2$, NADPH, SsuE

and purified **23,** produced cytochalasin Z16 (**24**), a carbonate containing known metabolite believed to be an intermediate in cytochalasin E biosynthesis. Its structure was confirmed by NMR, MS and X-ray crystallography (Figure 2-12)

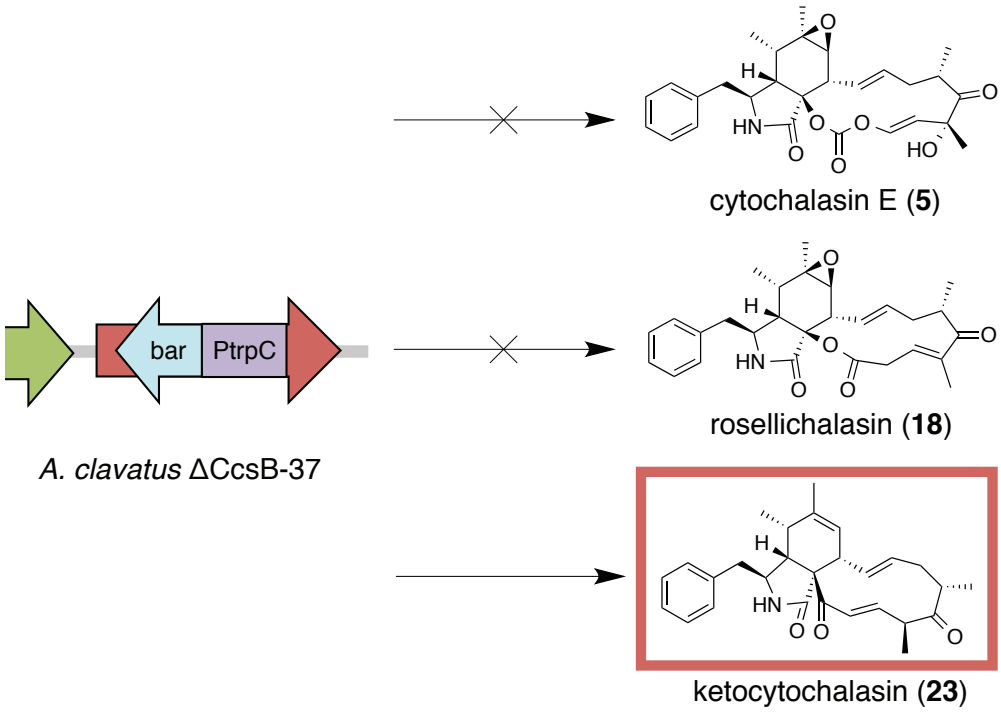

Figure 2-11. Change in metabolic profile for *A. clavatus* after CcsB gene disruption. Bar = glufosinate resistance, PtrpC = promotor sequence

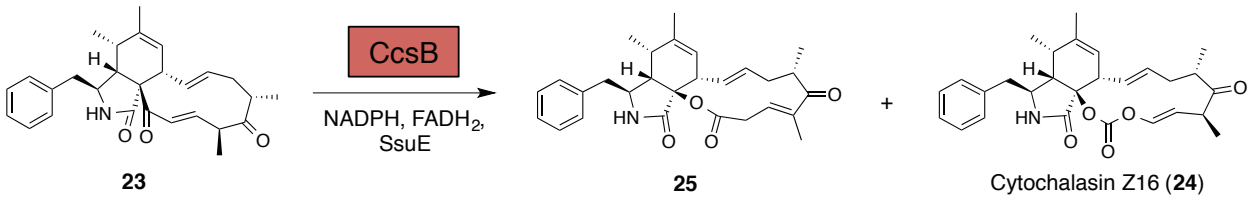

Figure 2-12. Isolated products (**25** and **24)** of *in vitro* assay with CcsB.

In addition to **24**, CcsB also produced an ester-containing natural product named iso-precytochalasin (**25**) that contained an isomerized double bond in conjugation with the macrocyclic ketone. Iso-precytochalasin (**25**) was isolated and its structure determined by NMR and MS. The presence of **25** in the reaction mixture suggested that it might be an intermediate *en route* to **24**. Interestingly, CcsB was unable to convert it to **24** in the *in vitro* assay, which led to the theory that **25** was a shunt product and a possible artifact of our assay conditions. Indeed, increasing the buffer pH from 7 to 9 increased the titre of **25** and made **24** nearly undetectable by LC-MS. Changing the medium from dH_2O to D_2O saw an increase of the mass of **25** by 1 amu, which is the predicted result of spontaneous double bond isomerization. These results suggested a base-catalyzed isomerization of the true intermediate, precytochalasin (**26**), to the non-functional shunt product, **25** (Scheme 2-2). Isolation of **26** proved fruitless due to its rapid, spontaneous conversion to **25**. Interestingly, feeding of iso-precytochalasin (**25**) to wild type *A. clavatus* and *A. clavatus* ΔCcsB in a complementation assay saw the production of rosellichalasin, a cytochalasin structure commonly isolated from *A. clavatus*. Whether rosellichalasin production is simply an artifact of laboratory conditions or is produced naturally remains to be solved. Feeding of cytochalasin Z16 (**24**) in the same complementation assay saw the production of **5**, suggesting its role as an intermediate in the biosynthesis of **5**.

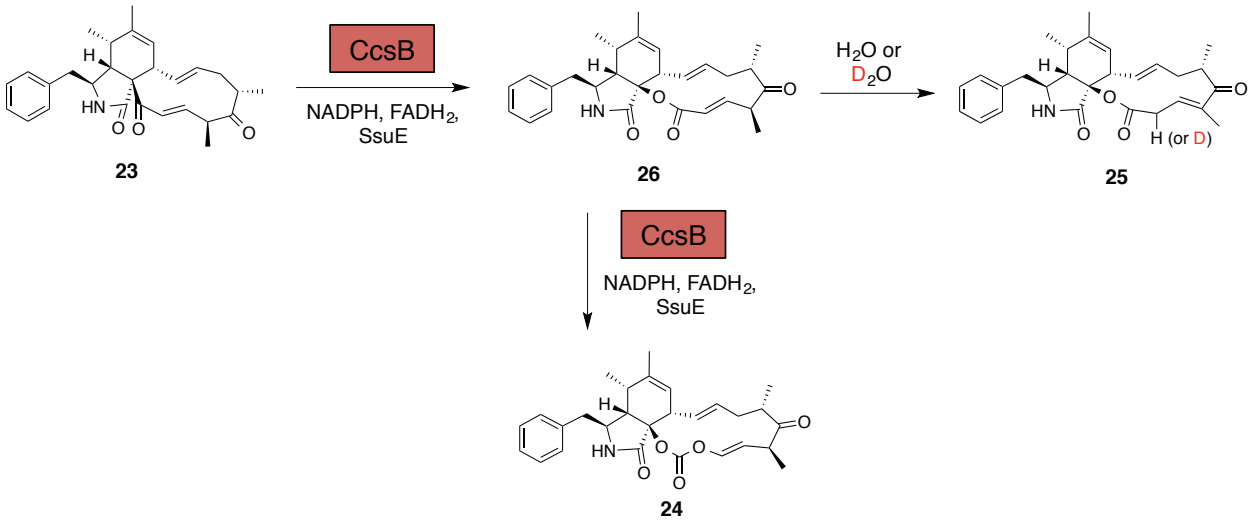

Scheme 2-2. Formation of **24** and shunt product **25** by CcsB. Intermediate **26** was transiently observed by LC-MS but isomerized readily to **25** during isolation.

2.2.3 Investigation into the mechanism of carbonate formation by CcsB

With the activity of CcsB elucidated, the remaining and arguably more interesting question remained: *how* does CcsB insert two oxygen atoms next to a conjugated ketone to create a vinyl carbonate? This transformation is unusual from both a synthetic and biosynthetic perspective. Oxidation of a vinyl ketone to a vinyl ester is notoriously difficult in organic synthesis as over-oxidation to the epoxy-ester is a common problem.[113] Additionally, there is little literature precedent for carbonate formation in nature, none of which are catalyzed by a BVMO.[114,115] Despite this limited information, we can elucidate a few clues about how CcsB functions by looking at its primary sequence. CcsB possesses the conserved domains for FAD, NADPH binding and also the conserved catalytic domain of BVMOs[116] (FxGxxxHxxxWP), a family of oxygenases that have been well studied and their mechanism elucidated in detail.[117]

Studies have found that the mechanism of BVMOs follow the accepted BV mechanism proposed by Criegee and others.[113,118] More specifically, the rules of migratory aptitude and retention of stereochemistry are similar between chemical and enzymatic synthesis. Cyclohexanone monooxygenase (CHMO) is a BVMO found in *Acinetobacter* NCIMB 9871 and is the most well characterized BVMO to date.[119,120] CcsB and CHMO share 23% sequence identity, suggesting the CHMO activity and mechanism could apply (at least in part) to CcsB. The mechanism of CHMO is shown in Figure 2-13.

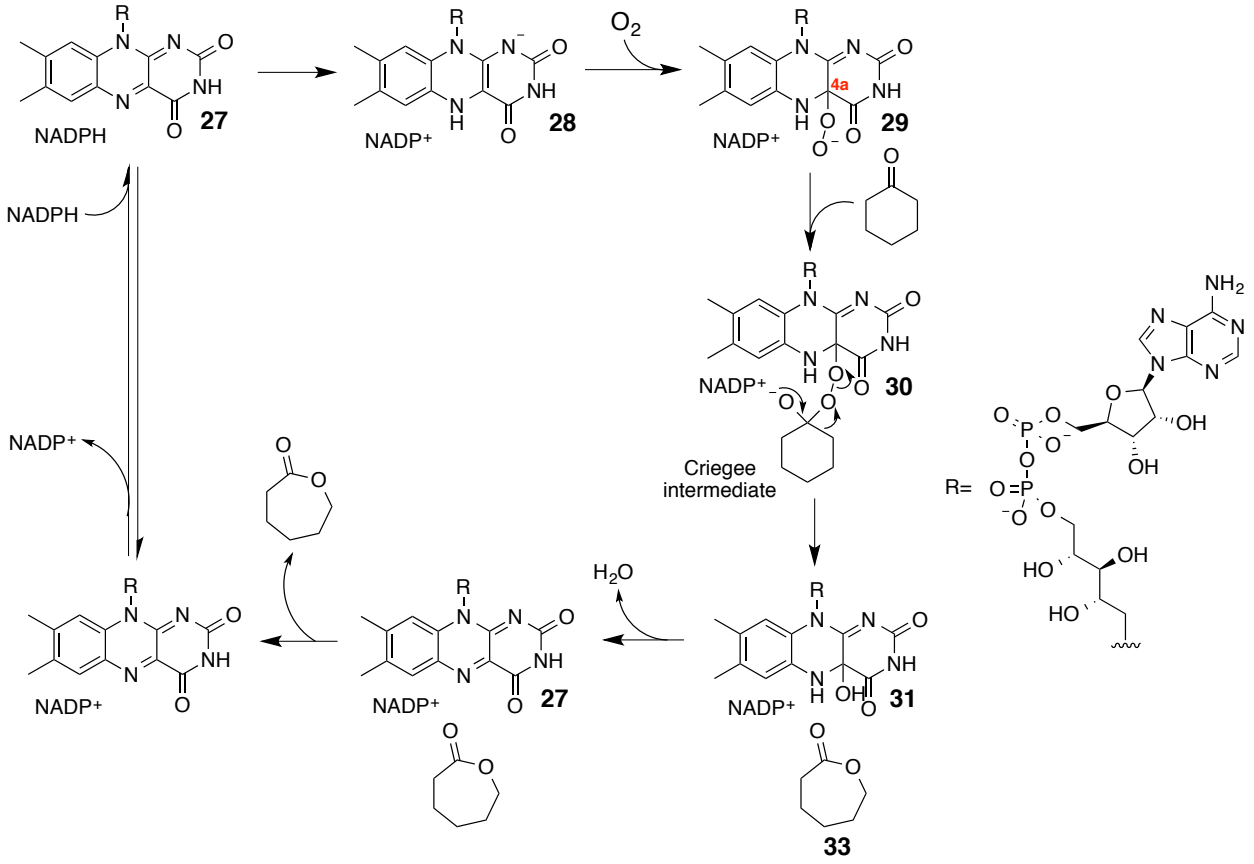

Figure 2-13. Mechanism of FAD-dependent cyclohexanone oxidation by CHMO. Modified from Leisch, H. *et al*[119]

The catalytic cycle begins with the reduction of the oxidized form of FAD (**27**) with NADPH. The reduced FAD (**28**) then reacts rapidly with oxygen to form the 4a-peroxy-FAD (**29**) and this species is the oxidant responsible for ester formation. Attack of the peroxy anion at the cyclohexanone ketone provides the classic Criegee intermediate (**30**) that results in C-C bond cleavage and migration onto the electrophilic oxygen, expanding the ring size with an ester group (**33**). The 4a-OH-FAD species (**31**) is rapidly converted to the oxidized form (**27**) with the expulsion of water. The newly formed lactone **33** is released from the enzyme first, followed by the $NADP^+$ co-factor. Binding of NADPH begins the cycle anew. The presence of a BVMO domain in CcsB suggests that initial ester formation may follow this mechanism. Isolation of isoprecytochalasin supports this theory as well, as the ester formation obeys the migratory rules of BV reactions, with the more substituted carbon having preference. It is peculiar that isoprecytochalasin (**25**) is not a substrate of CcsB as it shares similar structural features with its proposed ester containing intermediate **26**, barring that it is isomerized. This suggests that the double bond and/or the alpha-proton of the ketone (H18) are important for activity. This may also explain why ketocytochalasin D was not a substrate, because it contained a hydroxyl at H18 position instead of a hydrogen atom. Taking all these factors into account, a catalytic cycle for CcsB was proposed (Figure 2-14).

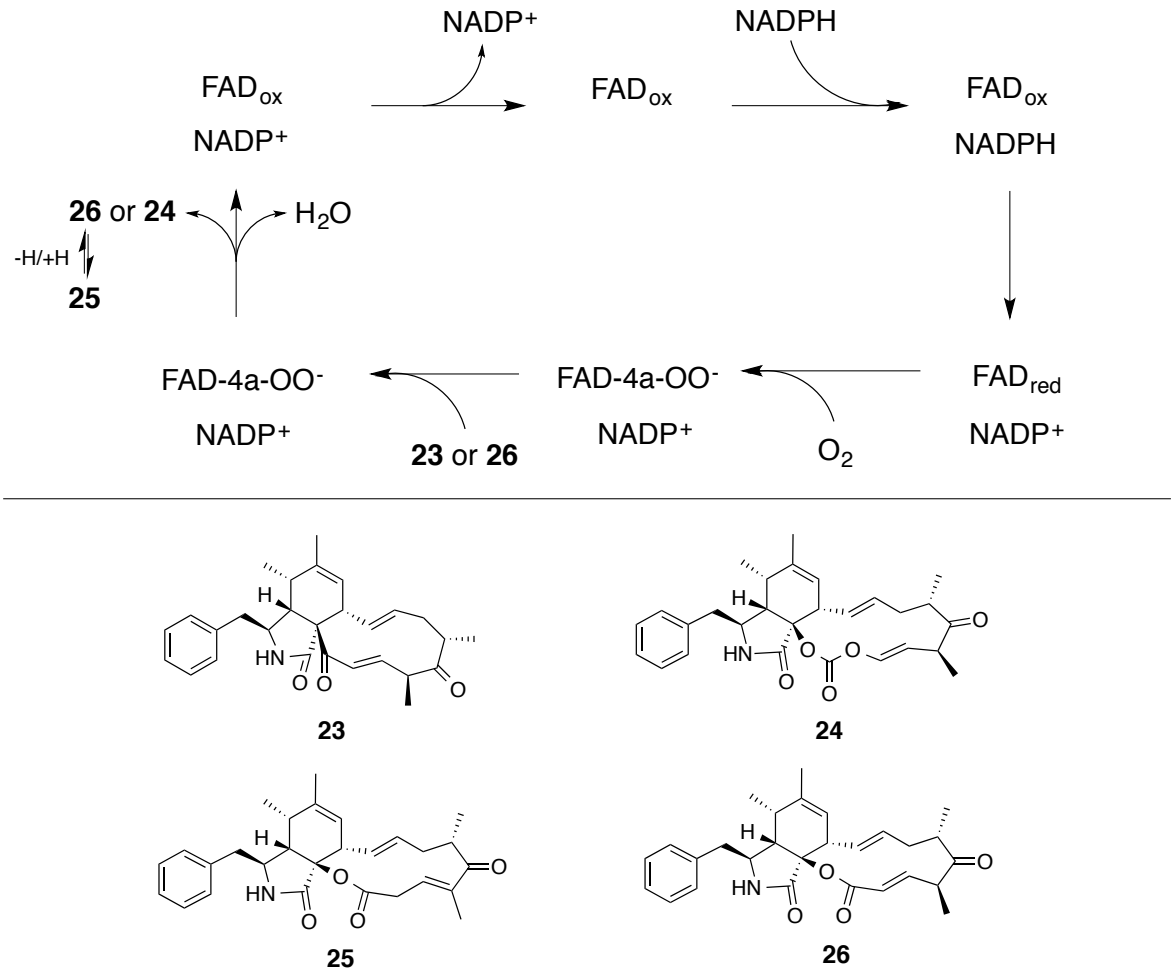

Figure 2-14. Proposed catalytic cycle of CcsB. Each round would install a single oxygen atom. Release of the product (either **26** or **24**) would result in either reuptake by CcsB for another round of oxidation or solvent-catalyzed isomerization to isoprecytochalasin (**25**).

The catalytic cycle and action of FAD was modeled closely after CHMO, with the exception that two rounds of catalysis were proposed to install the two oxygen atoms necessary for the carbonate. After one catalytic cycle, it is proposed that the cytochalasin product, one molecule of water, and $NADP^+$ are released into the reaction medium. After precytochalasin is released, it has one of two fates: CcsB either transforms it again to the carbonate, or it isomerizes to **25**. This hypothesis is supported by the observation that isolation of **25** is suppressed when

there are more than 2 equivalents of NADPH in the reaction mixture, with 8 equivalents resulting in trace amounts as detected by HPLC-MS.[116] The titre of **25** also increases when the pH of the enzymatic medium is above 8. This suggests that a competition exists between CcsB oxidation and solvent-catalyzed isomerization, which would most likely occur if the intermediate was released from the enzyme active site. It may be possible then that carbonate formation is the fortuitous result of a promiscuous enzyme that cannot distinguish between a ketone and ester-bearing starting material.

2.2.3.1 *In vitro* labeling studies of oxygen incorporation by CcsB

We set out to obtain experimental evidence for the double oxidation catalytic cycle of CcsB. If both oxygen atoms are inserted in a single oxidation cycle, we hypothesized that only one peroxy-flavin intermediate would be used per carbonate and therefore only one molecule of oxygen gas is needed. If the FAD cofactor was regenerated after each oxygen insertion, two molecules of oxygen gas would be needed. In order to determine the stoichiometry of molecular oxygen used, we decided to use a mixture of oxygen-16 and oxygen-18 gas. We modeled our experiment after a classical labeling study of prostaglandin E1 biosynthesis by Samuelsson.[121,122] In that study, oxygenation of 8,11,14-eicosatrienoic acid (**34**) occurred by incorporation of molecular oxygen in sheep seminal glands (Figure 2-15). The glands were incubated with [2-^{14}C]**-34** for ten minutes in an atmosphere consisting of 43% $^{16}O^{16}O$, 56% $^{18}O^{18}O$ and 1% $^{16}O^{18}O$. After chemical derivatization (to prevent equilibration of the label at the C9 position), the author used electron impact mass spectrometry (EI-MS) to determine heavy isotope incorporation. They concluded that based on the extremely low concentration of M+2 fragments and the high

ratio of M+4 fragments compared with their unlabeled counterparts, both oxygen atoms remaining in **39** and **40** must have originated from the same molecule of oxygen. Alternatively, if the oxygen atoms came from two molecules of oxygen, then the M+2 peaks would be much more prominent as each oxygen atom installed would have a ~50% chance of being a heavy isotope (**45** & **46)**.

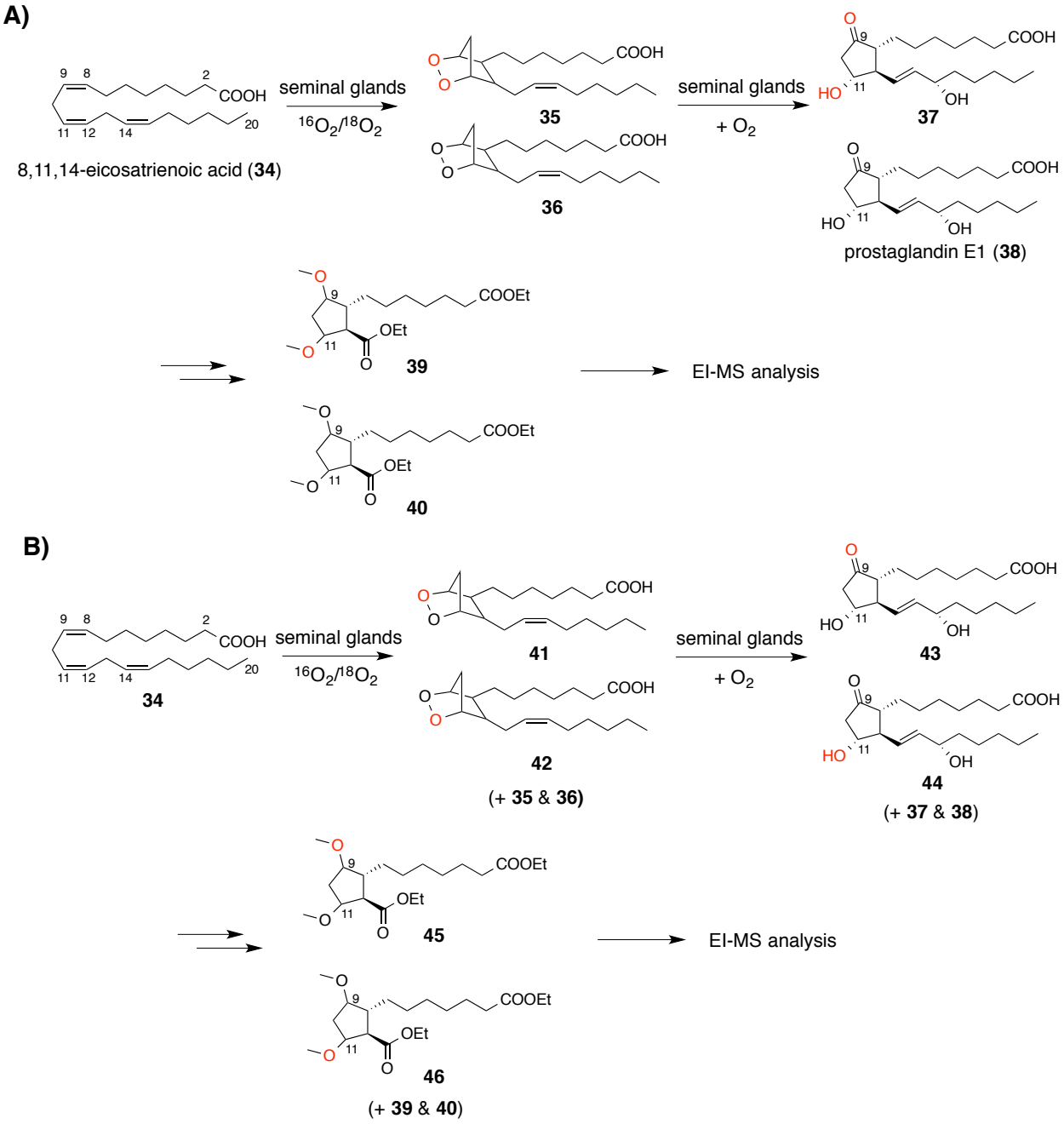

Figure 2-15. Outline of Samuelsson's study of oxygen incorporation in prostaglandin E1 biosynthesis. A) Expected products if a single molecule of oxygen is used; B) Expected products (four) if two molecules are used.

In order to accomplish our *in vitro* labeling study, we needed an apparatus that could permit accurate measurement and mixing of labeled and unlabeled oxygen gas and could facilitate an enzymatic reaction in this atmosphere. With assistance from Mr. Jason Dibbs, the department glassblower, we built the apparatus shown in Figure 2-16. Teflon tubing led from the oxygen tanks to a 3-opening, 2-way valve. This valve only permitted gas to enter from only one tank at a time with no possibility of the tanks being open simultaneously. The water-filled buret was used to accurately measure added oxygen so that a controlled ratio could be obtained. After adding the unlabeled oxygen, the buret was sealed and the glass chamber was charged with heavy oxygen. The buret was then opened and the next volume of oxygen was added, sealed for at least two minutes for adequate mixing. The glass chamber and reaction vessel were purged three times with the mixed atmosphere and then sealed to charge with the desired concentration. The enzymatic reaction was initiated by addition of CcsB via needle through the Teflon screw cap. Ball and socket joints at every junction allowed for flexibility and a fail-safe if the system became accidentally over-pressured.

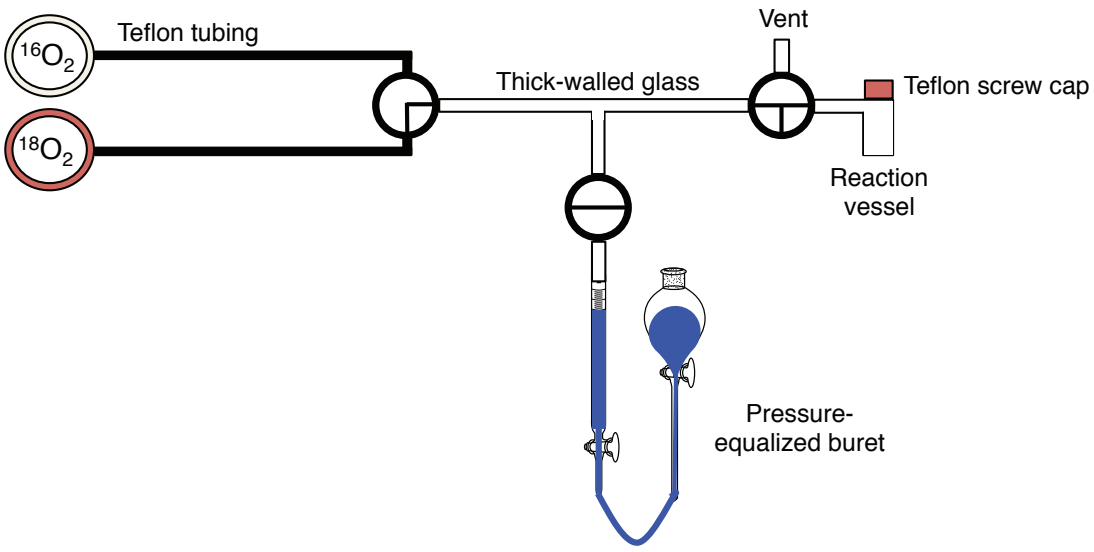

Figure 2-16. Schematic of the labeling apparatus used for the *in vitro* CcsB reaction

After three hours, the reaction was terminated by addition of MeOH, and the products were extracted with hexanes. The organic extract was analyzed by LC-MS-ESI (Figure 2-17). An extracted-ion mass chromatogram was used, scanning for the molecular formula of **24** ($C_{28}H_{33}NO_5$). The corresponding peak eluted after 19.73 minutes and the mass spectrum was obtained. The spectrum revealed the presence of three significant peaks, 464.2428 $(M+H)^+$, 466.2473 $(M+H+2)^+$ and 468.2525 $(M+H+4)^+$, that correspond to the unlabeled (**24**), singly (**47**) and doubly labeled (**48**) species. These results suggest that indeed two molecules of oxygen are used to synthesize the carbonate moiety. The high abundance of singly labeled cytochalasin Z16 points to the conclusion that two molecules of O_2 must be used. The singly labeled peak was ~60% of the abundance of the unlabeled while doubly labeled was approximately ~12% by peak height (after correcting for natural abundance). Initially, it would have been expected that if two molecules were used and each oxygen atom had an equal chance to be either ^{16}O or ^{18}O, it would be a statistical distribution of 1:2:1 (unlabeled/singly/doubly) because the singly labeled has two chances for labeling to occur (left or right of the carbonate). The obtained ratio of approximately

8:5:1 was probably a result of some residual $^{16}O_2$ gas dissolved in the buffer and kinetic isotope effects (KIE). The KIE could allow for selective loading of the lighter isotope of molecular oxygen onto FAD because the heavier isotope (although more abundant in the experimental atmosphere) would be kinetically slower to react.

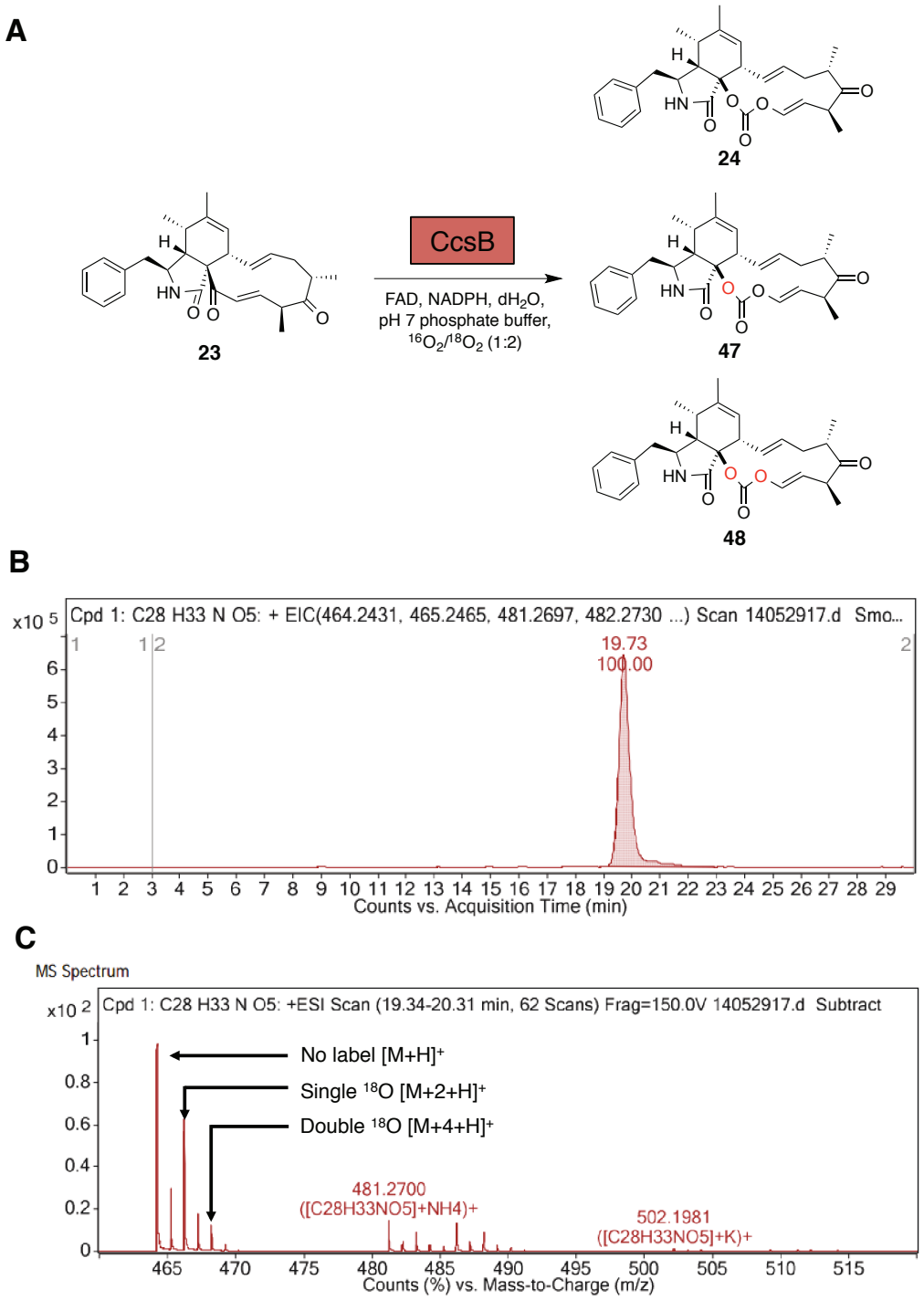

Figure 2-17. *In vitro* CcsB isotopic labeling assay. A) Outline of assay with conditions and possible products. Each additional oxygen label (red oxygen atom) would increase the mass by approximately 2 amu. B) LC-MS extracted ion chromatogram (EIC) for $C_{28}H_{33}NO_5$. C) ESI-MS spectrum for peak at 19.73 min. Parent ions for unlabeled, singly and doubly labeled found.

With a better picture of the catalytic mechanism of CcsB, we were able to propose an alternative (non-BV) mechanism for how the second oxygen could be introduced (Figure 2-18). The mechanism begins with a 4a-peroxy-flavin co-factor, presumably prepared in an analogous fashion to CHMO in Figure 2-12. The peroxy-flavin is deprotonated and nucleophilically attacks the ketone of ketocytochalasin, leading to the Criegee intermediate. Rearrangement in a typical BV fashion forms the ester with the most substituted carbon having migratory preference. CcsB would likely then release the oxidized $NADP^+$ into the reaction medium and reuptake NADPH to reduce the flavin co-factor for a second round of oxidation. The next equivalent of 4a-peroxy-flavin could then epoxidize the vinyl ester in an oxy-Michael fashion to afford the epoxy ester. Deprotonation of the acidic H18 proton would open the epoxide to the alpha-alkoxy moiety, which could close onto the ester forming a new, unstable epoxide. This intermediate could then rearrange into a carbonate, breaking a C-C bond into the vinyl system that upon re-protonation by the catalytic residue on the bottom face would furnish cytochalasin Z16 with the correct stereochemistry. Epoxide formation by a BVMO has been demonstrated during substrate scope experiments with CHMO.[119] The authors found that epoxide formation occurred with select substrates even when a ketone was present, suggesting the possibility of epoxidation as a side reaction. There is also precedent for this reaction in synthetic chemistry, in which carbonate formation occurs through an alpha-alkoxy ester rearrangement of a cyclic substrate, as demonstrated by Padwa and co-workers. [104]

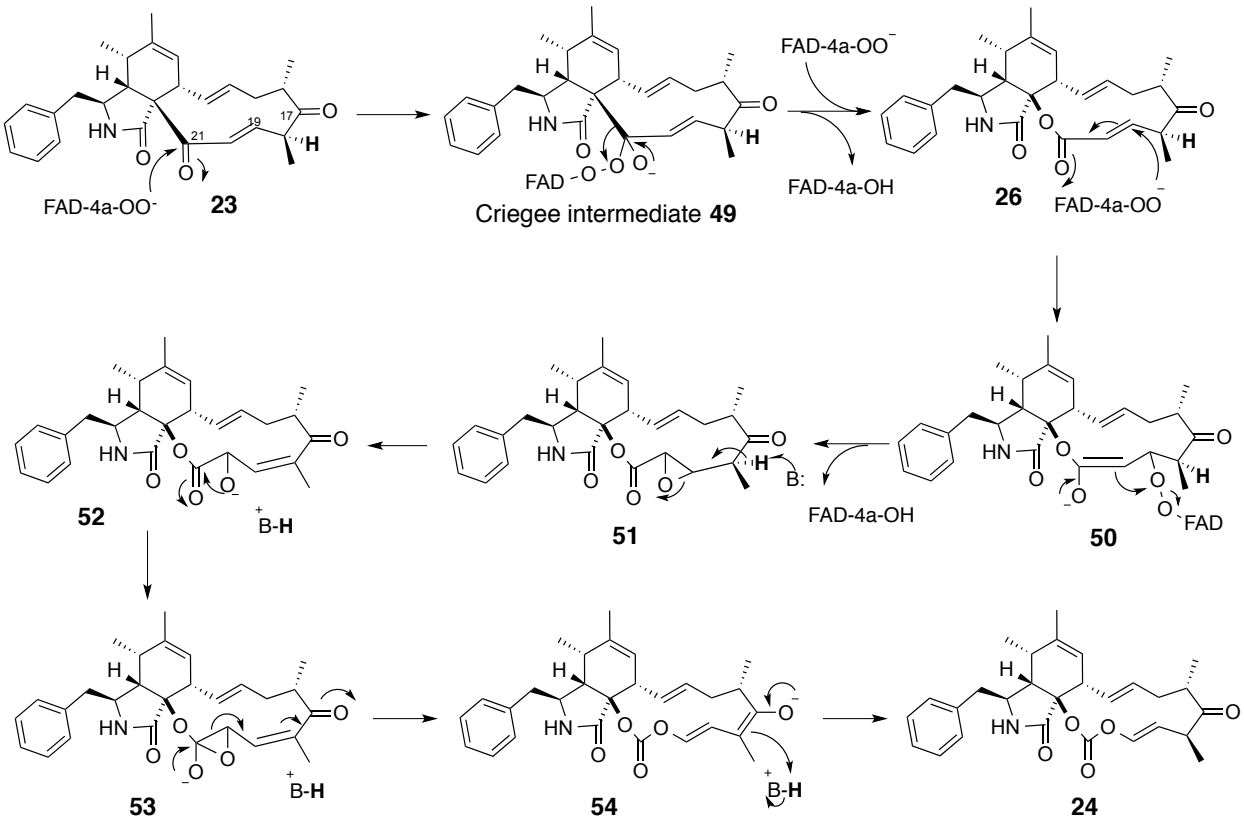

Figure 2-18. Proposed mechanism of carbonate formation by CcsB. Not pictured is hypothetical release of isoprecytochalasin and reuptake by CcsB.

2.3 Efforts towards the synthesis of the late-stage polyketide chain of CcsA

2.3.1 Introduction

With the confirmation that CcsB is indeed responsible for the step-wise transformation of a vinylgous ketone into the in-line carbonate of cytochalasin E, we set our sights on the PKS-NRPS enzyme, CcsA. Even though a great deal of information about the programming of fungal PKS-NRPS enzymes has been achieved through the engineering of chimeric enzymes[79,80,123], the exact operation of these enzymes is still mysterious. The existence and participation of proposed intermediates are far from conclusive. Our group, in collaboration with the Tang lab at UCLA, have studied the intermediates in hypothemycin biosynthesis, a fungal natural product synthesized by both a HR-PKS and a NR-PKS,[87] using chemically synthesized intermediates as *N*-acetylcysteamine (SNAC) esters. SNAC thioesters have been shown previously to be effective mimics of phosphopantetheine, the prosthetic group attached to a serine residue of the ACP domain, for recognition by PKS enzymes.[87,124,125] This systematic approach was conducted using ^{13}C-labelled intermediates and several synthetic intermediate SNAC esters. Incorporation of the ^{13}C label into hypothemycin indicated that the intermediates were recognized and transformed by the HR-PKS, Hpm8. Determination of the intermediates of a fungal PKS-NRPS has not been done, so we decided to explore the amino-acyl chain made by CcsA (**10**).

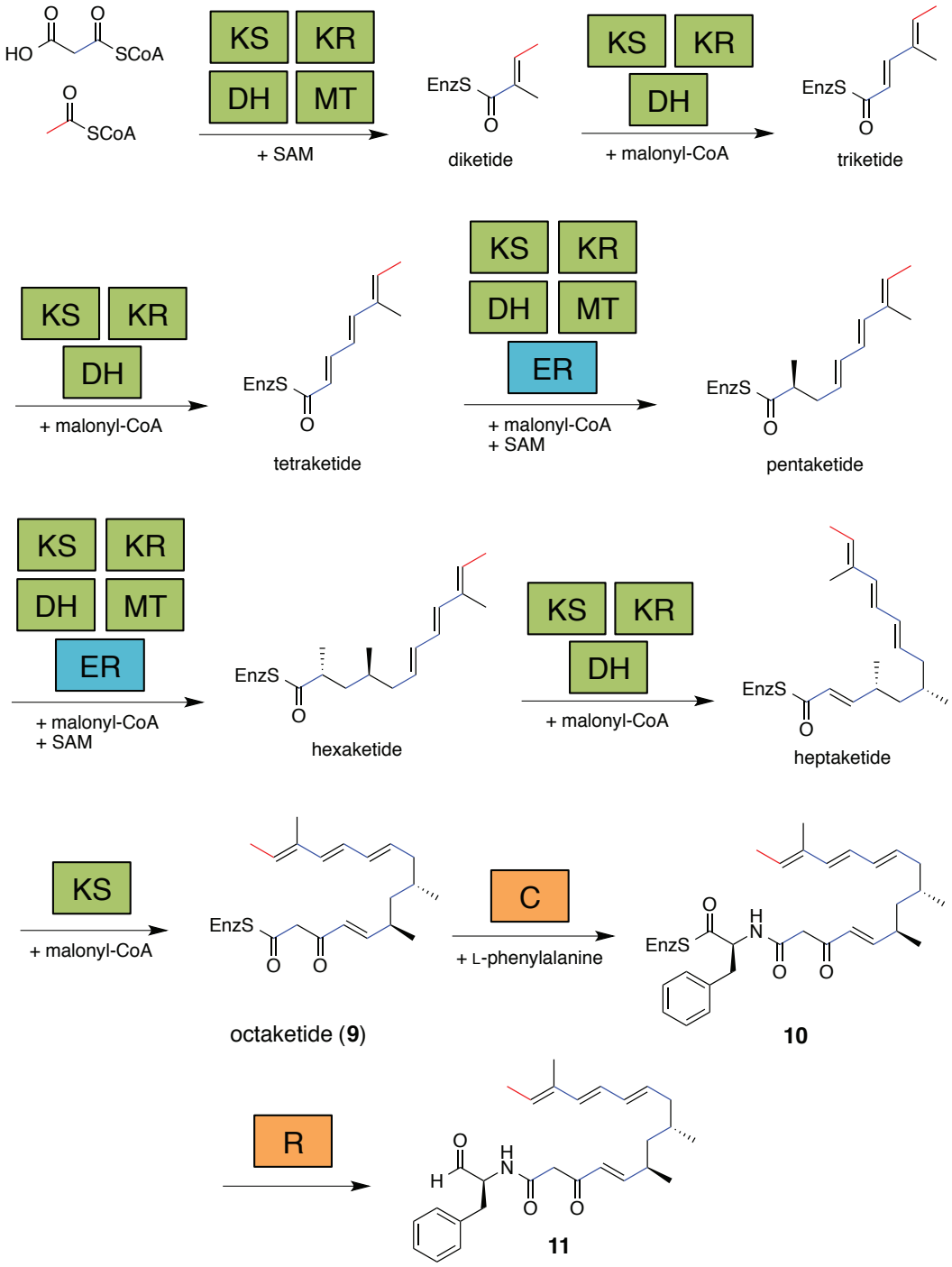

Figure 2-19. Proposed biosynthesis of enzyme bound amino acid-octaketide intermediate **10** of cytochalasin E by CcsA and CcsC (trans-acting ER) and released aldehyde **11**. Green domains = PKS domains of CcsA, orange = NRPS domains of CcsA, teal domain = CcsC (trans acting ER). Red bond indicates carbons incorporated by acetyl-CoA and blue indicates malonyl-CoA origin.

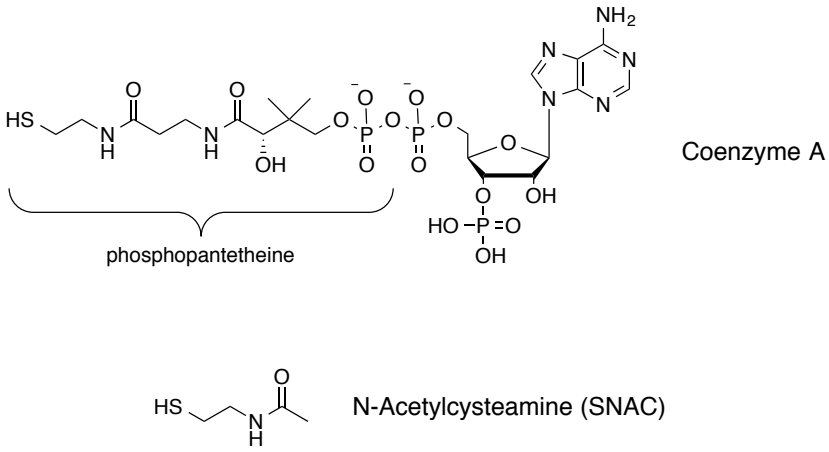

Figure 2-20. Structures of coenzyme A, phosphopantetheine and SNAC.

A detailed look at the proposed biosynthesis of the acyclic amino acid-octaketide intermediate generated by CcsA, in conjunction with CcsC (a trans-acting ER) can be found in Figure 2-19. Our ultimate goal is to use chemical synthesis to deconvolute the intermediate chemical reactions of CcsA and confirm the proposed off-loaded structure, aldehyde **11**. After 7 condensation reactions with one molecule of acetyl-CoA, 7 molecules of malonyl-CoA, and 3 molecules of SAM, CcsA is proposed to assemble an ACP bound octaketide **9**. The C domain would catalyze amide bond formation with the T domain-bound L-phenylalanine to form the amino-acyl intermediate **10**. The R domain is proposed to catalyze a $2e^-$ reduction to form an aldehyde before cyclization to the perhydro-isoindolone core of cytochalasin E.

Traditionally, a ^{13}C label is used in the proposed substrate and an isotopic enrichment in the final product can provide further proof of incorporation of the synthetic intermediate. This technique can be hampered by low incorporation rates and swamping of the ^{13}C label by the high concentration of unlabeled material synthesized by the PKS enzyme. Additionally, incorporation of a carbon-13 label in chemical synthesis is costly and can be plagued by low yields of small scale reactions. Therefore, we proposed that introduction of a late-stage intermediate would

circumvent the labeling problem by allowing us to only add phenylalanine and NADPH (leaving out acetate). Our previous work on hypothemycin and ^{13}C-labeled intermediates saw a positive correlation of label retention with intermediate maturity (i.e. a synthetic pentaketide intermediate is incorporated into the final product more readily than the triketide).[87] Additionally, studies with PKS-NRPS systems such as tenellin[79] and aspyridone[80] have shown that the PKS and NRPS portions operate independently (even when severed, see Chapter 1.5). These studies suggest that the chances of recognition and incorporation of an octaketide-SNAC thioester by the NRPS into the final product are high. If it is indeed recognized, this would provide convincing evidence for the polyketide intermediates and we could also determine the structure of the released product. To the author's knowledge, it would be the first time a SNAC ester intermediate has been recognized and transformed by an NRPS region.

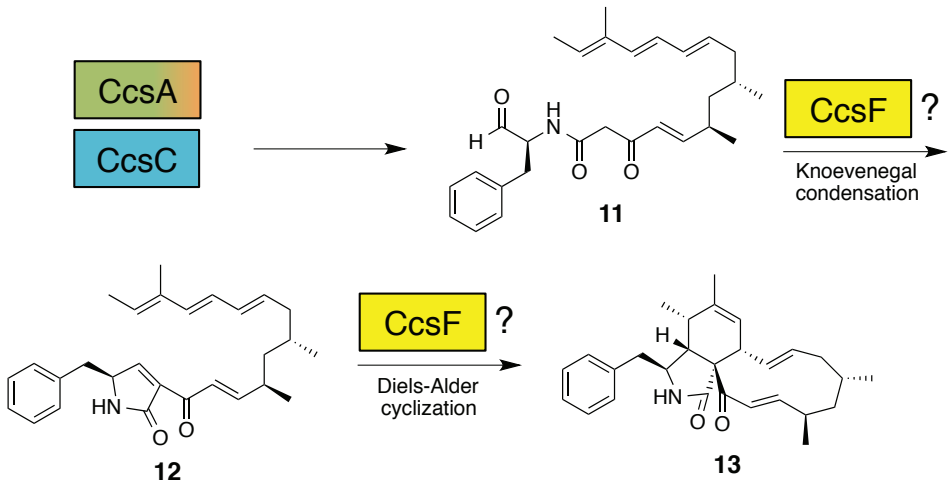

Figure 2-21. Proposed Knoevenagel condensation and Diels-Alder reaction in cytochalasin E biosynthesis.

Another motivation to probe the activity of CcsA and the structure of **11** is to confirm the proposed intramolecular Diels-Alder [4+2] cyclization that forms **13** (Figure 2-21). The current

proposal is based on transient aldehyde formation and either enzymatic or spontaneous intramolecular Diels-Alder cyclization. Enzymatic [4+2] cyclizations have been demonstrated in analogous systems, such as solanapyrone[126], lovastatin[127], and more recently equisetin[128], spinosyn A[37] and versipelostatin[129] (Figure 2-22). Enzymatic pericyclic reactions in biosynthesis appear to have two distinct benefits over spontaneous reactions, including an increase in the reaction rate of cyclization (as in the case of SpnF)[37] and/or resulting in an unfavorable stereochemistry (such as lovastatin hexaketide cyclization).[130] It is also interesting to note that cyclization of the lovastatin hexaketide **55** to **56** occurs during chain elongation by the PKS LovB (and presumably is catalyzed by the synthase as well) while cyclization of **57** to **58** occurs post-PKS.

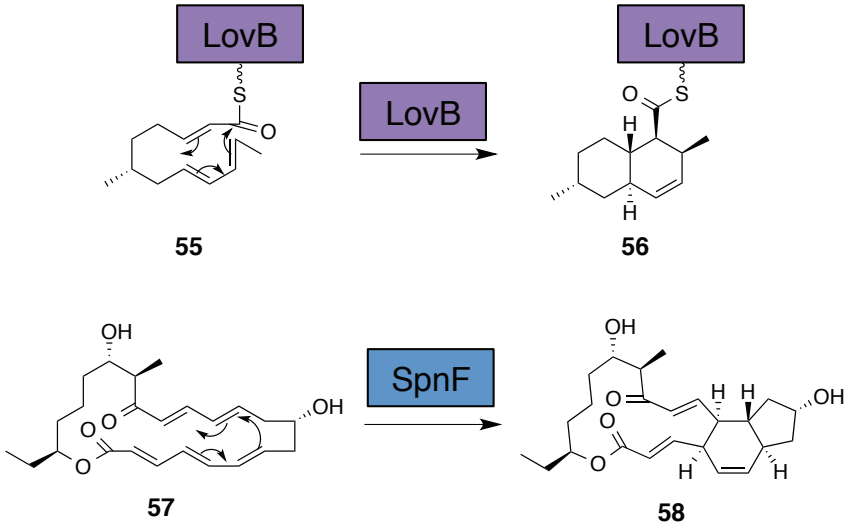

Figure 2-22. Enzymatic [4+2] intramolecular cyclizations in polyketide biosynthesis.

It is possible that many other cytochalasin metabolites experience this cyclization reaction, as the resultant tricyclic core is a common feature of the cytochalasin family. A candidate standalone enzyme that could be responsible for this reaction is CcsF, a protein with no assigned

function in the cytochalasin E gene cluster (Figure 2-3). Bioinformatic analysis of CcsF reveals that most of the homologs of CcsF are found in other PKS-NRPS gene clusters, including the one responsible for chaetoglobosin A biosynthesis in *P. globosum*.[100] Chaetoglobosin A is also proposed to undergo a [4+2] cyclization during its biosynthesis. Exploring the activity of CcsF might also inform the investigation of chaetoglobosin biosynthesis. With a greater understanding of these pericyclic enzymes, not only would we obtain a broader understanding of the biosynthesis of all cytochalasin analogs, but could also expand the repertoire of "cycloadditions" possible or even utilizing them in a cascade fashion, as seen with pyrollidinomycins.[131]

2.3.2 Project objectives

In collaboration with Prof. Yi Tang's lab at UCLA, we targeted the elucidation of the ultimate product of CcsA, and the possibility that Diels-Alder cyclization could be catalyzed by CcsF. In this project, our lab is responsible for the synthesis of the proposed biosynthetic intermediate **59**, and the Tang lab will clone, express, and purify the enzymes CcsA, CcsC and CcsF (Figure 2-23). After the expression and synthesis is complete, the enzymes will be assayed with the synthetic intermediates and LC-MS and NMR will analyze their resultant products. If the proposed octaketide thioester intermediate is recognized by the NRPS portion of CcsA, only phenylalanine and NADPH will be required in the assay to transform it to the final released product **11**. Synthesis of **12** will also be investigated in a divergent fashion from **11**, as more than half of the molecules are identical.

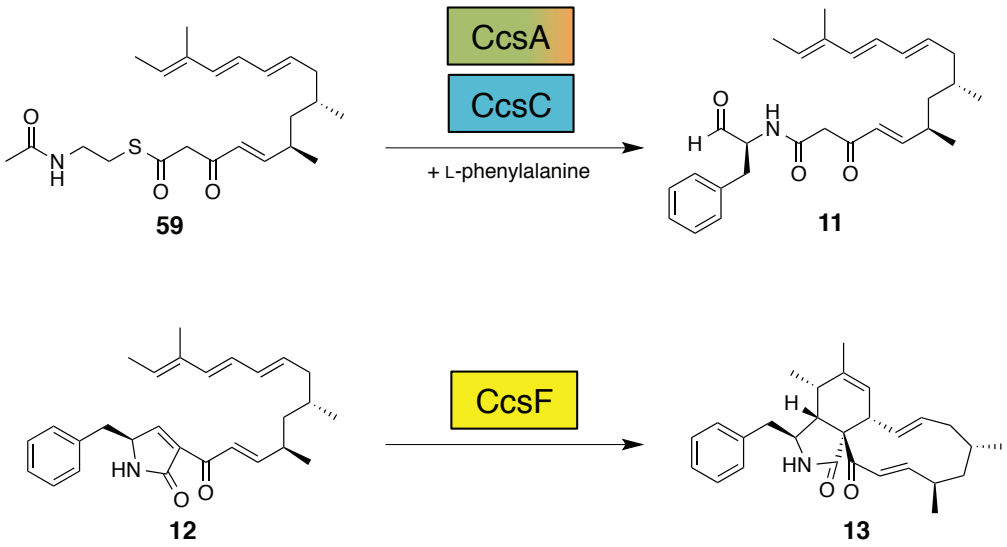

Figure 2-23. Proposed enzymatic assays and products for the identification of the products of enzymes CcsA and CcsF. Both proposed substrates (and possibly the products) are targets for synthesis.

2.3.3 Synthesis of proposed "late stage" octaketide SNAC thioester and pre-Diels Alderase substrate

Synthesis of proposed polyketide intermediates (especially late-stage) can be a daunting task, with stereochemical control of methyl groups and other functionality required. Even more frustrating is the possibility of synthesizing a proposed substrate, only to learn that the enzyme requires a different substrate (see Chapter 2.2.2.2). Fortunately, we performed labeling studies (Figure 2-7), which indicated the parts of cytochalasin E that were derived of acetate units, as well as those that were from phenylalanine, SAM and molecular oxygen. This allowed us to postulate what the structures of the intermediates and final product of CcsA might be with reasonable certainty. In 2013, the Oikawa group reported the heterologous expression of CcsA in *Aspergillus oryzae*, a fungal expression host that is typically used for sake production.[132] The authors were able to reconstitute CcsA activity and also isolate the released product **60** (Figure 2-

24). The structure of **60** corroborated labeling studies, in particular, the lack a ketone at position C17. Unfortunately, the absolute stereochemistries of the methyl groups in this intermediate are ambiguous, but we can make the reasonable assumption that the stereochemistry of cytochalasin E would remain unchanged from the CcsA-generated intermediate **11** to the final product **5**. Although hydroxylation is hypothesized to occur at C18 by a P450 monooxygenase post PKS assembly, these enzymes typically proceed with retention of stereochemistry.[133] One other notable outcome of the work done by Oikawa and co-workers is that the reductase domain seemingly reduced the enzyme-attached thioester to an alcohol (not the proposed aldehyde), although it is not clear if this is the true intermediate or a shunt product. If alcohol **60** were the true intermediate, then oxidation to an aldehyde would be needed before cyclization could occur. We designed the synthesis to allow derailment to **60**, if it was deemed necessary.

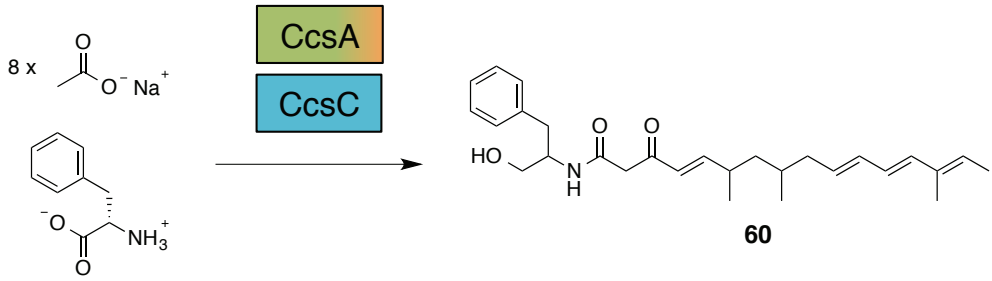

Figure 2-24. Cytochalasin backbone production by CcsA and CcsC as observed by Oikawa and co-workers.[132]

A retrosynthetic strategy for the synthesis of **12** and **59** can be found in Scheme 2-3. The targets were split into three fragments. The strategy was to combine all three fragments through trans-selective Horner-Wadsworth-Emmons (HWE) olefinations. This proposal allows for the convenient synthesis of both **12** and **59** through a divergent strategy, by using two identical

fragments – sometimes termed the "tail". Simply modifying the "head group" to contain the cyclized phenylalanine as a deoxy-tetramic acid (**64**) and keeping the phosphonate for olefination would be sufficient for synthesizing **12**. Another advantage to this strategy is that it could be used to synthesize **60** using a different head group.

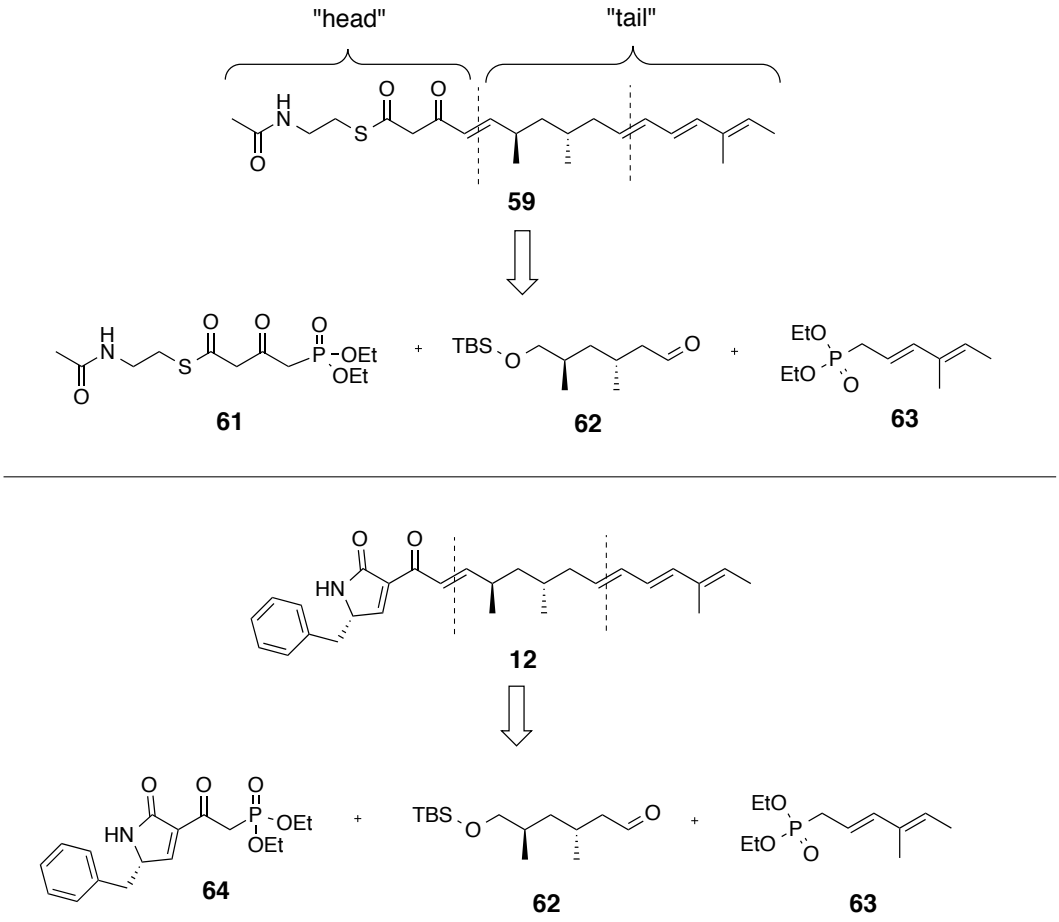

Scheme 2-3. Retrosynthetic analysis of **59** and **12**. Fragments **62** and **63** are referred to as the tail group while **61** is the head group and the differentiating factor for both syntheses.

2.3.3.1 Synthesis of 61, the head group of 59.

The synthesis of SNAC-containing **61** began with Meldrum's acid, which was employed to build the beta-keto phosphonate. Coupling of phosphonoacetic acid to Meldrum's acid using 1-ethyl-3-(3-dimethylaminopropyl)carbodiimide (EDC) and 4-dimethylaminopyridine (DMAP) led to derivative **65**.[134] Heating this compound at 100°C in the presence of *N*-acetyl-cysteamine (HSNAC) assembled **61** in 59% overall yield.

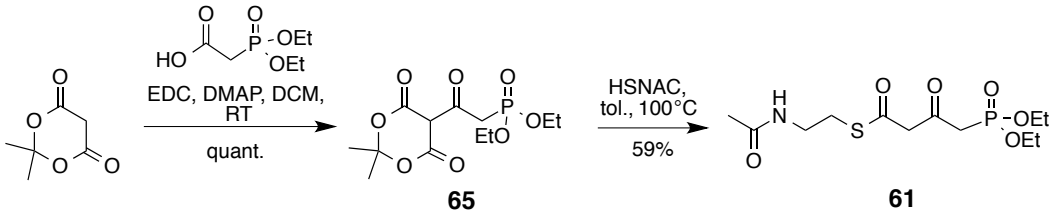

Scheme 2-4. Synthesis of **61** through acylation and electrocyclic ring opening of Meldrum's acid.

2.3.3.2 Synthesis of the CcsA mature chain middle fragment 62

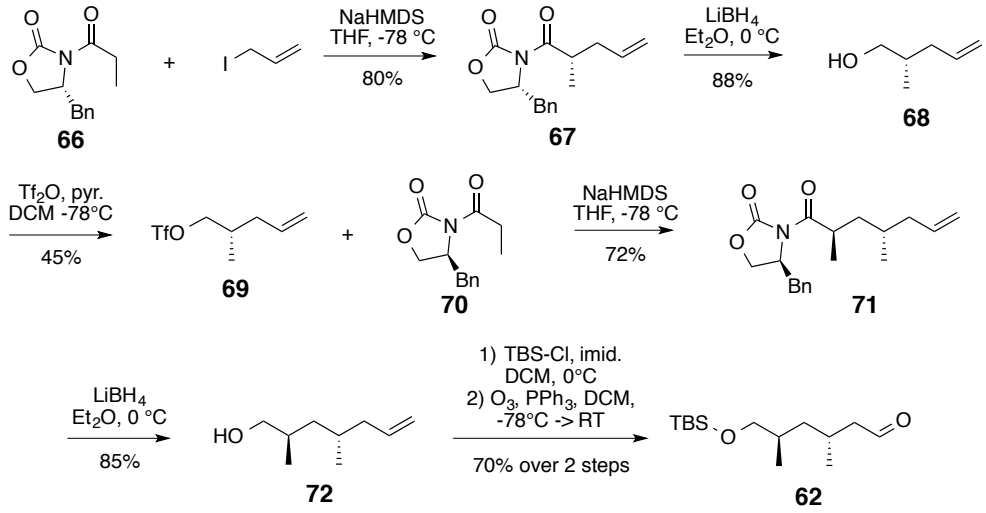

Scheme 2-5. Synthesis of fragment B, using Evans' chiral oxazolidinone chemistry.

The strategy for synthesizing fragment B is outlined in Scheme 2-5. Construction of the two stereocentres presented the largest challenge. Evans' chiral oxazolidinone chemistry was used because it is robust and considered by some to be the benchmark for stereochemical induction. Luckily, compounds **67** and epi-**71** had been previously synthesized using this chemistry with great reported d.e. (>96%) in both cases.[135,136] Fragment B was synthesized starting from *N*-propionylated 4-(*R*)-benzyloxazolidinone **66**. The *Z*-enolate was made selectively with NaHMDS, and was reacted with allyl iodide in 80% yield. Reduction of the resulting amide bond to primary alcohol **68** using lithium borohydride removed the chiral auxiliary. Chiral alcohol **68** was activated with triflic anhydride. Nucleophilic displacement of the triflate with propionylated (*S*)-oxazolidinone furnishes **71,** and was isolated as a single stereoisomer. The chiral auxiliary was removed with lithium borohydride, and the resultant

alcohol **72** was subsequently protected as a silyl ether and used immediately in an ozonolysis reaction to yield **62**.

2.3.3.3 Synthesis of allylic phosphonate 63

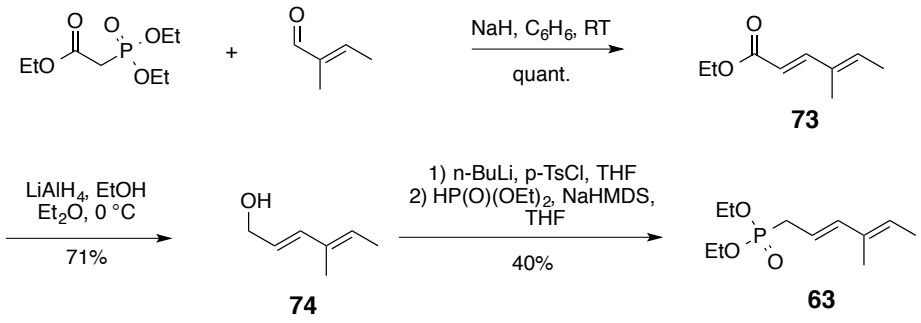

Scheme 2-6. Synthesis of **63** by HWE olefination

The allylic phosphonate **63** was assembled by first reacting triethylphosphonoacetate and tiglic aldehyde by Horner-Wadsworth-Emmons (HWE) olefination to yield intermediate **73**. The conjugated ester was reduced to the allylic alcohol using monoethoxyaluminum hydride in moderate yield. The allylic alcohol was converted to the allylic phosphonate by first tosylating the free hydroxyl group, then displacing the tosyl in an S_N2 fashion with freshly prepared sodium diethylphosphite. Fidelity of the relative stereochemistry of the methyl groups was verified using nOe experiments and observing the correlation between the two methyl peaks.

2.3.3.4 Synthesis of the tail segment of 59 and attempts at olefination with the head piece

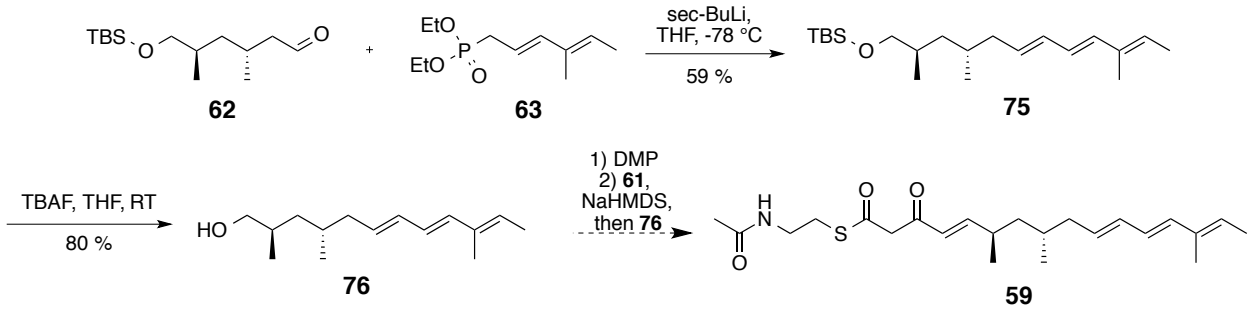

Scheme 2-7. Synthetic scheme depicting HWE olefination connecting **62** and **63**, yielding triene **75** and proposed steps to **59**.

Allylic phosphonate **63** was deprotonated by *sec*-BuLi to generate the reactive ylide species. Treatment with aldehyde **62** generated the expected triene, with all three bonds in the *E* configuration. Deprotection of the bulky silyl ether with fluoride anion generated the triene alcohol, which was set-up for oxidation by Dess-Martin periodinane to generate the alpha-substituted aldehyde. As the triene alcohol was hypothesized to be sensitive to acid and light, several test reactions were attempted with a commercially available aliphatic aldehyde to determine acid-free conditions (Scheme 2-8).

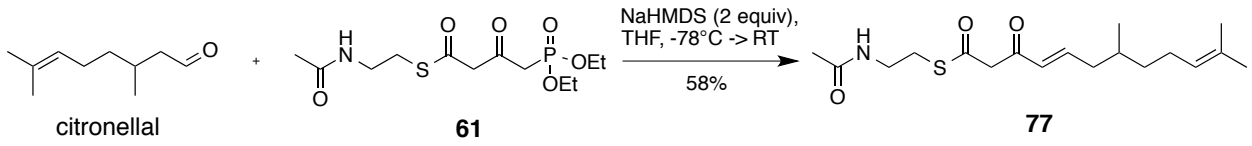

Scheme 2-8. Synthesis of **77**, using test reaction conditions to determine viability of reaction.

Treatment of **61** with two equivalents of base generated the dianion ylide, which reacts at the phosphonate alpha carbon (most basic) to presumably generate the oxaphosphetane which

would rearrange to form the *E* double bond selectively following the established HWE mechanism.[137,138] Phosphate buffer (pH=7) was used to avoid exposure of the product to acid and special care was taken to minimize light exposure. The success of the test reaction suggests that the proposed final step is a viable route to construction of the desired product. The evaluation of the final proposed step for synthesis of **59** is currently ongoing in our group.

2.3.3.5 Synthesis of 78, and proposed divergent synthesis to assemble 12 and 60

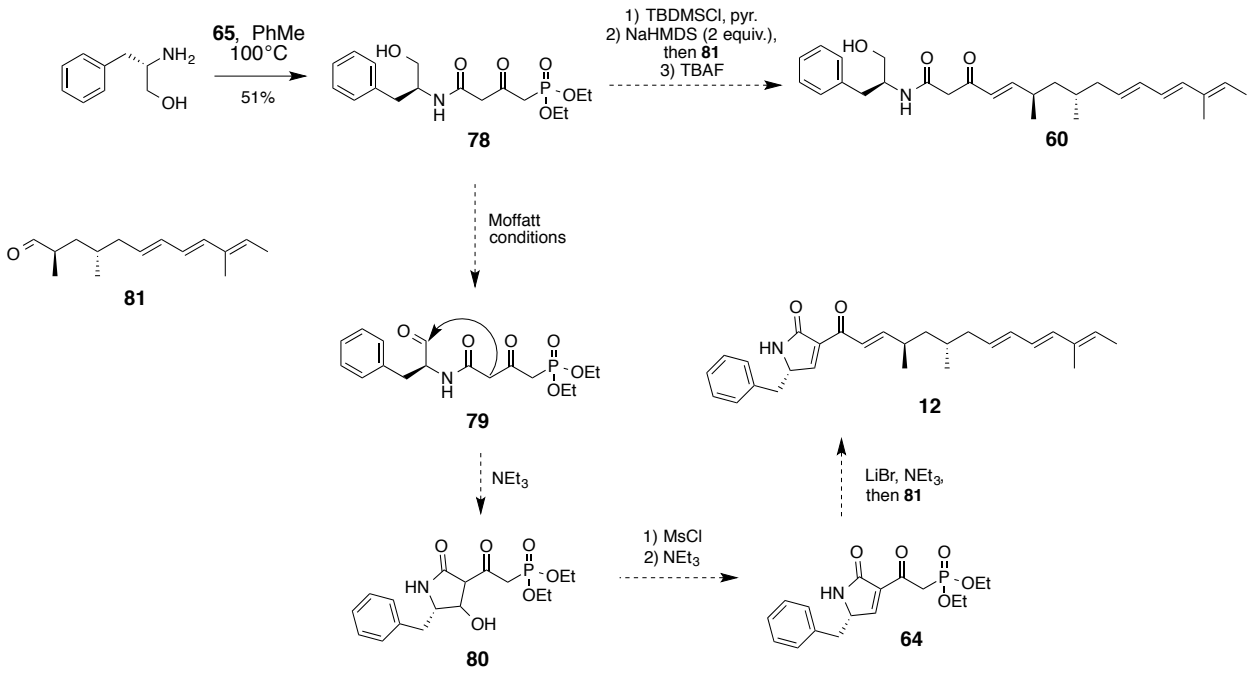

Scheme 2-9. Proposed synthesis for trienes **12** and **60** using a divergent strategy from phosphonate **78**.

Although the synthesis of **12** was not undertaken due to time constraints, a reasonable proposal for its synthesis can be drafted. Starting with L-phenylalaninol, heating to 100°C with **65** in toluene provided phosphono-amide **77** in 51% yield**.** This intermediate was devised as a

divergence point to allow for the synthesis of both **60** and **12** from a common intermediate. The synthesis of **64** was devised to take a biomimetic approach, proposing Knoevenagel type cyclization to furnish the deoxy-tetramic acid. Oxidation in modified Pfitzner-Moffatt conditions would synthesize **79** and avoid the deleterious use of base that could possibly catalyze unwanted HWE dimerization.[138] Lactam formation by mild base would synthesize **80**, which could be mesylated and eliminated to furnish **64**. The tetramic acid phosphonate **64** could be extended to the final product **12** through a HWE olefination using mild Rathke conditions. Alternatively, protecting the hydroxyl of **77** and performing the olefination could synthesize **60** after deprotection.

2.4 Conclusions and future work

In the chapter, the biosynthesis of cytochalasin E was explored in detail. We started with *in vivo* isotopic labeling of cytochalasin E using the biosynthetic enzymes in *A. clavatus*. This allowed us to map out the origins of most of the carbon and oxygen atoms and gave us insight into how the macrocyclic carbonate was made. CcsB, a BVMO, was isolated, purified and its activity was investigated using synthetic and naturally obtained substrates **22** and **23**. After formation of carbonate **24** was detected, a mechanism was proposed. Attempts to synthesize the proposed octaketide SNAC intermediate **59** were also undertaken. A proposal for synthesis of possible pre-Diels-Alder substrate **12** was made.

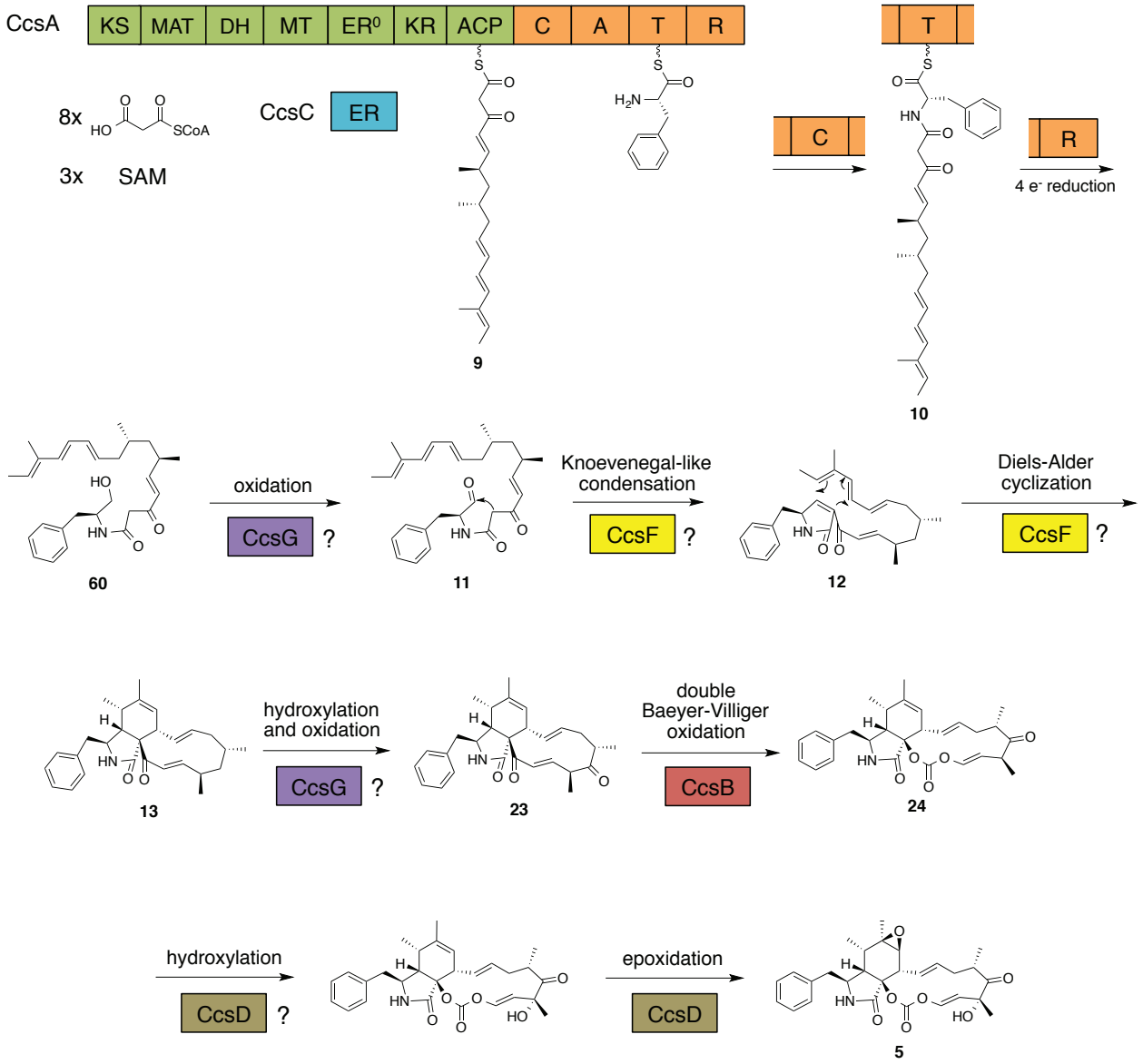

Figure 2-25. Updated proposed biosynthesis of cytochalasin E. The roles of CcsD, CcsG and CcsF remain to be elucidated.

With the biological role of CcsB elucidated, we can make a substantial update to the proposed biosynthesis of cytochalasin E (Figure 2-25). The structure of CcsB substrate **23** suggests that carbonate formation occurs after Diels-Alder cyclization but before epoxide and 3° hydroxyl installation. This is intriguing considering that the labeling studies indicated that the

ketone at C18 was installed post-PKS, suggesting the work of an oxygenase enzyme. Since there are only two in the gene cluster and four distinct oxidation reactions that take place (aldehyde formation, double hydroxylation, oxidation to ketone, and epoxidation), this may mean that a *trans*-acting oxygenase acts during cytochalasin E biosynthesis.

Future work would include further determination of the mechanism of CcsB. Synthesis of potential inhibitors to obtain a crystal structure would be an ideal course of action. Alternatively, trying to replicate the epoxy-ester rearrangement of **51** to **24** on the bench could add credence to that mechanism. Once the syntheses of **59** and **12** are finished, testing with CcsA would be possible. Exploration of the chain released product and potential activity of CcsF would be the main avenues of investigation.

3 Probing the timing and selectivity of lovastatin LovB methyltransferase, a domain of a fungal iterative HR-PKS

3.1 Introduction

3.1.1 Lovastatin: discovery and biosynthesis

Lovastatin is a commercially successful cholesterol-lowering drug, having sales of as much as $11.5B US by 2011.[139,140] Lovastatin (**81**) (sometimes referred to as mevinolin) induces its cholesterol-lowering activity through competitive inhibition of 3-hydroxy-3-methyl-glutaryl-CoA reductase (HMG-CoA reductase), an early enzyme in the cholesterol biosynthetic pathway.[141] It was originally discovered by Merck scientists in 1980 through activity-guided fractionation of *Aspergillus terreus* extracts in search of HMG-CoA inhibition.[15] Lovastatin research led to the development of the semi-synthetic derivative simvastatin (**83**), which is identical to lovastatin save an extra methyl group on its side chain (Figure 3-1).[142] Another structurally related statin is compactin (**84**), which was isolated from *Penicillium citrinium* in 1976.[143] Compactin was discovered before lovastatin but is considerably less active and struggled to experience the same commercial success.[140] Lovastatin is not only a success story for blockbuster drugs of natural product origin, but is also the product of one of the best-characterized fungal polyketide biosynthetic pathways.

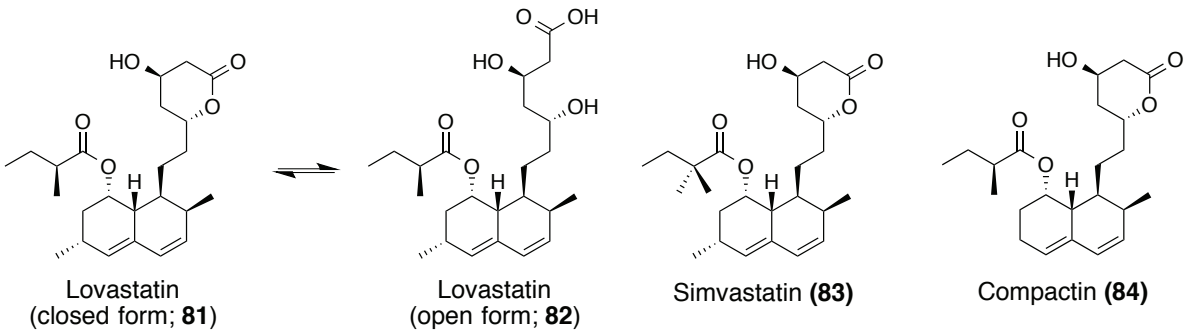

Figure 3-1. Structures of lovastatin (in both open and closed lactone forms) and structurally related statins.

The gene cluster responsible for production of **81** in *A. terreus* is outlined in Figure **3-2**. The gene cluster was first published in 1999[45] and has since been rediscovered in *Monascus pilosus,*[144] another fungal species that produces **81**. The gene cluster contains two PKS genes, lovB and lovF that are responsible for synthesizing the nonaketide and diketide portions of **81**, respectively.[45] The cluster also contains a cytochrome P450 encoding gene, lovA, that is responsible for oxygenation and double bond installation.[145] LovI and LovE are regulators of lovastatin production while lovD and lovG encode thioesterases. Finally, lvrA is hypothesized to be the gene responsible for resistance, as it encodes a protein that is highly homologous to HMG-CoA reductase.

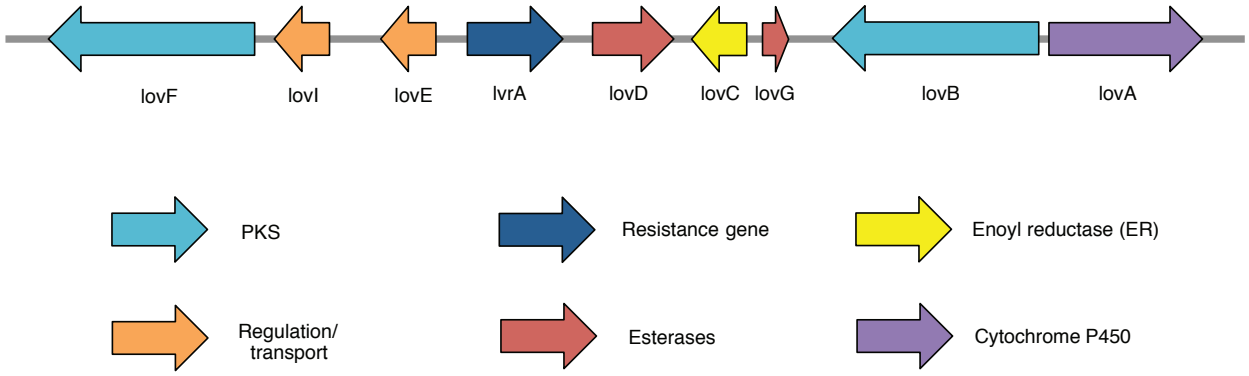

Figure 3-2**.** Cartoon representation of the lovastatin gene cluster in *Aspergillus terreus.*

The proposed biosynthesis of dihydromonacolin L (DML) can be found in Figure 3-3. DML, a biosynthetic precursor to lovastatin, has been prepared enzymatically from heterologously expressed LovB and LovC.[45] LovB is an unusual fungal iterative PKS as it contains parts of an NRPS module, including a C domain and part of an A domain (catalytic domain missing), suggesting a PKS-NRPS origin.[146] Phylogenetic and genetic engineering suggest an early evolutionary divergence due to LovB PKS domains being unable to operate properly after fusion with other NRPS domains.[123] As discussed in section 1.5, these NRPS fusions are often well tolerated.[44,79] It is interesting to note that while removing the C domain abolishes production of DML, adding it back in *trans* restores the activity of LovB. This is reminiscent of observations with aspyridone biosynthesis, in which the PKS and NRPS domains of AspA can communicate in *cis* or *trans*, with no appreciable change in activity.[80] This suggests that while the C domain may not function in a classical way, it is still important for LovB activity.

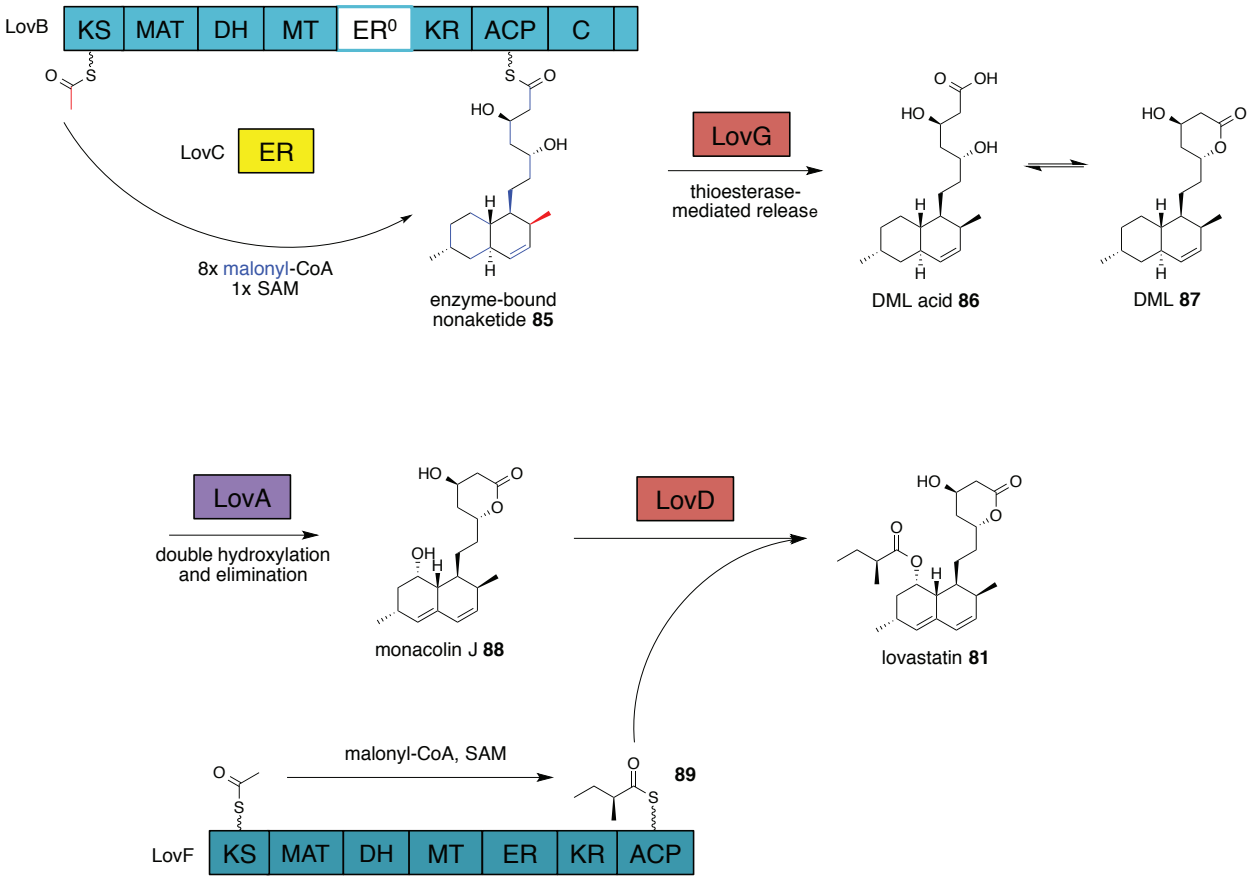

Figure 3-3. Biosynthesis of lovastatin by *Aspergillus terreus*.

LovB shares another trait with PKS-NRPS enzymes, featuring a redox-inactive ER domain with concomitant use of a *trans*-acting ER (LovC) instead. Along with LovC, LovB catalyzes approximately 35 chemical reactions to furnish ACP-bound nonaketide **85**. Interestingly, LovB is also hypothesized to catalyze an intramolecular Diels-Alder reaction at the hexaketide stage to form the a *trans* decalin with disfavored stereochemistry (Figure 2-22).[130] After cyclization, the hexaketide is proposed to be extended and functionalized to nonaketide **85**. A thioesterase (LovG) catalyzes the release of **85**, as LovB is missing either a TE domain (as seen in other HR-PKSs) or an R domain (typical for PKS-NRPSs) that could be used for self-

catalyzed chain release.[147] Once the thioester is hydrolyzed, DML is in equilibrium between its open **86** and closed forms **87**. LovA then catalyzes a double hydroxylation that results in elimination of one of the hydroxyls to furnish conjugated diene **88**.[145] LovF, a HR-PKS, synthesizes an ACP-bound methylated diketide **89** that again is unable to be released, due to the lack of a TE domain.[148] LovD compensates for the missing domain by catalyzing chain release through ester formation with monacolin J, to furnish **81**. LovD has been demonstrated to have relaxed substrate specificity and can accept 2(*S*)-methylbutyrate-CoA in the place of the ACP-bound diketide, although with lower yield. Tang and co-workers have used this promiscuity to their advantage and published a series of LovD mutants that can synthesize simvastatin **83** from **88** and 2,2-dimethylbutyrate thioester donors *in vitro* or in whole cells.[149-151] Much of lovastatin biosynthesis has been mapped, with all of the post-PKS enzymes expressed and their activity characterized. This chapter will focus on LovB and the programming of its tailoring domains, specifically on the pattern of methylation by the MT domain.

3.1.2 Previous work with LovB: characterization, expression and engineering

The earliest indications of the polyketide origins of lovastatin (and the participation of a PKS) came from a suite of whole-cell labeling studies.[152-155] *Aspergillus terreus* was fermented in the presence of doubly labeled acetate, labeled SAM or in an $^{18}O_2$ rich atmosphere and the sites of isotopic labeling were determined by ^{13}C-NMR and changes in chemical shift (Chapter 2.2). These results culminated in the labeling pattern shown in Figure 3-4. Doubly carbon-13 labeled acetate was used to determine if acetate units were intact when incorporated or if they were broken down beforehand. Using this swath of isotopically enhanced precursors allowed

researchers to map every non-hydrogen atom in lovastatin and suggest that two separate PKS chains are made. Once the PKS origin was elucidated, the hunt for the enzymes responsible for their synthesis was on.

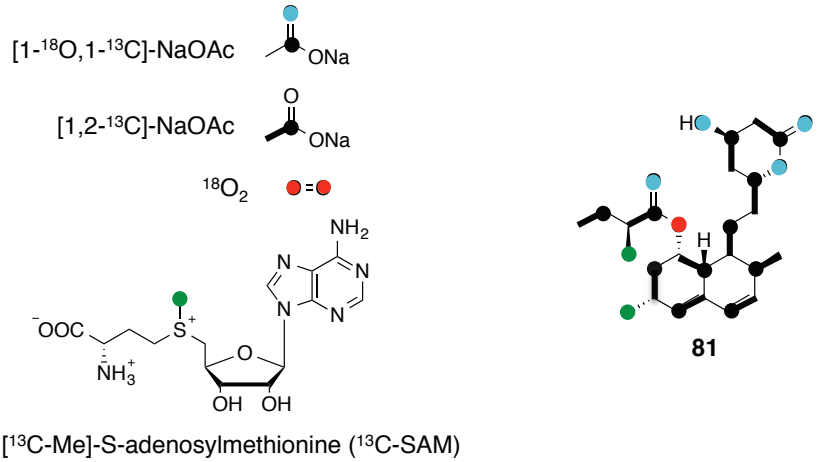

Figure 3-4. Summary of whole-cell labeling studies of lovastatin by *Aspergillus terreus*.[152-155]

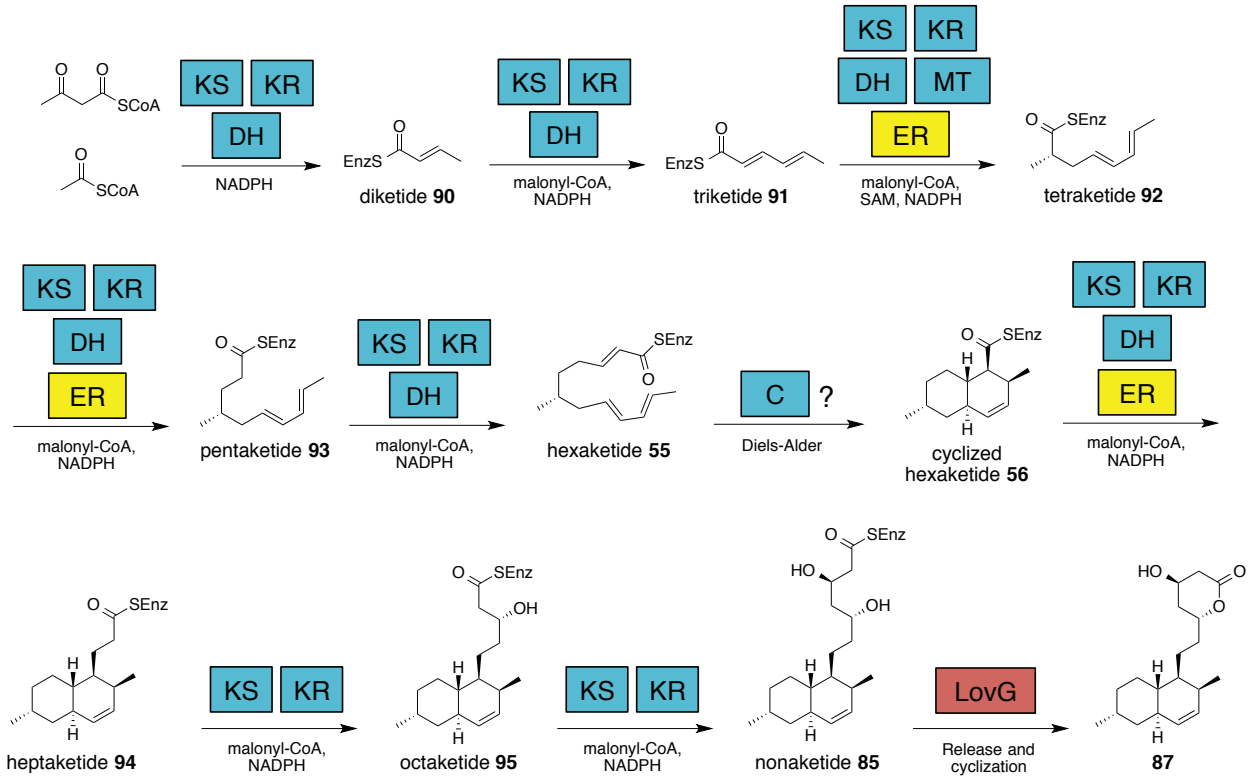

Figure 3-5. In depth proposal for **96** assembly by LovB. Domains and co-factors required at each step are listed.

Once **87** had been isolated from both *A. terreus*[156] and *M. pilosus*[157] and had been hypothesized to be a biosynthetic precursor of **81**, a proposal for its biosynthesis could be made (Figure 3-5). Diketide **90** could be assembled by condensation of a molecule of acetyl-CoA and malonyl-CoA and subsequent reduction and elimination by the KR and DH domains respectively. Extending **90** by two carbons and installing another double bond using the KR and DH tailoring domains synthesizes triketide **91**. Synthesis of the tetraketide (**92**) is mechanistically important, as it is the first stage in which the MT and *trans*-ER are required. Interestingly, this is the only time that the MT is active during the biosynthesis of **87**. This point also marks a major divergence from between lovastatin and compactin biosynthesis, as

compactin could be considered to be an unmethylated lovastatin. Pentaketide **93** is then formed, using KR, DH and LovC and is extended to the linear hexaketide **55** by the KR and DH domains. The linear hexaketide is then proposed to be cyclized through an enzyme-catalyzed intramolecular Diels-Alder (DA) to furnish the bicyclic hexaketide **56**. This reaction is discussed in more detail in Chapter 2. Recent isolation of a pre-DA product using a LovB fusion protein that has the native C domain swapped for the NRPS domains from EqxS (equisetin synthase) suggests that the C domain may be the responsible agent for the intramolecular cyclization reaction.[123] Investigation of the role of the C domain in Diels-Alder catalysis is currently ongoing in our lab. The cyclized hexaketide is then extended by three acetate units to furnish the enzyme bound nonaketide **85,** which is released by a *trans*-TE (such as LovG).

LovB was heterologously expressed first in 1999 in *Aspergillus nidulans*[45] and then a decade later in an engineered strain of *Saccharomyces cerevisiae*.[78] This is an impressive achievement as these large multimodular (~1 MDa) proteins are notoriously difficult to express and purify.[45] Using the *A. nidulans* system, Vederas, Hutchinson and co-workers were able to successfully express and purify LovB and LovC and assay both enzymes for **87** production.[45] Although the expression level was low, the authors were able to characterize the products of LovB both with and without LovC (Figure 3-6). With purified, active LovB in hand the authors were able to gain insight into how LovB is programmed. They discovered that LovB synthesized aberrant shunt products (**96** and **97**) in the absence of the *trans*-acting ER LovC, none of which contained any reduced double bonds (confirming that the *cis*-ER is redox inactive). These pyrone shunt products can be rationalized by the mechanism proposed in Figure 3-6C.[45] The authors hypothesized that in the case of non-functional enoyl reduction, the tailoring domains active at the tetra- and pentaketide stages may not function properly and the enzyme is "stalled". LovB

could then use the functioning core domains (KS and MAT) to extend the chain by two ketide units and catalyze self-release through pyrone formation. This would prevent the enzyme from being permanently inhibited. The varying chain length of pyrones makes sense as LovC is required at both the tetraketide (resulting in **96**), and the pentaketide (**97**) stage. The structures of pyrones **96** and **97** were confirmed through chemical synthesis.[158]

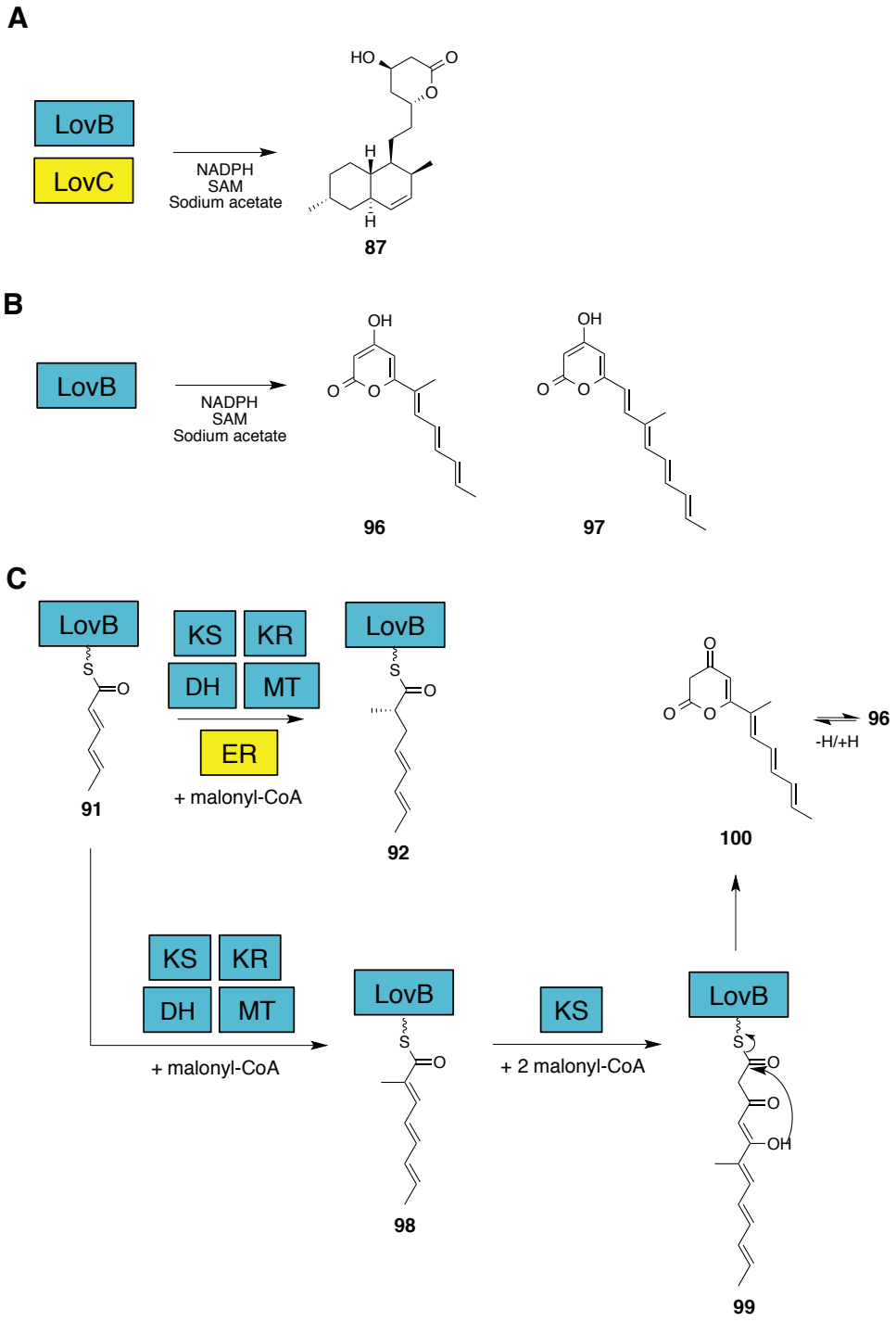

Figure 3-6. Results of initial *in vitro* assays of LovB and LovC (yellow ER).[45] A) Production of **87** by LovB and LovC with proper cofactors. Note that product release was the probable result of endogenous *trans*-TE. B) Production of pyrones **96** and **97** by LovB in the absence of LovC. C) Top: normal tetraketide product (**92**) formed when LovC is present. Bottom: Mechanism of pyrone formation by LovB resulting in self catalyzed off-loading (no TE necessary).

Pyrone formation by LovB in the absence of LovC is not an isolated phenomenon. In 2009, Tang, Vederas and co-workers were able to substantially increase the yield of LovB using an engineered strain of *S. cerevisiae*.[78] This system improved expression and allowed for functional assays of LovB in the absence of necessary cofactors (Figure 3-7). Testing LovB in cofactor restricting conditions can illustrate how the domains operate in isolation, without the need for using truncated proteins or isolated domains. Truncated synthase experiments restrict the possibility of protein-protein interactions, which are important for proper PKS function.[80] LovB was tested independently with all cofactors present and production of pyrones **96** and **97** was noted (Figure 3-7A, similar result as in Figure 3-6). When NADPH was removed from the assay, a novel shorter pyrone **101** was found (Figure 3-7B). This result is be rationalized by a non-functional KR (no NADPH) preventing normal diketide formation (**90**). LovB then extends the starter unit by two acetate units and off-loads in a similar mechanism to Figure 3-6B. More pyrones of various chain lengths (**102**, **103**, **104**) were isolated when SAM was withheld from the assay (Figure 3-7CD). New shunt products **105** and **106** were also isolated from the SAM-free assays. The authors concluded that these might be the result of a single chain extension and hydrolysis followed by decarboxylation as a minor product release mechanism.

In Figure 3-7E and F, LovC was replaced by MlcG, the *trans*-ER used in compactin (**84**) biosynthesis to determine the nature of the interaction between LovC and MT during tetraketide biosynthesis. The structure of **84** is nearly identical to **81** except for the extra methyl group on **81**. The HR-PKS responsible for nonaketide biosynthesis of compactin has a MT but it is thought to be inactive (since it is not used).[159] MlcG shares high sequence similarity with LovC (83%; 72% identity), suggesting that it could interact with LovB through proper protein-protein interactions. Surprisingly, MlcG restored the activity of SAM-free LovB and a methyl-

free DML product **107** was isolated. Even more surprising was that LovB combined with MlcG was able to synthesize DML (**87**) when SAM was added back. These results demonstrate that the *trans*-ER complementation is necessary for normal LovB polyketide production and that tetraketide methylation is key for proper LovB:LovC interactions. Pyrone formation to off-load aberrant products has been found in other systems as well, suggesting it might be a ubiquitous mechanism for off-loading in fungal PKS-NRPS systems.[123]

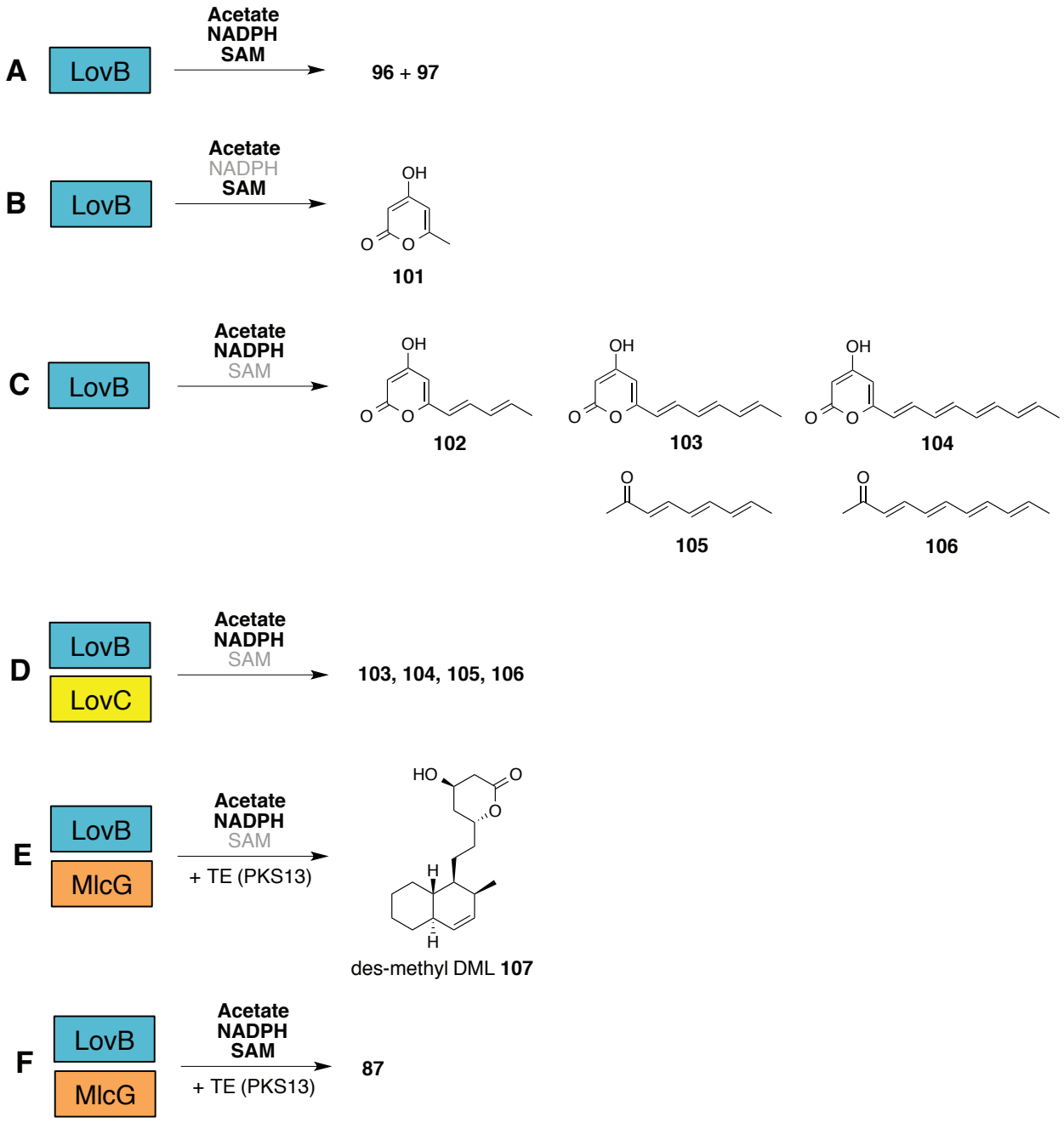

Figure 3-7. Results of *in vitro* LovB assays using *S. cerevisiae* expression system. Bold co-factors were present in the enzyme reaction while greyed ones were absent. MlcG is a trans-ER from the compactin biosynthetic pathway in *Penicillium citrinum*. PKS13 is a broad specificity TE from *Giberella zeae* used for chain release from LovB. **105** and **106** are hypothesized to be resulting from a minor off-loading mechanism of hydrolysis and decarboxylation.

3.1.3 Project objectives

We aim to gain a deeper understanding of LovB and the basis for domain selectivity (a.k.a. the "programming" of LovB). Specifically, we decided to assay the methyltransferase domain of LovB as it is arguably the simplest in its programming because it only operates once at the tetraketide stage. The assays with full LovB exclude the possibility of aberrant behavior due to the lack of protein-protein interactions or improper folding resulting from the rest of the megasynthase being missing. This should allow for the native conformation and activity of the MT. The Tang lab, specifically Ralph A. Cacho and Bo Wang, were responsible for expression, and enzyme kinetic assays while our work centered on the synthesis of the substrates and products used for testing. We first targeted determination of the substrate for the MT domain and assay of LovB with only SAM present in the reaction mixture. Absence of NADPH can prevent competing reactions (such as ketoreduction) from taking place. We will elucidate the basis for selectivity by preparing less desirable substrates that are either too short (triketide) or too long (pentaketide) and determine if there is any substrate selectivity. If these are methylated, it may indicate that additional domains may be involved in proper functionalization. If the MT domain demonstrates high discrimination on its own, it would suggest that the methylation reaction selectivity is intrinsic to this domain alone.

3.2 Results and discussion[§]

3.2.1 Testing the methyltransferase domain of LovB

The chimeric proteins discussed in chapter 1.5 and the *in vitro* assays with LovB represent the bulk of the knowledge that we have for the programming of PKS-NRPS domains. Characterizing these domains and their selectivity has proved to be a very challenging task. The first hurdle was reliable expression and reconstitution of the activity of LovB and development of the assay for screening any possible products (LC-MS).[78] The next difficulty is assaying individual domains in a complex system to get an idea of their selective activity. An understanding of the precise mechanism of domain selectivity could also assist in the development of selective irreversible inhibitors that could lock the system at each polyketide stage. This would be beneficial from a structural biology point of view to obtain crystal structures and snapshots of how these megasynthases look in a 3D sense, at a given stage. Until then, we just have theories of how these domains selectively operate.

One of the difficulties in assaying these domains stems from their multiple modes of reactivity. These domains are active at multiple, separate polyketide stages and this complicates the knowledge we obtain about their reactivity. The MT domain on the other hand is much simpler, displaying very high selectivity for only the tetraketide stage over the eight other possible substrates (di, tri, pentaketide, etc.). Interestingly, with all the pyrone shunt products isolated from erroneous LovB activity, none have been found with methylation at any stage other than the tetraketide. If we understand the basis for its high selectivity, maybe we can apply the programming rules to more complicated domains as well.

[§] Enzymatic testing was undertaken in Prof. Yi Tang's lab at UCLA by graduate students Ralph A. Cacho and Bo Wang.

Studying the methyltransferase domain of LovB may provide knowledge outside of domain selectivity. In an exhaustive review of the structure and mechanisms of PKS domains, Prof. Keatinge-Clay referred to the MT as the most poorly understood domain.[77] This is remarkable, considering that the MT domain is a unique feature of fungal PKS systems, separating it from mammalian FAS[160] and bacterial type I PKS systems like DEBS (Chapter 1.2).[161] In contrast to MTs, methylation in modular type I PKSs is typically achieved through starter unit selection (by the AT) of methyl-malonate instead of malonate.[26] In addition, the MT catalyzed methylation during **81** biosynthesis improves the activity two-fold over **84**.[15] Adding another methyl group to **81** leads to **83** and another doubling of potency (Figure 3-8).[162] These are examples of the well documented "magic methyl effect" that has perplexed medicinal chemists[162] and prompted synthetic chemists to develop methylation reactions inspired by SAM and MTs.[163] Understanding how these MT domains work could lead to more methylated polyketide derivatives and possibly an enhancement in potency through the magic methyl effect.

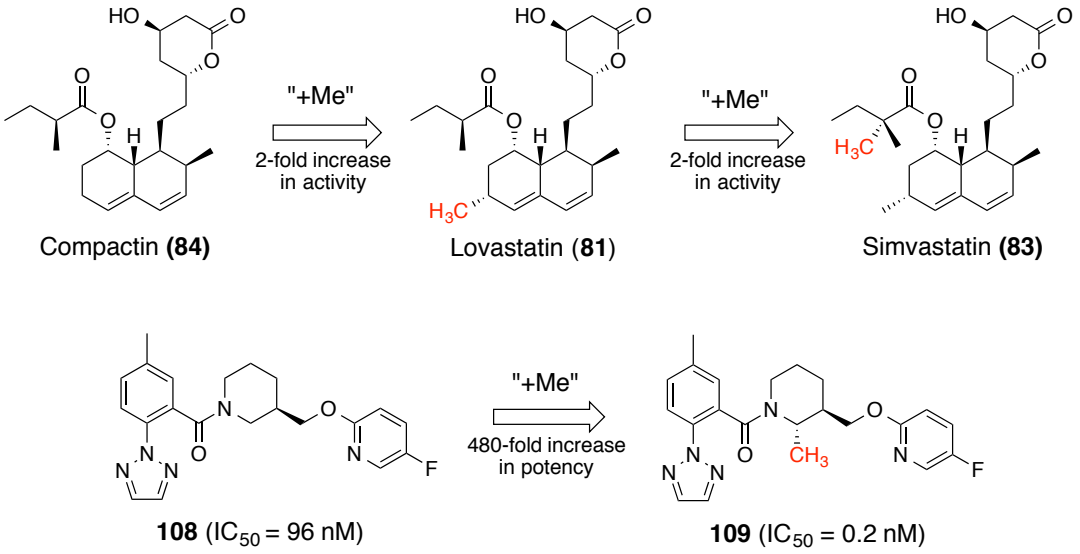

Figure 3-8. Examples of the magic methyl effect. Top example: gradual increase of activity of HMG-CoA inhibitors as methylation increases. Bottom example: 480-fold increase in potency of **109**, a selective inhibitor of orexin-1 receptor for treatment of insomnia.[162]

In order to assay the MT domain of LovB for its activity, we need to hypothesize what its substrate might be. An overview of the formation of tetraketide **92** and the predicted order of domain reactivity is shown in Figure 3-9. The first step is chain extension catalyzed by the KS domain to furnish ACP-bound intermediate **110**. We hypothesized that MT would be the first domain to react for two reasons. First, methylation has been shown to occur in pyrone formation (**96** and **97**) when LovC was not present (Figure 3-6). This indicates that methylation should occur before enoyl reduction. Second, electrophilic methylation by SAM at the α position of β-keto-thioester **110** would be much more favorable as the pK_a of the alpha proton is much lower than if enoyl reduction had occurred (~13[164] vs ~26[165] in DMSO). One interesting implication of methylation being the first tailoring domain to act on intermediate **110**, is that the stereochemistry of the methyl group would be set by the *trans*-ER and not the MT. This makes sense as beta-keto thioesters can readily epimerize in water due to rapid keto/enol tautomerization.[42]

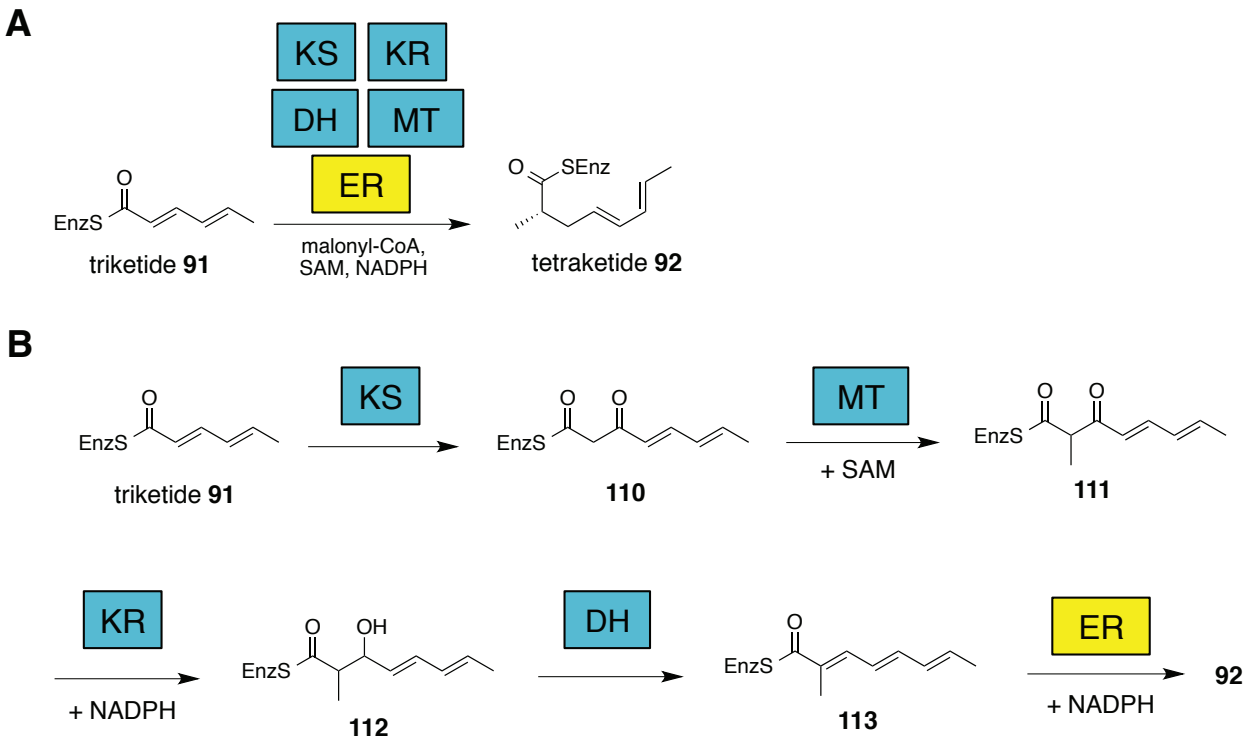

Figure 3-9. Role of MT domain in synthesis of **92**. A) Overall transformation of triketide **91** to **92**. B) Predicted order of reactivity and substrates for each domain in the biosynthesis of **92**.

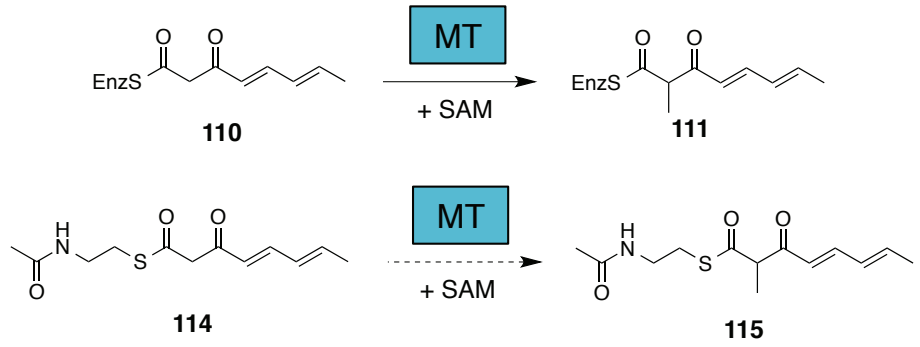

Scheme 3-1. Hypothesized reactions catalyzed by the LovB MT domain. Top: Biological reaction catalyzed by MT. Bottom: hypothesized reaction as SNAC esters.

3.2.2 Synthesis of 115, product standard of LovB MT tetraketide assay

Armed with a hypothesis of what the substrate for the MT assay might be, we sought to synthesize **110** and **111** as SNAC esters, which would mimic the phosphopantetheinyl arm for recognition by the domains of LovB (Scheme 3-1, more in Chapter 2). Drew Hawranik, a previous member of our group, synthesized **114**, while I synthesized the methylated standard **115**. The synthetic scheme can be found in Scheme 3-2.

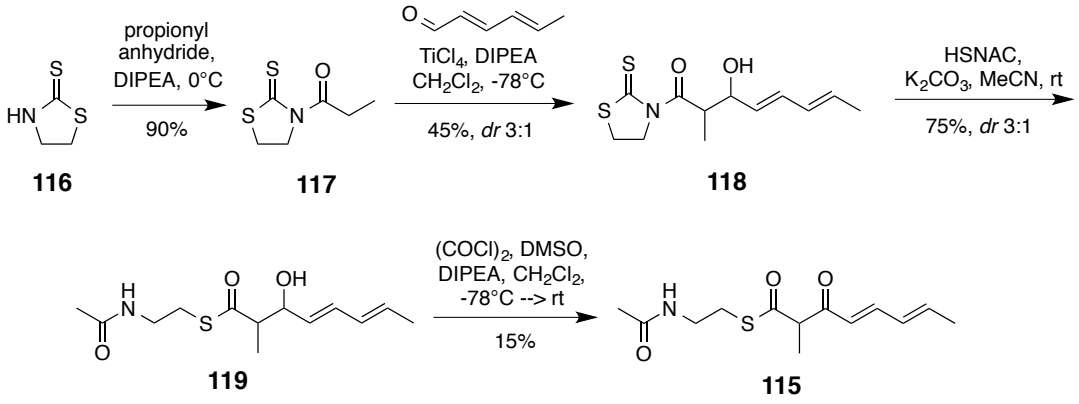

Scheme 3-2. Synthesis of tetraketide SNAC ester **115** product standard

The strategy used to assemble methylated tetraketide **115** was developed in part by Dr. Zhizeng Gao to synthesize α-methyl-β-hydroxy-SNAC thioesters for hypothemycin biosynthesis.[87] In that synthesis, he used Crimmins' chiral auxiliary[166] to obtain the diastereomers required for the enzymatic assay. One important difference in the synthesis of **115** is that no stereoselectivity is needed for this synthesis as the product rapidly epimerizes through enol/keto tautomerization. This meant that one could use a simpler version of the chiral auxiliary **116**, referred to as the 'Crimmins core', to make the synthesis more cost-effective. Starting from thiazolidine-2-thione **116**, propionylation in the presence of propionic anhydride and a weak base

allowed for the facile synthesis of **117**. Synthesis of **118** was achieved using a titanium-catalyzed aldol reaction using the propionyl Crimmins core as a titanium enolate with $TiCl_4$ and diisopropylethylamine (DIPEA) and the commercially available (2*E*,4*E*)-2,4-hexadienal as the electrophile. This resulted in β-hydroxy-amide **118** with the amide bond reacting as an activated carbonyl that could be readily converted to the SNAC ester **119** at room temperature in 86% yield. The SNAC ester **119** was oxidized to the β-keto SNAC ester **115** using Swern conditions. The oxidation of β-hydroxy-SNAC esters to their β-keto derivatives are notoriously low yielding[167], presumably due to β-elimination to furnish the conjugated, substituted triene SNAC.

3.2.3 Testing of tetraketide SNAC 114 with LovB and SAM

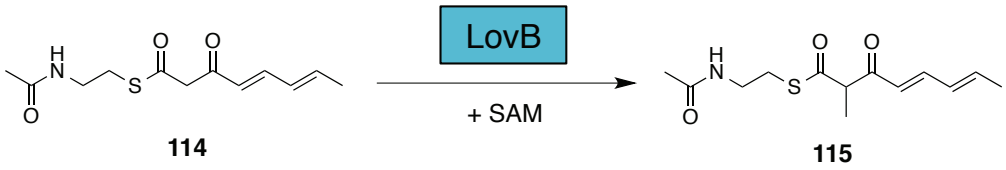

Figure 3-10. Transformation of SNAC-tetraketide **114** to **115** by LovB. The DH and KR domains were rendered unable to function due to the lack of NADPH.

With the substrate and expected products available, our collaborators were able to determine if the MT domain (and LovB in general) could transform SNAC ester **114**. Gratifyingly, LovB was able to methylate **114** and produce a compound with the same mass and chromatographic properties as synthetic standard **115** (Figure 3-10). This success prompted us to design substrates to determine the basis for recognition by the MT domain. A simplified tetraketide **120** was designed to test if functionality was a determining factor (Figure 3-11).

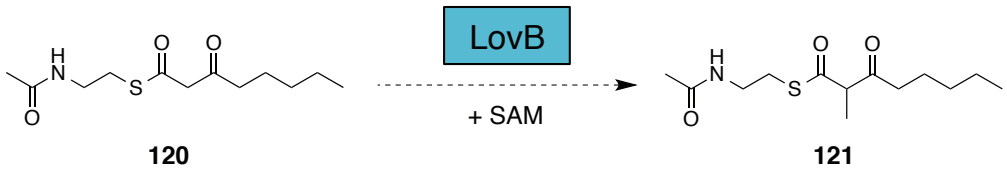

Figure 3-11. Proposed transformation of simplified tetraketide **120** to **121** by LovB and SAM co-factor.

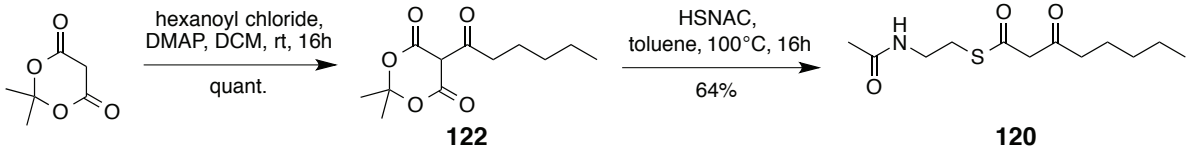

Scheme 3-3. Synthesis of **120** using acylated Meldrum's acid and HSNAC

Scheme 3-3 depicts the synthetic strategy for assembling the simplified MT substrate **120**. Acylating and heating Meldrum's acid in the presence of a nucleophile assembles SNAC ester **120** in a manner similar to **61** in Chapter 2. This convenient synthesis allowed for the rapid assembly of the substrate **120**. The methylated standard **121** was assembled using similar methodology in Scheme 3-2 and can be seen in Scheme 3-4. Using propionylated Crimmins core **117**, the β-hydroxy amide **123** can be synthesized using titanium chloride aldol conditions seen previously. The core can then be displaced with SNAC to yield **124** and the hydroxyl group was oxidized to β-keto thioester **121** using Dess-Martin periodinane (DMP).

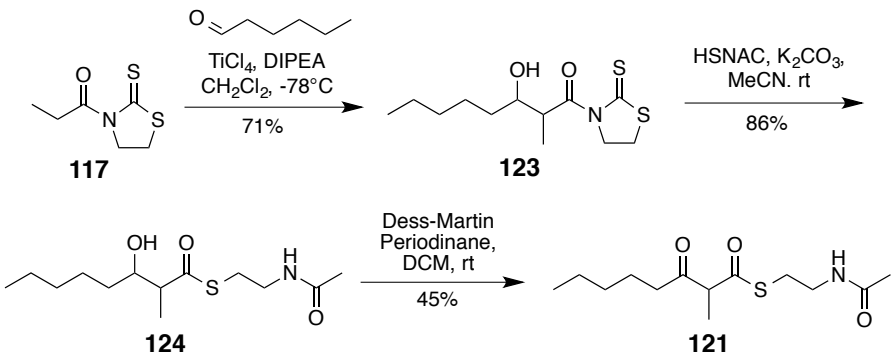

Scheme 3-4. Synthesis of simplified tetraketide SNAC ester standard **121** using titanium enolate-aldol chemistry.

3.2.4 Testing simplified tetraketide SNAC 120 and expanding the substrate scope of LovB-MT

Simplified tetraketide substrate **120** and product standard **121** were sent to our collaborators at UCLA for *in vitro* testing. Using the same assay as in Figure 3-10, LovB-MT was able to transform **120** to **121** although a much slower conversion rate was observed. With this result, we set out to determine the selectivity of the MT domain for other polyketide stages (triketide **91** and pentaketide **93**). We predicted that the MT domain would exhibit selectivity for the tetraketide substrate over premature or later stages (Figure 3-12). We made this prediction because in all *in vitro* studies of LovB, no products have been found with an unusual methylation pattern. If this hypothesis were true, it would provide convincing evidence for a substrate length-based selectivity rather than specific functionality recognition. Conveniently, the synthesis of tetraketide SNAC ester **114** provided a platform for the syntheses of multiple SNAC esters, including natural triketide SNAC **125** and product standard **126** as well as part of the synthesis of pentaketide SNACs **129** and **131**, and standards **130** and **132**.

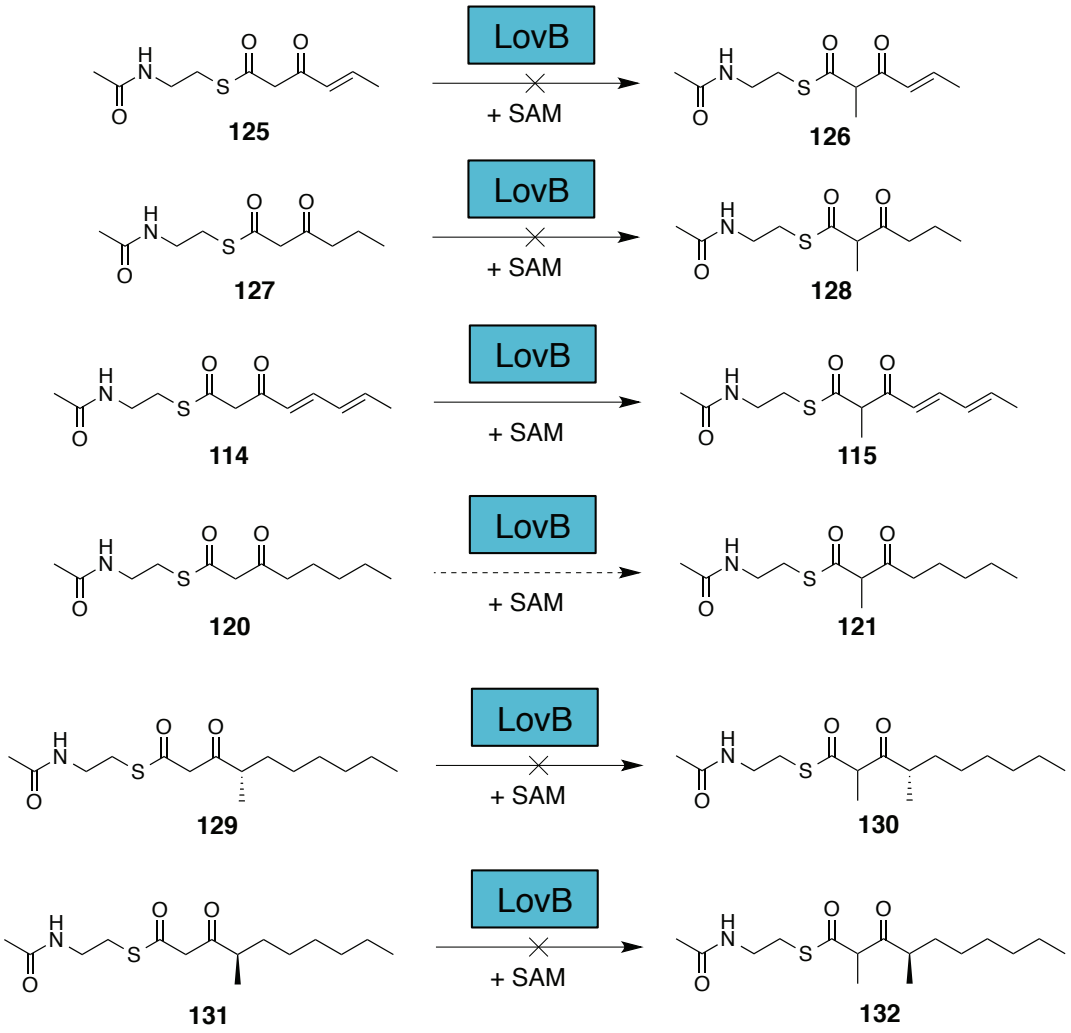

Figure 3-12. Evaluation of possible substrates for the MT domain of LovB. Pictured are the triketide SNAC esters **125** and **127** and their expected products **126** and **128**, the tetraketide SNAC esters **114** and **120** and their products **115** and **121** and the simplified pentaketide substrates with natural (**129**) and unnatural (**131**) stereochemistry. Dashed arrows depict our prediction for LovB MT activity while arrows with X's are reactions predicted to be unsuccessful.

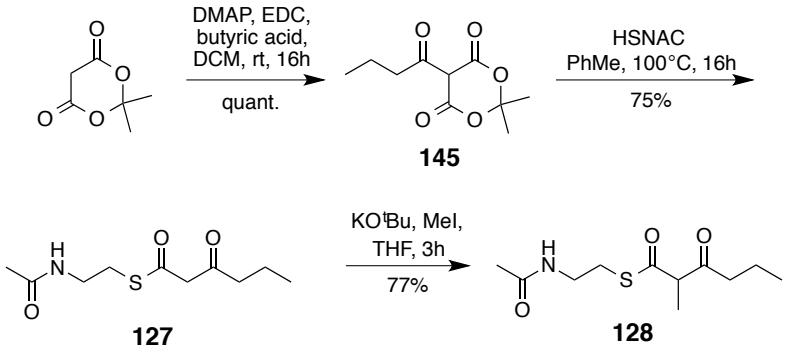

Scheme 3-5. Synthesis of simplified triketide **125** and its standard **126** by direct electrophilic methylation with methyl iodide.

Synthesis of triketide SNAC **125** and product standard **126** was easily completed using the chemistry as shown in Scheme 3-2 and Scheme 3-4. The simplified triketide **127** was synthesized using the Meldrum's acid route shown in Scheme 3-5. A more convenient route was taken to the methylated triketide by monomethylating **127** with strong base to yield **128**. Synthesis of the pentaketide SNAC with natural stereochemistry (**129**) was completed by Randy Sanichar, a current graduate student in our lab, while I finished pentaketide SNAC **131** with the unnatural stereochemistry (Scheme 3-6). Evans's chiral auxiliary was employed to generate the stereochemistry needed for the methyl group based on both its convenience and strong literature precedent.[168] Starting from (*R*)-Evans' chiral auxiliary, compound **133** was synthesized using chemistry discussed in Scheme 2-5. The acylated oxazolidinone **133** was deprotonated by sodium hexamethyldisilazane (NaHMDS) to give the *Z*-enolate selectively before methyl iodide was added as the electrophilic methyl source to yield **134**. The chiral auxiliary was removed using $LiBH_4$ to give chiral alcohol **135** that matched literature data.[169] Alcohol **135** was used in a divergent fashion to synthesize both **131** and **132** (Scheme 3-7). Oxidation of **135** to the aldehyde was facilitated in mild Swern conditions to prevent epimerization of the resultant α-methyl aldehyde. The crude aldehyde was then used immediately in a titanium-enolate aldol addition to

synthesize **137**. Transformation of **137** to **131** was then accomplished using chemistry described in previous SNAC ester syntheses in this chapter. The reactions used in the conversion of **135** to **131** were also used to synthesize the methyl standard **132**. The difference was in the titanium enolate used, using the propionylated Crimmins core instead of the acetylated.

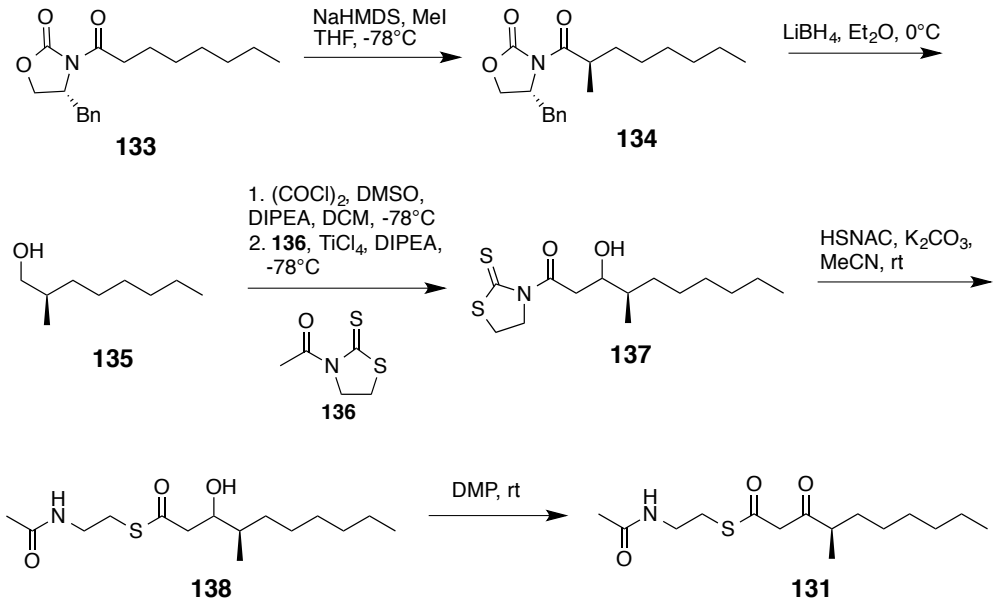

Scheme 3-6. Synthesis of pentaketide SNAC **131** (unnatural stereochemistry)

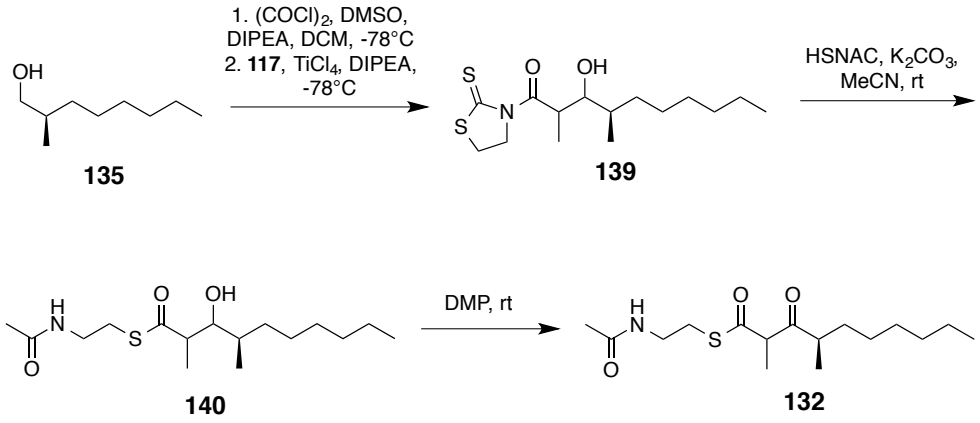

Scheme 3-7. Synthesis of pentaketide methyl standard **132** (unnatural stereochemistry) from chiral alcohol **135.**

3.2.5 Testing triketide and pentaketide SNAC esters for MT activity

At the time of writing, all substrates were synthesized and sent to UCLA for testing. In order to evaluate each substrate for activity and for ease of comparison, the turnover number (K_{cat}) and Michaelis-Menten constant (K_m) were calculated for each substrate and the specificity constant (K_{cat}/K_m) was determined. The specificity constant is used in enzyme kinetics to determine an enzyme's (or in this case catalytic domain of an enzyme) preference for one substrate over another.[170] If the specificity constant is high, this indicates tighter binding and higher turnover of that substrate. The data for the substrates that have been tested so far is found in Table 3-1.

Substrate tested	Specificity constant (nM/min)
Triketide SNAC (natural; **125**)	0.479
Triketide SNAC (simplified; **127**)	0.242
Tetraketide SNAC (natural; **114**)	1130
Tetraketide SNAC (simplified; **120**)	3.63

Table 3-1. Specificity constants for tetraketide and triketide SNAC esters tested for MT activity

A few pieces of valuable information can be gleaned from these data. First, the specificity for the natural substrate **114** is 3 orders of magnitude higher than its saturated, chain length analogue **120**. This level of discrimination indicates that there is a recognition element beyond chain length. Interestingly, the unsaturated, natural triketide SNAC substrate **125** was recognized and transformed by the MT domain, albeit at a much slower rate. This is surprising since no products of LovB, shunt or otherwise, have been found with alternative methylation. If the triketide (and possibly the pentaketide, data pending) is a substrate, then why has methylation never been observed? One theory that explains this data could be that the MT domain simply reacts faster at the tetraketide stage and is always in direct competition with the KR domain (Figure 3-13). Once the MAT and KS domain synthesize enzyme-bound intermediate **110**, two different theoretical reaction paths are possible (black and red arrows). We propose that based on kinetic data and selectivity constant, methylation occurs first (black arrows). The ketoreductase can then reduce the beta-ketone to yield **112** after methylation has occurred. If the KR reduces the beta-ketone of **110** to the hydroxyl group first, methylation may no longer be viable due to the rise in pKa of the α-protons (red arrows; Figure 3-13). The KR domain must compete with the MT domain at every ketide stage in **87** production and the MT is simply faster at the

tetraketide stage. This data could provide the first substantial evidence for a kinetic basis of selectivity for iterative PKS domains.

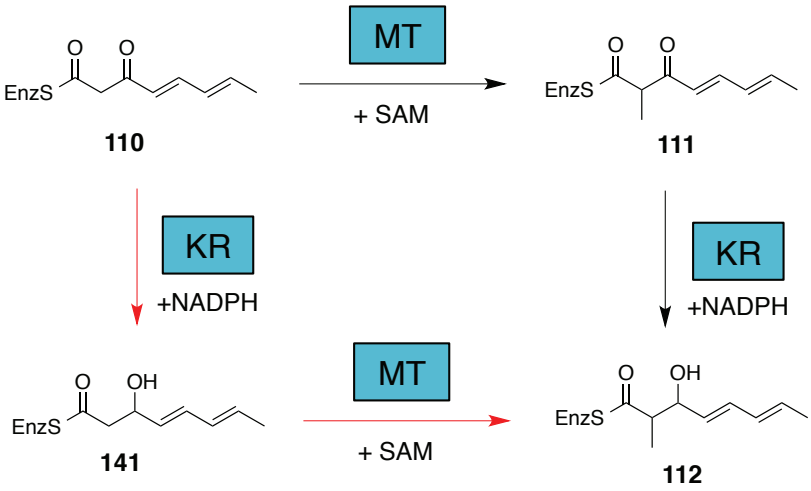

Figure 3-13. Competition between KR and MT domain at tetraketide **(92)** formation by LovB. Red arrows indicate reaction path where KR operates first and MT second while the black arrows indicate methyl transfer first and reduction second.

3.3 Conclusions

The biosynthetic machinery of lovastatin (**81**) is arguably the most thoroughly studied of all known fungal polyketides. Notably missing from our knowledge of fungal polyketide biosynthesis (including **81**) is a detailed understanding of how the iterative PKS enzymes operate. The basis for the selective activity of each domain has perplexed natural product biologists and chemists since the discovery of 6-MSA synthase in 1970.[52] This chapter provides evidence for the kinetic basis for reactivity of each domain. The theory emerging from this chapter is that the ACP carrying the growing polyketide chain doesn't selectively shuttle the growing chain to the domains in the correct order, but may actually sample all of them. The selectivity may arise from substrate recognition and the fastest reaction simply occurs first. Our collaborators working in the Tang lab at UCLA are testing this hypothesis using a LovB-DH^0 mutant that has functioning MT and KR domains but is unable to process the intermediates further due to an inactive DH domain (Figure 3-14). Luckily, all of the product standards required for these assays are intermediates in previous syntheses. These studies are ongoing and early results corroborate well with this theory.

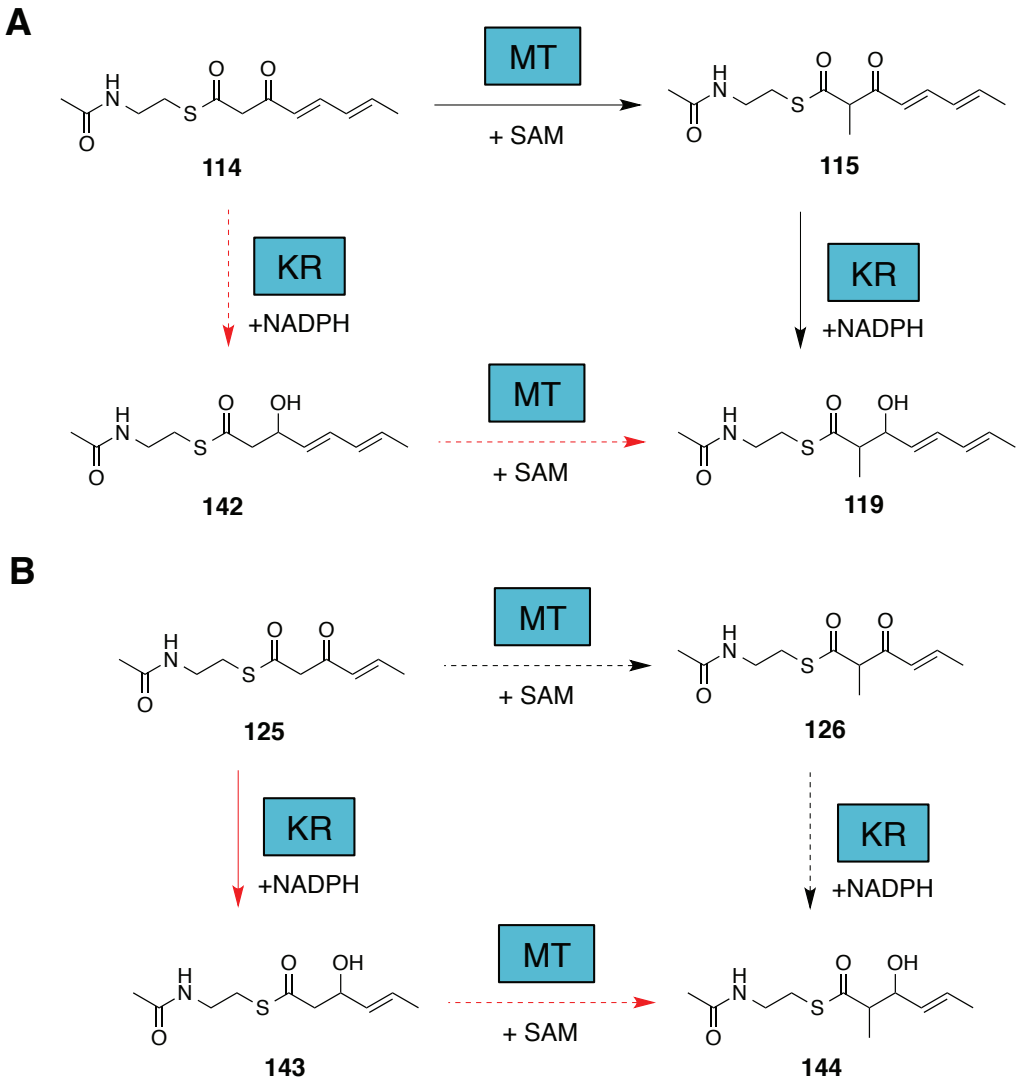

Figure 3-14. Outline of two MT/KR competition assays with LovB-DH^0 AND NADPH, SAM. **A)** Tetraketide SNAC substrate **114** with the three possible products. LC-MS will be used to analyze enzyme extracts for the accumulation of any intermediates. **B)** Triketide SNAC **125** and possible products of MT/KR competition assay. The predicted accumulated product will be **143** as methylation occurs slowly and the reduction by the KR is predicted to be much faster. All products are intermediates in syntheses discussed in this chapter and have been sent for testing.

Although we have made strides in understanding how iterative MT domains work, many questions remain. What is the recognition element that differentiates the natural tetraketide SNAC **114** from the chain length analogue **120**? In that vein, can we reprogram the MT domain to outcompete the KR domain and methylate the growing polyketide more than once? How will

this change affect DML (**87**) biosynthesis (especially the Diels-Alder cyclization)? Does this rule of kinetic selectivity apply to other domains, such as the *trans*-ER and the DH? Understanding the full scope of this theory could be the key to unlocking the genetic engineering potential of iterative PKS systems.

4 Experimental Procedures

4.1 General experimental

4.1.1 Solvents, Reagents and Solutions

All reactions involving air or moisture sensitive reactants were conducted under a positive pressure of dry argon. All solvents, chemicals, biochemicals, and reagents were reagent grade and used as supplied unless otherwise stated. For anhydrous reactions, solvents were dried according to the procedures detailed in Armarego and Chai.[171] Tetrahydrofuran and diethyl ether were distilled over sodium and benzophenone under at atmosphere of dry argon. Acetonitrile, dichloromethane, methanol were distilled over calcium hydride. Triethylamine, DMSO, pyridine were dried over 4Å MS. Solvent removal was achieved under reduced pressure with a diaphragm pump attached to a Büchi rotary evaporator and finished with a high-powered vacuum, unless the compound was considered volatile. Reagents were purchased from Sigma-Aldrich unless indicated. Deionized water was obtained from a Milli-Q reagent water system (Millipore Co., Milford, MA). Unless otherwise specified, solutions of NH4Cl, NaHCO3, HCl, NaOH, and Na2S2O3 refer to aqueous solutions. Brine refers to a saturated solution of NaCl. All reactions and fractions from column chromatography were monitored by thin layer chromatography (TLC). Compounds were visualized by exposure to UV light and by dipping the plates in 1% $Ce(SO_4)_2 \cdot 4H_2O$ 2.5% $(NH_4)Mo_7O_{24} \cdot 4H_2O$ in 10% H_2SO_4 followed by heating with a heat gun. Flash chromatography was performed according to the method of Still et al.[172] on silica gel (EM Science, 60Å, 230-400 mesh).

4.1.2 Characterization and instrumentation

Optical rotations were measured on Perkin Elmer 241 polarimeter with a microcell (10 cm, 1 mL) at 23°C unless otherwise specified. Nuclear magnetic resonance (NMR) spectra were obtained on Varian Inova 400, Varian DD2 400, Varian 500 (equipped with cryo-probe) or Varian VNMRS 600 MHz. ^{1}H NMR chemical shifts are reported in parts per million (ppm) using the residual proton resonance of solvents as reference: $CDCl_3$ δ 7.26, and CD_2Cl_2 δ 5.32. ^{13}C NMR chemical shifts are reported relative to $CDCl_3$ δ 77.0 or CD_2Cl_2 δ 53.8. Infrared spectra (IR) were recorded on a Nicolet Magna 750 or a 20SX FT-IR spectrometer. Film Cast refers to the evaporation of a solution on a NaCl plate. Mass spectra were recorded on a Kratos IMS-50 (high resolution, electron impact ionization (EI)), and a Agilent Technologies 6220 oaTOF (high resolution, electrospray (ESI)).

4.2 Biological procedures

4.2.1 Whole-cell isotopic labeling with *A. clavatus*

A. clavatus T2 is inoculated in fresh PD medium (4 × 50 mL), and incubated in a closed system at 30°C. The closed system is connected via Tygon tubing to a water trap (to remove condensation), a stirring 3M KOH trap (to remove excess CO_2) and an aquarium pump (controlled by a Variac, 3-5 V). A pressure- equalizing burette containing (0.5 g/L $CuSO_4$ is filled with either $^{16}O_2$ or $^{18}O_2$ to create a slightly over-pressurized system. As the oxygen is consumed, more is added. In the first 24 h of growth 50 ml $^{16}O_2$ consumed. In the following 49 h, 1130 ml $^{18}O_2$ is consumed, and finally, 170 ml $^{16}O_2$ is consumed in the final 14 h. **5** is isolated by EtOAc extraction and SiO_2 gel chromatography (97:3 CH_2Cl_2-MeOH), and characterized by ^{1}H-NMR and ^{13}C-NMR.

4.2.2 Isolation of cytochalasin D (7) from *Zygosporium masonii*

The producer organism, *Z. masonii*, was obtained from the University of Alberta Microfungus Collection and Herbarium (UAMH) as a frozen mycelia suspension (1 mL). This was thawed, and transferred to a potato-dextrose-agar (PDA) petri dish (~10 mL), and maintained at room temperature for several days. Upon sporulation of the organism on solid media, a swab of the spores was transferred into freshly autoclaved potato-dextrose (PD) liquid medium (2x25 mL in 125 mL flasks). These were incubated at 27 °C, with shaking at 225 rpm for seven days, at which point white spheres representing the organism were observed in the flask. These were transferred aseptically into large flasks (2x500 mL) containing autoclaved PD liquid medium and shaken at 225 rpm and 27 °C for 10-12 days. The cultures (including media) were pulverized in a Waring blender and then stirred with an equal volume of ethyl acetate (EtOAc) for 2 h at 4 °C. This mixture was filtered through cheesecloth, and the organic and

aqueous layers were separated. The aqueous layer was washed with one volume of EtOAc, and the combined organic layers were dried with brine (one volume) and then over anhydrous Na_2SO_4. The drying agent was filtered and the organic layer was evaporated to give the crude extract. For larger amounts of crude extract, cytochalasin D could be crystallized directly from acetone. Smaller amounts were purified by consecutive columns of silica-gel chromatography, eluted by 97:3 CH_2Cl_2:MeOH followed by 1:1 EtOAc:hexanes. 1M H_2SO_4 was used as a TLC stain and an orange colour was observed. The title product was isolated as a white solid (31-70 mg/L yield), and spectra were consistent with literature.

4.2.3 *In vitro* isotopic labeling of 24 by CcsB

CcsB was obtained as a frozen stock solution from our collaborators in Prof. Yi Tang's lab at UCLA. CcsB was heterologously expressed and purified according to Hu et al.[116] CcsB stock solution (50 µL) was thawed before use. The assay conditions were as follows: 50 mM phosphate buffer (pH = 7), 0.4 mM ketocytochalasin (**23**), 20 µL FAD, 1.6 mM NADPH, and 10 µM CcsB with a final volume of 100 µL. The assay was conducted at 28°C in an eppendorf tube within a custom built apparatus sealed in an atmosphere of ~60% $^{18}O_2$ and ~40% $^{16}O_2$ gas. After 2 hours, the reaction was terminated with 100 µL of MeOH and was extracted twice with 200 µL of hexanes. The organic layer was removed, dried and reconstituted in 60 µL of MeOH for liquid chromatography-mass spectrometry (LC-MS). LC-MS was conducted with both positive and negative ionization modes with a Phenomenex Luna 5 µm, 2.0 mmx100mm C18 reverse phase column. Samples were separated on a linear gradient of 5% acetonitrile (0.1% formic acid) to 95% acetonitrile (0.1% formic acid) at a flow rate of 0.1 mL/min.

4.3 Synthesis and characterization

Characterization of cytochalasin D (7) isolated from *Z. masonii*

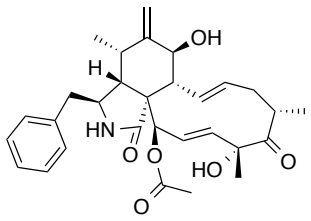

White solid; $[\alpha]_D$ -31.34 (c = 4.90, $CHCl_3$). IR ($CHCl_3$, cast): 3416, 2969, 2938, 1739, 1702, 1690 cm^{-1}. ^{1}H-NMR (600 MHz, $CDCl_3$): δ (ppm) 7.31 (d, 2H, *J* = 7.6 Hz), 7.26 (s, 1H), 7.24 (s, 1H), 7.14-7.12 (m, 2H), 6.11 (dd, 1H, *J* = 15.8, 2.7 Hz), 5.69 (dd, 1H, *J* = 15.6, 9.8 Hz), 5.63 (app t, 1H, *J* = 2.5 Hz), 5.50 (s, 1H), 5.36-5.30 (ddd, 1H, *J* = 15.8, 10.2, 5.2 Hz), 5.29 (d, 1H, *J* = 1.7 Hz), 5.14 (dd, 1H, *J* = 15.8, 2.3 Hz), 5.08 (s, 1H), 4.62 (br s, 1H), 3.81 (dd, 1H, *J* = 10.5, 0.8 Hz), 3.23 (dt, 1H, *J* = 8.8, 4.2 Hz), 2.87-2.79 (m, 2H), 2.75-2.71 (m, 2H), 2.67 (dd, 1H, *J* = 13.4, 9.4 Hz), 2.51 (app q, 1H, *J* = 11.3 Hz), 2.25 (s, 3H), 2.15 (dd, 1H, *J* = 5.1, 3.4 Hz), 2.03-2.00 (m, 1H), 1.50 (s, 3H), 1.19 (d, 3H, *J* = 6.9 Hz), 0.95 (d, 3H, *J* = 6.7 Hz) ^{13}C-NMR (125 MHz, $CDCl_3$): δ (ppm) 210.2, 173.6, 169.7, 147.6, 137.3, 134.3, 134.1, 132.3, 130.7, 129.1, 129.0, 127.6, 127.1, 114.5, 77.7, 69.9, 53.5, 53.3, 50.1, 47.0, 45.4, 42.4, 37.8, 32.7, 29.7, 24.2, 20.8, 19.4, 13.7. HRMS (ESI) Calcd for $C_{30}H_{38}NO_6$ 508.2694, found 508.2694 $[M+H]^+$.

Synthesis of desacetyl-cytochalasin D (21)

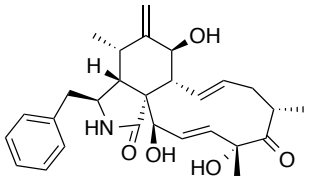

A fresh solution of NaOMe in methanol (1M) was prepared by dissolving hexanes-washed sodium (23 mg) in dry methanol (1 mL) at 0 °C. To a solution of cytochalasin D (41 mg, 0.081 mmol) in dry methanol (2 mL) was added NaOMe (45 mL of 1M solution), which was stirred at room temperature for 2 hours. When the reaction was deemed complete by TLC, the mixture was quenched with an equal amount of HCl (45 ml of a 1M solution) and the solvent was removed under reduced pressure. The residue was taken up in $CDCl_3$, dried over Na_2SO_4 and analyzed by NMR. The crude colourless oil was used immediately without further purification (36 mg, 97%). $[\alpha]_D$ = -21.51 (c 4.80, $CHCl_3$). IR ($CHCl_3$, cast): 3400.1, 3086.0, 3062, 2967, 2932, 2851, 1700, 1686 cm^{-1}. ^{1}H-NMR (500 MHz, $CDCl_3$): δ (ppm) 7.35 (t, 2H, *J*=7.3 Hz), 7.25-7.23 (m, 1H), 7.16 (d, 2H, *J*=7.0 Hz), 6.26 (dd, 1H, *J* = 15.9, 2.6 Hz), 5.71 (dd, 1H, *J* = 15.8, 9.0 Hz), 5.45 (dd, 1H, *J* = 15.9, 2.3 Hz), 5.38 (br s, 1H), 5.36-5.32 (m, 1H), 5.31 (ddd, 1H, *J* = 15.3, 10.2, 4.8 Hz), 5.17-5.12 (m, 1H), 4.67 (br s, 1H), 4.14-4.10 (m, 1H), 3.83 (d, 1H, *J* = 11.2 Hz), 3.23 (app dt, 1H, *J* = 8.7, 4.1 Hz), 2.97-2.90 (m, 2H), 2.87 (app t, 1H, *J* = 10.2 Hz), 2.81-2.72 (m, 1H), 2.65-2.58 (m, 2H), 2.53 (app q, 1H, *J* = 11.9 Hz), 2.05 (dd, 1H, *J* = 13.0, 5.2 Hz), 1.58 (s, 3H), 1.23 (d, 3H, *J* = 6.9 Hz), 1.15 (d, 3H, *J* = 6.7 Hz). ^{13}C-NMR (100 MHz, $CDCl_3$): δ (ppm) 210.2, 174.9, 148.1, 137.3, 137.0, 133.7, 131.1, 129.2, 128.9, 127.2, 127.1, 114.1, 77.8, 76.6, 69.7, 54.2, 53.5, 50.2, 45.7, 45.4, 42.4, 37.7, 32.9, 24.3, 19.4, 13.9. HR-MS (ESI) Calcd for $C_{28}H_{36}NO_5$ 488.2407, found 488.2399 $[M+Na]^+$.

Synthesis of ketocytochalasin D (22)

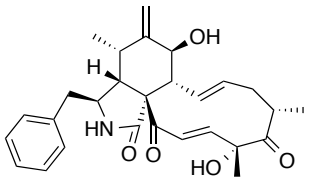

To avoid over oxidation during this reaction, careful NMR analysis was used to monitor reaction progress. Specifically, the doublets corresponding to the hydrogen atoms attached to C20 and C19 of the starting material (6.22 and 5.45 ppm respectively) were followed. In the desired product these peaks shifted to 6.97 and 6.35 ppm. Over-oxidation resulted in a slight upfield shift of these signals. **21** (19 mg, 0.04 mmol) was dissolved in CD_2Cl_2 (2 mL), in a dried round bottom flask (5 mL). A solution of Dess-Martin periodinane (17 mg, 0.04 mmol) in CD_2Cl_2 (1 mL) was also prepared. Aliquots (0.1-0.2 mL) of the periodinane were added to Zygosporin D and stirred at room temperature. The reaction progress was monitored by NMR spectroscopy every 30-60 minutes, and more periodinane was added until reaction progress showed 50-65% completion (further reaction resulted in doubly-oxidized product which is difficult to separate). The reaction was quenched with isopropanol (0.5 mL) and evaporated under reduced pressure. The residue was directly purified by silica gel chromatography, using an eluent of 1:1 hexanes:EtOAc. The title product was obtained as a white solid (8.7 mg, 47%). Compound **22** appears as a single, purple spot on thin layer SiO_2 plate stained with H_2SO_4 (1 M) (R_f = 0.4, 5% MeOH in CH_2Cl_2). $[\alpha]_D$ -40.22 (*c* 0.87, $CHCl_3$). IR ($CHCl_3$): 3417, 3292, 2969, 2933, 1685, 1619, 1454, 1375, 1015, 754 cm^-1; ^{1}H-NMR (600 MHz, $CDCl_3$): δ (ppm) 7.32 (t, 2H, *J* = 7.5 Hz), 7.25 (t, 1H, *J* = 7.4 Hz), 7.12 (d, 2H, *J* = 7.0 Hz), 6.97 (d, 1H, *J* = 15.7 Hz), 6.35 (d, 1H, *J* = 15.7 Hz), 5.80 (ddd, 1H, *J* = 15.5, 9.8, 0.9 Hz), 5.58 (br s, 1H), 5.25 (s, 1H), 5.19 (ddd, 1H, *J* = 15.5, 10.9, 4.7), 5.08 (s, 1H), 4.71 (br s, 1H), 4.06 (d, 1H, *J* = 10.1 Hz), 3.34-3.28

(m, 1H), 3.24 (dd, 1H, J = 5.9, 2.4 Hz), 2.83-2.75 (m, 1H), 2.72 (ddd, 1H, J = 10.9, 6.8, 1.3 Hz), 2.67 (dd, 1H, J = 13.4, 5.5 Hz), 2.57 (dt, 1H, J = 13.1, 11.0 Hz), 2.46 (dd, 1H, J = 13.3, 8.9 Hz), 2.41 (app t, 1H, J = 9.9 Hz), 2.12-2.07 (m, 1H), 1.64 (s, 3H), 1.21 (d, 3H, J = 6.8 Hz), 1.00 (d, 3H, J = 6.7 Hz). ^{13}C-NMR (125 MHz, $CDCl_3$): δ (ppm) 209.9, 197.4, 172.7, 148.5, 143.3, 137.0, 135.0, 134.3, 129.8, 129.3, 128.9, 127.0, 114.4, 78.6, 71.5, 64.1, 53.1, 51.7, 45.2, 44.2, 42.9, 38.3, 31.6, 23.6, 19.8, 13.0. HRMS (ESI) calcd for $C_{28}H_{33}NO_5Na$ 486.2241, found 486.2251 $[M+Na]^+$.

Diethyl 2-(2,2-dimethyl-4,6-dioxo-1,3-dioxan-5-yl)-2-oxoethylphosphonate (65)

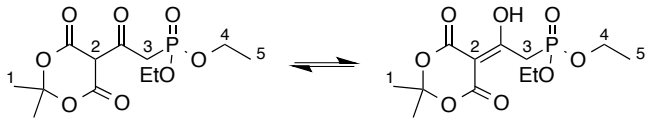

The known compound **65**[173] was prepared by a different procedure. Freshly recrystallized Meldrum's acid (0.721 g, 5 mmol), diethyl phosphonoacetic acid (0.981 g, 5 mmol) and dimethylaminopyridine (DMAP, 0.671 g, 5.5 mmol) were dissolved in dry CH_2Cl_2 (13 mL) and stirred at room temperature for 5 minutes under Ar. 1-Ethyl-3-(3-dimethylaminopropyl)carbodiimide (EDC, 0.940 g, 5 mmol) was then added in one portion and the reaction was stirred at room temperature for 16h in which time a change in colour from colourless to bright yellow was noted. The solution was quenched with 1M HCl (25 mL), the layers were separated and the aqueous was extracted (3 x 20 mL CH_2Cl_2). The organic layers were pooled, washed with brine and dried over anhydrous Na_2SO_4. The solvent was removed *in vacuo* to yield a crude yellow oil that was used immediately without purification (1.602g, quant.). (0:100 keto:enol) ^{1}H NMR (500 MHz, CD_2Cl_2) δ 4.11 (dq, 4H, *J* = 8.3, 7.1 Hz, H4), 3.86 (d, 1H, *J* = 23.9 Hz, H3), 1.71 (s, 6H, H1), 1.28 (td, 2H, *J* = 7.1, 0.6 Hz, H5). ^{13}C NMR (126 MHz, CD_2Cl_2) δ 187.8, 105.6, 93.7, 63.3, 34.8 (d, *J* = 126.5 Hz), 27.0, 16.5.

***S*-2-acetamidoethyl-4-(diethoxyphosphoryl)-3-oxobutanethioate (61)**

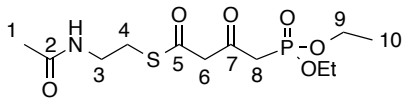

Compound **65** (0.502 g, 1.55 mmol) and *N*-acetylcysteamine (0.25 mL, 2.23 mmol) were dissolved in dry toluene (10 mL) and heated to 100 °C for 16h. The solvent was removed *in vacuo* and the crude oil was subjected to flash column chromatography. Eluting with EtOAc first, then 10% MeOH in EtOAc yielded the correct product as a slightly yellow oil (0.635 g, 41%). The title compound was isolated as a single spot on a SiO_2 TLC plate (R_f = 0.6, 5:1 EtOAc:MeOH). IR ($CHCl_3$, cast) 3294, 2984, 2932, 1726, 1675, 1250, 1025 cm^{-1}; ^1H NMR (600 MHz, CD_2Cl_2) δ 6.81 (s, 1H, NH), 5.60 (d, 0.4H, *J* = 3.1 Hz, enol-H6), 4.15 – 4.03 (m, 4H, H9), 3.89 (s, 1.6H, keto-H6), 3.36 (q, 2H, *J* = 6.5 Hz, H3), 3.20 (d, 1.6H, *J* = 22.5 Hz, keto-H8), 3.04 (t, 2H, *J* = 6.6 Hz, H4), 2.74 (d, 0.4H, *J* = 22.3 Hz, enol-H8), 1.89 (s, 3H, H1), 1.33 – 1.25 (m, 6H, H10); ^{13}C NMR (151 MHz, CD_2Cl_2) δ 197.1, 196.7 (d, J = 6.3 Hz), 194.3, 172.9, 172.9, 170.0, 104.2 (d, J = 7.6 Hz), 65.4 (d, J = 6.5 Hz), 60.5, 45.1 (d, J = 126.7 Hz), 41.8, 41.3, 36.1 (d, J = 135.1 Hz), 31.9, 30.7, 25.4, 25.3, 18.8, 18.8, 18.7; HR-MS (ESI) Calcd for $C_{12}H_{22}NO_6PSNa$ 362.0798, found 362.0793.

(*R*)-4-Benzyl-3-((*S*)-2-methyl-4-pentenoyl)-2-oxazolidinone (67):

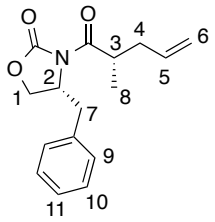

(*R*)-4-benzyl-3-propionyl-oxazolidinone (9.14 g, 39.2 mmol) was dissolved in dry THF (110 mL) and cooled to -78 °C using a dry ice/acetone bath. Sodium hexmethyldisilazide (NaHMDS, 41.2 mL, 1M) was added dropwise via addition funnel and the mixture was stirred at -78 °C for 15 min. Allyl iodide (5.38 mL, 58.8 mmol) was added dropwise at -78 °C and the reaction was allowed to warm to room temperature over 16h. The reaction was quenched with NH_4Cl (50 mL) and the aqueous and organic were separated. The aqueous was extracted with ether (3 x 50 mL) and the organic was combined and washed with brine. Drying over anhydrous Na_2SO_4 and removing the solvent *en vacuo* yielded a crude yellow-orange oil. Purification on flash column chromatography (SiO_2, 9:1 hexanes/EtOAc) yielded a pure yellow oil (4.12 g, 39%). $[\alpha]_D$ = -38.5 (*c* 1.0, $CHCl_3$); ref $[\alpha]^{20}_D$ = -39.0 (c 1.0, $CHCl_3$)[174]; IR ($CHCl_3$, cast) 3029, 3063, 2978, 2935, 1780, 1699, 1640, 1604, 1583 cm^{-1}; ^1H NMR (600 MHz, $CDCl_3$) δ 7.36 – 7.30 (m, 2H, H10), 7.30 – 7.24 (m, 1H, H11), 7.24 – 7.19 (m, 2H, H9), 5.83 (ddt, *J* = 17.2, 10.1, 7.0 Hz, 1H, H5), 5.14 – 5.03 (m, 2H, H6), 4.68 (ddt, *J* = 9.8, 7.6, 3.2 Hz, 1H, H2), 4.22 – 4.12 (m, 2H, H1), 3.87 (dq, *J* = 6.8, 6.8 Hz, 1H, H3), 3.29 (dd, *J* = 13.4, 3.4 Hz, 1H, H7), 2.70 (dd, *J* = 13.4, 9.9 Hz, 1H, H7'), 2.53 (dtt, *J* = 13.7, 6.8, 1.3 Hz, 1H, H4), 2.28 – 2.20 (m, 1H, H4'), 1.19 (d, *J* = 6.8 Hz, 3H, H8); ^{13}C NMR (151 MHz, $CDCl_3$) δ 176.54, 153.14, 135.41, 135.30, 129.44, 128.97, 127.35, 117.24, 77.27, 77.06, 76.85, 66.05, 55.43, 38.15, 38.02, 37.20, 16.47. HRMS (ESI) Calcd for $C_{16}H_{19}NO_3Na$ $([M+Na])^+$ 296.1262, found 296.1253.

(*S*)-2-methyl-4-pentenol (68):

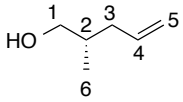

This known product was prepared according to a previously published procedure.[135] Absolute EtOH (1.06 mL, 18.2 mmol) and **67** (4.12 g, 15.1 mmol) were dissolved in dry ether (120 mL) and cooled to 0 °C using an ice-water bath. $LiBH_4$ (9.12 mL, 2M) was added dropwise via syringe and the temperature was maintained 0 °C for 1.5h. The reaction was quenched with 1M NaOH (60 mL) and stirred until the solution was clear. The layers were separated and the aqueous was extracted with ether (3 x 60 mL). The organic was pooled, washed with brine and dried over anhydrous Na_2SO_4. The organic solvent was removed *in vacuo* to yield a clear, colourless, volatile oil. The crude was subjected to flash column chromatography (SiO_2, 1:1 pentanes/ether) and used immediately due to its volatile nature (1.40g, 93%). ^{1}H NMR (500 MHz, $CDCl_3$) δ 5.86 – 5.74 (m, 1H, H4), 5.08 – 4.97 (m, 2H, H5), 3.50 (dd, *J* = 10.6, 6.2 Hz, 1H, H1), 3.44 (dd, *J* = 10.6, 6.1 Hz, 1H, H1'), 2.21 – 2.12 (m, 1H, H3), 1.98 – 1.88 (m, 1H, H3'), 1.73 (m, 1H, H2), 0.91 (d, *J* = 6.8 Hz, 3H, H6); ^{13}C NMR (126 MHz, $CDCl_3$) δ 136.9, 116.0, 67.8, 37.8, 35.6, 16.3. MS (GC): found 82.1 (M-H_2O).

(*S*)-4-benzyl-3-((2*R*,4*S*)-2,4-dimethyl-6-heptenoyl)-2-oxazolidinone (71):

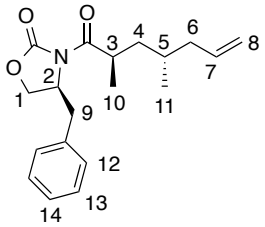

Compound **71** was synthesized using a known procedure.[136] **68** was dissolved in 30 mL dry CH_2Cl_2 and cooled to -78 °C in a dry ice/acetone bath. Dry pyridine (0.34 mL, 4.2 mmol) was added dropwise and spun at -78 °C for 10 min. Triflic anhydride (0.70 mL, 4.12 mmol) was added dropwise and the temperature was maintained until TLC analysis showed no remaining starting material (1.5 h). The reaction was quenched with dH_2O (10 mL) and the layers were separated. The aqueous was extracted with DCM (3 x 10 mL) and the organic was pooled, washed with dH_2O (2 x 20 mL), brine (20 mL) and dried over anhydrous Na_2SO_4. The solvent was removed *in vacuo* and a cloudy, crude yellow oil was found. The crude triflate was used immediately without purification. (*S*)-4-benzyl-3-propionyl-oxazolidinone (1.80 g, 7.68 mmol) was dissolved in 14 mL dry THF and cooled to -78 °C. NaHMDS (7.68 mL, 1M) was added dropwise and the reaction was maintained at -78 °C for 30 min. The colour changed from colourless to yellow. The crude triflate was dissolved in 3 mL dry THF and added dropwise to the reaction at -78 °C. The reaction was allowed to warm gradially to room temp over 16 h. The solution was quenched with slow addition of 14 mL of NH_4Cl solution. The aqueous and organic layers were separated and the aqueous was extracted with EtOAc (3 x 15 mL). The organic layers were pooled, washed with brine and dried over anhydrous Na_2SO_4. The solvent was removed *in vacuo* and the crude yellow oil was subjected to flash column chromatography (SiO_2, 10:1 hexanes/EtOAc) to yield a yellow oil (0.266 g, 24%). Compound **71** was isolated as a single spot on thin layer chromatography (SiO_2, R_f = 0.8, 2:1 hexanes:EtOAc). ^1H NMR (500 MHz,

$CHCl_3$) δ 7.32 (m, 2H, H13), 7.29 – 7.24 (m, 1H, H14), 7.23 – 7.18 (m, 2H, H12), 5.78 (ddt, *J* = 17.2, 10.2, 7.1 Hz, 1H, H7), 5.07 – 4.98 (m, 2H, H8), 4.72 – 4.64 (m, 1H, H2), 4.22 – 4.12 (m, 2H, H1), 3.93 – 3.82 (m, 1H, H3), 3.28 (dd, *J* = 13.3, 3.4 Hz, 1H, H9), 2.74 (dd, *J* = 13.3, 9.7 Hz, 1H, H9'), 2.10 (m, 1H, H6), 1.96 (m, 1H, H6'), 1.66 – 1.59 (m, 2H, H4+H5), 1.45 (m, 1H, H4'), 1.15 (d, *J* = 6.7 Hz, 3H, H10), 0.94 (d, *J* = 6.1 Hz, 3H, H11); ^{13}C NMR (126 MHz, $CDCl_3$) δ 177.6, 153.0, 137.0, 135.4, 129.4, 128.9, 127.3, 116.0, 77.3, 77.1, 76.8, 65.9, 61.3, 55.3, 49.0, 41.7, 40.2, 38.0, 38.0, 36.3, 35.3, 30.5, 19.7, 18.9, 16.7, 14.1, 7.5. HRMS (ESI): Calcd for $C_{19}H_{25}NO_3Na$ $([M+Na])^+$ 338.1727, found 338.1728.

(2*R*,4*S*)-2,4-dimethyl-6-heptenol (72):

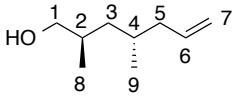

Compound **72** was prepared in the same fashion as **68** and used immediately. Compound **72** appears as a single spot on thin layer SiO_2 plates (R_f = 0.6, 2:1 hexanes/EtOAc). Yellow oil (0.105 g, 66%) ^{1}H NMR (500 MHz, $CDCl_3$) δ 5.87 – 5.74 (m, 1H, H6), 5.06 – 4.98 (m, 2H, H7), 3.55 – 3.46 (m, 1H, H1), 3.44 (dd, 1H, *J* = 10.5, 6.6 Hz, H1'), 2.06 (m, 1H, H5), 2.01 – 1.91 (m, 1H, H5'), 1.79 – 1.71 (m, 1H, H3), 1.68 – 1.60 (m, 1H, H3'), 1.31 (br s, 1H, OH), 1.17 (m, 2H, H2+H4), 0.92 (d, 3H, *J* = 6.7 Hz, H8), 0.89 (d, 3H, *J* = 6.6 Hz, H9); ^{13}C NMR (126 MHz, $CDCl_3$) δ 137.5, 115.7, 77.3, 77.0, 76.8, 69.0, 65.9, 42.3, 40.1, 33.2, 29.9, 22.3, 19.1, 16.2, 15.2, 14.1.

***tert*-Butyl((3*R*,4*S*)-2,4-dimethyl-6-heptenyloxy)dimethylsilane:**

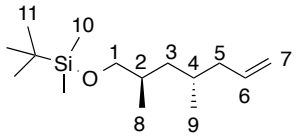

This compound was prepared using a known procedure.[175] **72** (72 mg, 0.51 mmol), *tert*-butyldimethylchlorosilane (TBDMSCl, 153mg, 1.01 mmol) and imidazole (138 mg, 2.20 mmol) were dissolved in 7 mL of dry DCM at 0°C. The reaction was allowed to warm to room temperature over 16h and the solvent was removed *in vacuo*. The crude oil was reconstituted in EtOAc (7 mL) and washed sequentially with $KHSO_4$ (1N), dH_2O, brine and dried over Na_2SO_4. The solvent was once again removed *en vacuo* and the crude colourless oil was used without purification. ^{1}H NMR (500 MHz, CD_2Cl_2) δ 5.80 (ddt, *J* = 17.3, 10.2, 7.2 Hz, 1H, H5), 5.04 – 4.93 (m, 2H, H7), 3.42 (dd, *J* = 9.7, 5.8 Hz, 1H, H1), 3.35 (dd, *J* = 9.7, 6.6 Hz, 1H, H1'), 2.07 – 1.98 (m, 1H, H5), 1.96 – 1.86 (m, 1H, H5'), 1.74 – 1.55 (m, 2H H2+H4), 1.16 (m, 1H, H3), 1.06 (m, 1H, H3'), 0.89 (s, 10H, H11), 0.87 (s, 14H, TBDMS-Cl), 0.85 (d, *J* = 2.9 Hz, 3H, H8), 0.84 (d, *J* = 3.0 Hz, 3H, H9), 0.04 (s, 6H, H10), 0.03 (s, 8H, TBDMS-Cl); ^{13}C NMR (125 MHz, CD_2Cl_2) δ 138.2, 115.5, 69.3, 42.6, 40.6, 33.6, 30.4, 26.0, 25.8, 19.3, 16.6, -2.9, -5.3.

(3*R*,5*R*)-6-(*tert*-butyldimethylsilyloxy)-3,5-dimethylhexanal (62):

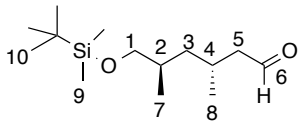

This molecule has been prepared previously in a different relative stereochemistry and by a different procedure.[176] Silyl ether-**72** (206 mg, 0.803 mmol) was dissolved in 5 mL of dry DCM and cooled to -78 °C. Ozone was bubbled through the reaction via an ozonator until the solvent turned a pale blue (~15 min) while the temperature was maintained. The voltage was turned off and pure oxygen gas was bubbled through until the colour changed back to colourless (5 min). Argon was then flushed through the system (still at -78°C) and triphenylphosphine (0.469 g, 1.79 mmol) was added. The reaction was allowed to warm to room temperature over 16 h and the DCM was subsequently removed *in vacuo*. The resulting slurry was reconstituted in pentanes and filtered. After the precipitate was washed twice with pentanes, the filtrate was decanted and the solvent was removed to yield a crude yellow oil with some white solid (PPh_3). The crude was purified using flash column chromatography (SiO_2, 3% to 20% ether in pentanes) to yield a pure clear colourless oil (145 mg, 70%). Title compound was isolated as a single spot by TLC (SiO_2, R_f = 0.5, 10% Et_2O in hexanes). $[\alpha]_D$ = 22.6 (*c* 1.1, $CHCl_3$); IR ($CHCl_3$, cast) 2956, 2929, 2857, 1728 cm^{-1}; ^1H NMR (500 MHz, CD_2Cl_2) δ 9.73 (t, *J* = 2.3 Hz, 1H, H6), 3.46 – 3.32 (m, 2H, H1), 2.36 (ddd, *J* = 16.0, 5.8, 2.1 Hz, 1H, H5), 2.24 (ddd, *J* = 16.0, 7.6, 2.5 Hz, 1H, H5'), 2.20 – 2.09 (m, 1H, H4), 1.68 (m, 1H, H2), 1.30 (ddd, *J* = 13.9, 9.4, 4.8 Hz, 1H, H3), 1.05 (ddt, *J* = 13.7, 9.3, 4.7 Hz, 1H, H3'), 0.93 (d, *J* = 6.6 Hz, 3H H8), 0.89 (s, 8H, H10), 0.87 (d, *J* = 6.6 Hz, 3H, H7), 0.04 (s, 6H, H9); ^{13}C NMR (125 MHz, CD_2Cl_2) δ 203.0, 69.0, 52.2, 41.0, 33.6, 25.9, 19.8, 18.6, 16.5, -5.3; HRMS (ESI) Calcd for C14H31O2Si 259.2088, found 259.2084 $[M+H]^+$

(2*E*,4*E*)-ethyl 4-methyl-2,4-hexadienoate (73):

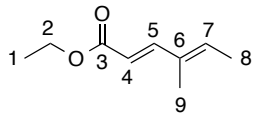

This known compound was synthesized using an established procedure.[177] Sodium hydride (2.5 g, 62.4 mmol, 60% suspension in oil) was dissolved in 0.5 L dry THF at room temperature. Triethylphosphonoacetate (10.9 mL, 59.4 mmol) was added dropwise via syringe and the reaction was maintained at room temperature for 1 h. Tiglic aldehyde (5.75 mL, 59.4 mmol) was added dropwise and the reaction was stirred for 3 h. The reaction changed colour from colourless to slightly yellow. The solution was then quenched with ~5 g of ice and left for 16 h. Water (200 mL) was added and the bulk of the THF was removed *en vacuo*. The aqueous was then washed with ether (3 x 200 mL), the subsequent organic layers were pooled and then washed with brine. Concentrating *in vacuo* yielded a yellow oil that was purified by flash column chromatography (SiO_2, 3:1 hexanes/EtOAc). The final product **73** was isolated as a yellow oil (6.53 g, 78%). IR (CH_2Cl_2, cast) 2981, 2925, 2857, 1714, 1633, 1622 cm^{-1}; ^1H NMR (500 MHz, $CHCl_3$) δ 7.31 (d, J = 15.7 Hz, 1H, H4), 6.02 – 5.93 (m, 1H, H5), 5.78 (dt, J = 15.7, 0.7 Hz, 1H, H7), 4.20 (q, J = 7.2 Hz, 2H, H2), 1.81 (dd, J = 7.0, 1.1 Hz, 3H, H8), 1.77 (s, 3H, H9), 1.29 (t, J = 7.1 Hz, 3H, H1). ^{13}C NMR (126 MHz, $CDCl_3$) δ 167.5, 149.3, 136.1, 133.7, 115.2, 60.0, 20.9, 14.3, 11.7. HR-MS (ESI): Calcd for $C_9H_{14}O_2Na$ 177.0886, found 177.0888.

(2*E*,4*E*)-4-methylhexa-2,4-dienol (74):

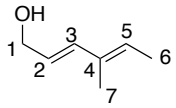

The title compound has been synthesized previously.[177] Dry ether (14 mL) was charged with $LiAlH_4$ (0.38 g, 10 mmol) and cooled to 0 °C using an ice-water bath. Absolute EtOH (0.58 mL, 9.92 mmol) was added dropwise and gas evolution was noted. Meanwhile, 18 mL of ether was charged with **73** (1.00 g, 6.48 mmol) and cooled to 0 °C. The preformed lithium aluminum monoethoxyhydride solution was added to **73** via cannula and stirred for 1 h. The solution was quenched by very slow addition of Rochelle's salt (15 mL) at 0 °C. The layers were separated and the aqueous was extracted with ether (3 x 15 mL). The organic layers were pooled, washed with brine and dried over Na_2SO_4. The solvent was then removed *in vacuo* and the crude liquid was subjected to flash column chromatography (SiO_2, 3:1 hexanes/EtOAc) to yield a colourless oil (405 mg, 56%). IR (CHCl3, cast) 3350, 2983, 2921, 2862, 1671 cm^{-1}; ^1H NMR (500 MHz, $CDCl_3$) δ 6.23 (d, *J* = 15.6 Hz, 1H, H3), 5.68 (dt, *J* = 15.7, 6.2 Hz, 1H, H2), 5.55 (q, *J* = 6.8 Hz, 1H, H5), 4.15 (d, *J* = 6.2 Hz, 2H, H2), 1.75 – 1.68 (m, 6H, H6 + H7). ^{13}C NMR (126 MHz, $CDCl_3$) δ 136.6, 133.8, 127.4, 124.8, 63.8, 13.8, 12.0. HRMS (GC) Calcd for: $C_7H_{12}O$ 112.0888, found 112.0888.

Diethyl (2*E*,4*E*)-4-methylhexa-2,4-dienylphosphonate (63):

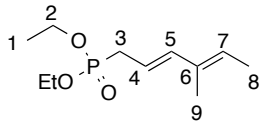

Known allylic phosphonate **74** was prepared using a previously established procedure.[178] **74** (226 mg, 2.01 mmol) was dissolved in 5 mL of dry THF and cooled to -78 °C in a dry ice/acetone bath. *n*-BuLi (0.80 mL, 2.5 mmol) was added dropwise via syringe and the reaction was maintained at -78 °C for 10 min. Tosyl chloride (TsCl, 421 mg, 2.21 mmol) was dissolved in 2 mL of dry THF and added to alkoxide **74** dropwise via syringe at -78 °C. The reaction was maintained at -78 °C for 1 h. Meanwhile, diethyl phosphite (0.43 mL, 3.32 mmol) was dissolved in dry THF (5 mL) and cooled to 0 °C. NaHMDS was added dropwise and the solution was stirred for 30 min at 0 °C. The freshly prepared sodium diethylphosphite was added to the tosylate solution via cannula and the reaction was stirred at -78 °C. After gently warming to room temperature over 16 h, the reaction was partitioned between 10 mL of pH 7 buffer (100 mM sodium phosphate) and 20 mL of dry ether. The layers were separated and the organic was washed with sat'd $NaHCO_3$ (20 mL), dH_2O (2 x 20 mL) and dried over Na_2SO_4. The crude was concentrated *in vacuo* to yield a crude yellow oil. The crude was purified using flash chromatography (Al_2O_3, ether then EtOAc) to yield a clear, colourless oil (186 mg, 40%). IR (CH_2Cl_2, cast) 3038, 2984, 2909, 2863, 1444, 1392, 1254, 1058, 1038 cm^{-1}; ^1H NMR (500 MHz, $CDCl_2$) δ 6.22 – 6.13 (m, 1H, H5), 5.57 – 5.41 (m, 2H, H4+H7), 4.05 (m, 4H, H2), 2.59 (dddd, *J* = 22.2, 7.6, 1.4, 0.7 Hz, 2H, H3), 1.76 – 1.68 (m, 6H, H8+H9), 1.29 (t, J = 7.1 Hz, 6H, H1). ^{13}C NMR (125 MHz, CD_2Cl_2) δ 139.7 (d, J = 14.6 Hz), 134.4 (d, J = 4.2 Hz), 126.9 (d, J = 4.1 Hz), 115.4 (d, J = 12.0 Hz), 63.9 (d, J = 5.9 Hz), 62.2 (d, J = 6.7 Hz), 31.0 (d, J = 139.4 Hz), 16.6

(d, J = 5.8 Hz), 16.3 (d, J = 6.7 Hz), 13.8 (d, J = 1.4 Hz), 12.1. HRMS (ESI) Calcd for $C_{11}H_{21}O_3PNa$ 255.1121, found 255.1120.

***tert*-Butyldimethyl((2*R*,4*S*,6*E*,8*E*,10*E*)-2,4,10-trimethyldodeca-6,8,10-trienyloxy)silane (75):**

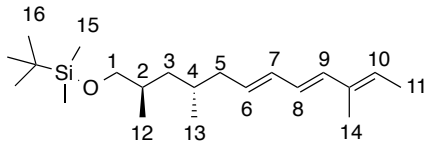

The title compound was synthesized using a published procedure.[178] A stirred solution of **63** (49.5 mg, 0.213 mmol) in 2 mL of dry THF was first cooled to -78°C, then *sec*-BuLi (0.15 mL, 1.4 M in cyclohexane) was added dropwise via syringe. The reaction was stirred at -78 °C for 20 min after which a solution of **62** (42.4 mg, 0.164 mmol) in 2 mL of dry THF was added dropwise via syringe. The reaction was allowed to warm to room temperature over 16 h. The solution was quenched with 3 mL pH = 7 buffer (100 mM sodium phosphate) and 6 mL ether. The layers were separated and the aqueous extracted with ether (3 x 5 mL). The organic was pooled, washed with brine and dried over $MgSO_4$. Concentrating *in vacuo* yielded a crude yellow oil. Purification by flash column chromatography (base-washed SiO_2, pentanes) afforded the product as a colourless oil (27 mg, 50%). Compound 75 was isolated as a single spot by TLC (base-washed SiO_2, R_f = 0.9, hexanes). $[\alpha]_D$ = 7.2 (*c* 1.28, $CHCl_3$); IR ($CHCl_3$, cast) 3021, 2955, 2927, 2856, 1471, 1462, 1387 cm^{-1}, ^1H NMR (500 MHz, CD_2Cl_2) δ 6.15 – 6.12 (m, 2H, H8+H9), 6.12-6.04 (m, 1H, H7), 5.67 (dt, 1H, *J* = 14.7, 7.4 Hz, H6), 5.58 – 5.46 (m, 1H, H10), 3.43 (dd, 1H, *J* = 9.7, 5.8 Hz, H1), 3.35 (dd, 1H, *J* = 9.7, 6.6 Hz, H1'), 2.19 – 2.01 (m, 1H, H5), 2.01 – 1.88 (m, 1H, H5'), 1.75 – 1.74 (s, 3H, H14), 1.73 (d, 3H, *J* = 1.1 Hz, H11), 1.70 – 1.56 (m, 2H, H2+H4), 1.17 (ddd, 1H, *J* = 13.9, 9.4, 4.7 Hz, H3), 1.06 (ddd, 1H, *J* = 13.7, 9.4, 4.9 Hz, H3'), 0.89 (s, 9H, H16), 0.85 (d, 3H, *J* = 3.4 Hz, H12), 0.84 (d, 3H, *J* = 3.4 Hz, H13), 0.04 (s, 6H, H15); ^{13}C NMR (126 MHz, CD_2Cl_2) δ 135.6, 135.2, 132.7, 132.7, 132.5, 126.8, 126.6, 69.3, 54.2, 54.0, 53.7, 53.5, 53.3, 41.6, 40.7, 33.7, 31.0, 30.0, 26.0, 19.4, 18.6, 16.6, 14.0, 12.0, -5.3.

(2*R*,4*S*,6*E*,8*E*,10*E*)-2,4,10-trimethyldodeca-6,8,10-triene-1-ol (76):

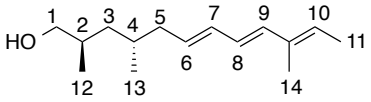

This procedure was adapted from a published method.[179] To a stirred solution of **75** (12.8 mg, 0.038 mmol) in 0.5 mL of dry THF was added a solution of tetrabutylammonium fluoride (TBAF, 0.1 mL, 1M in THF) dropwise via syringe. The reaction was spun at room temperature for 2.5 h and quenched with dH_2O and ether (0.5 mL each). The layers were separated and the aqueous was extracted with ether (3 x 0.5 mL). The organic layers were pooled, washed with water, brine and dried over Na_2SO_4. The solvent was removed *in vacuo* to yield a clear colourless oil. Purification by flash column chromatography (base-washed SiO_2, 10% EtOAc in hexanes) yielded a pure colourless oil (6.8 mg, 80%). Title compound isolated as a single spot by thin layer chromatography (base-washed SiO_2, R_f = 0.2, 9:1 hexanes:EtOAc). $[\alpha]_D$ = 23.65 (c = 0.49, $CHCl_3$); IR (CHCl3, cast) 3369, 2958, 2926, 1723, 1461, 1378 cm^{-1}; ^1H NMR (500 MHz, CD_2Cl_2) δ 6.18 – 6.10 (m, 2H, H8+H9), 6.10 – 6.02 (m, 1H, H7), 5.67 (dt, *J* = 14.7, 7.4 Hz, 1H, H6), 5.54 (qd, *J* = 6.9, 1.1 Hz, 1H, H10), 3.44 (dd, *J* = 10.4, 5.8 Hz, 1H), 3.36 (dd, *J* = 10.4, 6.5 Hz, 1H), 2.08 (m, 1H, H5), 1.98 (m, 1H, H5'), 1.84 – 1.64 (m, 6H, H14+H11), 1.71 – 1.66 (m, 1H, H2), 1.65 – 1.56 (m, 1H, H4), 1.21 – 1.04 (m, 2H, H3), 0.90 – 0.84 (m, 6H, H12+H13); ^{13}C NMR (126 MHz, CD_2Cl_2) δ 135.7, 135.1, 132.6, 132.6, 126.9, 126.6, 69.1, 41.6, 40.5, 33.6, 31.9, 30.9, 23.0, 19.3, 16.4, 14.2, 14.0, 12.0. HRMS (EI) Calcd for $C_{15}H_{26}O$ 222.1984, found 222.1989.

(*E*)-*S*-2-acetamidoethyl 7,11-dimethyl-3-oxododeca-4,10-dienethiolate (77):

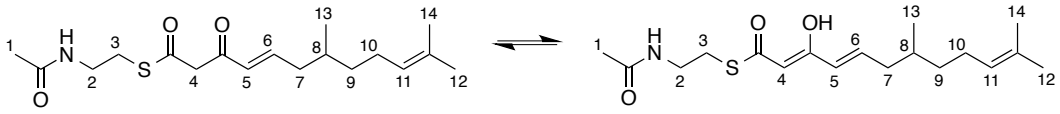

Title compound **77** was prepared using a procedure adapted from Pronin *et al.*[180] Phosphonate **61** (10.8 mg, 31.6 μmol) was dissolved in 1 mL of dry THF and spun at -78°C. NaHMDS (1 M, 70 μL) was added dropwise and the mixture was spun at -78°C for 15 min. Citronellal (5.7 μL, 29 μmol) was added dropwise and the reaction was stirred for 45 minutes and allowed to warmed to room temperature over 16h. The mixture was then quenched with a drop of pH 7 phosphate buffer and concentrated *in vacuo*. Immediate purification using flash column chromatography (base-washed SiO_2, EtOAc) to yield a colourless oil (5.6 mg, 58%). Compound 77 was isolated as a single spot by TLC (base-washed SiO_2, R_f = 0.4, pure EtOAc). ^{1}H NMR (500 MHz, $CHCl_3$) δ 6.89 (dt, 0.4H, *J* = 15.7, 7.4 Hz, keto-H6), 6.76 (dt, 0.6H, *J* = 15.3, 7.6 Hz, enol-H6), 6.15 (dd, 0.4H, *J* = 15.8, 1.4 Hz, keto-H5), 5.91 (br s, 1H, N-H), 5.72 (dd, 0.6H, *J* = 15.5, 1.5 Hz, enol-H5), 5.44 (s, 0.6H, enol-H4), 5.10-5.06 (m, 1H, *J* = 7.0, 5.6, 2.8, 1.4 Hz, H11), 3.84 (s, 0.8H, keto-H4), 3.59 – 3.39 (m, 2H, H2), 3.14-3.06 (m, 2H, H3), 2.33 – 2.16 (m, 1H, H7+H10), 2.14 – 1.99 (m, 2H, H7'+H10'), 1.69 (s, 3H, H1), 1.64 (dd, 3H, *J* = 13.7, 6.9 Hz, H14), 1.55 (s, 3H, H12), 1.40 – 1.30 (m, 2H, H9), 1.29 – 1.13 (m, 1H, H8), 0.91 (d, 1.2H, *J* = 6.7 Hz, keto-H13), 0.89 (d, *J* = 5.6 Hz, 1.8H, enol-H13); ^{13}C NMR (126 MHz, $CDCl_3$) δ 194.5, 192.6, 191.3, 170.4, 170.3, 167.4, 150.0, 143.0, 131.7, 131.5, 130.6, 124.9, 124.4, 124.2, 99.7, 77.3, 77.0, 76.8, 54.9, 40.3, 40.1, 40.0, 39.3, 36.8, 32.5, 32.2, 29.3, 28.0, 25.8, 25.6, 25.5, 23.3, 23.2, 19.6, 17.7.

Diethyl-4-(1-hydroxy-3-phenylpropanyl-2-amino)-2,4-dioxobutylphosphonate (78):

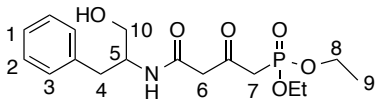

This procedure was adapted from the synthesis of **61**. A stirred solution of crude **65** (1.05g, 3.26 mmol), L-phenylalaninol (0.490g, 3.26 mmol) and 50 mL of dry MeCN (over 4Å MS) was heated to reflux over 16h. The resulting solution was concentrated *in vacuo* and reconstituted in EtOAc (30 mL). The organic was washed with $KHSO_4$ (1N), $NaHCO_3$ (sat'd), brine and dried over anhydrous Na_2SO_4. The solvent was removed *in vacuo* and a clear yellow oil was found. Purification by flash column chromatography (SiO2, EtOAc, then 10% MeOH in EtOAc) yielded a pure yellow oil (0.616 g, 51%). Title compound was isolated as a single spot by TLC (SiO_2, R_f = 0.5, 10% MeOH in EtOAc). ^{1}H NMR (500 MHz, $CDCl_3$) δ 7.37 – 7.19 (m, 5H, H1+H2+H3), 6.96 (d, *J* = 8.1 Hz, 1H, N-H), 4.24 (ddd, *J* = 7.9, 4.7, 3.2 Hz, 1H, H5), 4.16 (tdd, *J* = 9.2, 7.0, 5.9 Hz, 4H, H8), 3.75 (d, *J* = 11.6 Hz, 1H, 10H), 3.54 (m, 3H, H10'+H6), 3.39 (dd, *J* = 22.5, 13.5 Hz, 1H, H7), 3.12 (dd, *J* = 22.7, 13.5 Hz, 1H, H7'), 2.90 (dd, *J* = 7.4, 3.6 Hz, 2H, H4), 1.85 (br s, 1H, OH), 1.36 (td, *J* = 7.1, 1.7 Hz, 6H, H9); ^{13}C NMR (126 MHz, $CDCl_3$) δ 197.22, 197.18, 165.53, 137.78, 129.26, 128.59, 128.56, 128.45, 126.58, 77.31, 77.26, 77.06, 76.81, 63.68, 63.53, 63.13, 63.11, 63.08, 63.06, 53.47, 53.30, 52.28, 51.55, 42.89, 41.88, 37.09, 37.00, 36.95, 16.34, 16.29; HRMS (ESI) Calcd for $C_{17}H_{26}NO_6PNa$ 394.1390, found 394.1395 $[M+Na]^+$

***N*-propionyl-thiazolidine-2-thiol (117):**

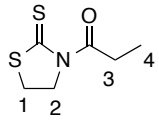

This compound has been synthesized previously by a different procedure.[181] Sodium hydride (1.67 g, 69.6 mmol) was added in one portion to 100 mL dry THF and stirred for 5 min before thiazolidine-2-thiol (5 g, 41.94 mmol) was added in 3 portions. After stirring the reaction at 0°C for 15 minutes, acetic anhydride (4.7 mL, 50.3 mmol) was added dropwise via syringe and the reaction was allowed to warm to room temperature over 16h. The reaction was quenched with slow addition of saturated NH_4Cl solution (100 mL) and the organic was extracted with EtOAc (3 x 100 mL). The organic was pooled, washed with brine, dried over anhydrous Na_2SO_4 and the solvent was removed *in vacuo* to yield a yellow crude oil. Purification using flash column chromatography (SiO_2, 4:1 hexanes:EtOAc) yielded the product as a bright yellow oil (5.81 g, 87%). IR ($CHCl_3$, cast) 2978, 2938, 1701 cm^{-1}; ^1H NMR (700 MHz, $CDCl_3$) δ 4.57 (t, 2H, J = 7.6 Hz, H2), δ 3.26 (t, 2H, J = 7.5 Hz, H1), 3.23 (q, 2H, J = 7.2 Hz, H3), 1.14 (dt, 3H, J = 15.3, 7.4 Hz, H4); ^{13}C NMR (175 MHz, $CDCl_3$) δ 201.5, 175.6, 56.0, 32.3, 28.3, 8.8. HRMS (ESI) Calcd for $C_6H_9NOS_2Na$ 198.0018, found 198.0014 $[M+Na]^+$.

(4*E*,6*E*)- 3-hydroxy-2-methyl-1-(2-thioxothiazolidin-3-yl)octa-4,6-diene-1-one (118):

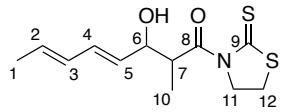

Compound **118** was synthesized using a previously developed procedure.[87] Propionyl thiazolidine (**117**; 1.00 g, 5.71 mmol) was dissolved in dry DCM (50 mL) and cooled to -78°C. $TiCl_4$ (1M in DCM, 6.28 mL) was added dropwise via syringe and stirred for 15 min before DIPEA (0.99 mL, 0.737 g) was added dropwise at -78°C. The reaction was spun at -78°C for one hour as the colour changed from bright orange to black-red. 2,4-hexadienal (0.95 mL, 8.56 mmol) was added dropwise and the temperature was maintained at -78°C for 30 min. Quenching with saturated, aqueous NH_4Cl (30 mL) changed the colour from dark red to bright yellow. The layers were separated, and the organic was extracted three times with EtOAc (30 mL). The organic was pooled, washed with brine and dried with anhydrous Na_2SO_4. The solvent was removed to yield a bright yellow oil. Purification using flash chromatography (SiO_2) with a 4:1 hexanes/EtOAc eluent yielded **118** as a bright yellow oil and a mixture of *syn* and *anti* diastereomers (0.8250 g , 56%). IR ($CHCl_3$, cast film) 3414, 2977, 2936, 1697 cm^{-1}; ^{1}H-NMR ($CDCl_3$, 500 MHz): **Diastereomer 1:** δ 6.23 (dd, 1H, *J* = 15.4, 10.5 Hz, H4), 6.05 (ddq, 1H, *J* = 15.6, 10.0, 1.5 Hz, H3), 5.73 (dq, 1H, *J* = 15.1, 6.8 Hz, H2), 5.53 (dd, 1H, *J* = 15.2, 6.3 Hz, H5), 4.68-4.62 (m, 1H, H7), 4.55-4.48 (m, 3H, H6+H11), 3.32-2.22 (m, 2H, H12), 2.51 (d, 1H, *J* = 3.2 Hz, OH), 1.78-1.74 (m, 3H, H1), 1.22 (d, 3H, *J* = 6.9 Hz, H10). **Diastereomer 2:** δ 6.59 (ddd, 1H, *J* = 15.3, 11.1, 1.4 Hz, H4), 6.01 (ddq, 1H, J = 10.8, 10.8, 1.6 Hz, H3), 5.63 (dd, 1H, J = 15.4, 6.0 Hz, H5), 5.56-5.50 (m, 1H, H2) 4.68-4.62 (m, 1H, H7), 4.60-4.56 (m, 1H, H7), 4.55-4.48 (m, 2H, H11), 3.32-2.22 (m, 2H, H12), 2.58 (d, 1H, *J* = 3.3 Hz, OH), 1.76 (m, 3H, H1), 1.24 (d, 3H, *J* = 7.0 Hz, H10). ^{13}C-NMR ($CDCl_3$, 125 MHz): **Diastereomer 1:** δ 201.9 (C1),

178.2 (C2), 132.0 (C6), 130.7 (C7), 130.5 (C8), 129.5 (C5), 73.1 (C4), 56.4 (C10), 44.6 (C3), 28.4 (C11), 18.1 (C9), 11.3 (C12). **Diastereomer 2:** δ 201.9 (C1), 178.2 (C2), 131.7 (C6), 128.5 (C7), 127.5 (C8), 126.9 (C5), 73.0 (C4), 56.4 (C10), 44.5 (C3), 28.4 (C11), 13.5 (C9), 11.3 (C12). HRMS (ESI) Calcd for $C_{12}H_{17}NO_2S_2Na$ 294.0593, found 294.0591 $[M+Na]^+$.

(4*E*,6*E*)-*S*-2-acetamidoethyl-3-hydroxy-2-methylocta-4,6-dienethiolate (119):

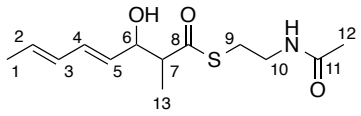

Compound **119** was synthesized using a published procedure.[87] **118** (206 mg, 0.761 mmol) was dissolved in 10 mL dry MeCN and K_2CO_3 (0.158 g, 1.141 mmol) and stirred at room temperature. *N*-acetylcysteamine (0.799 mmol, 85 μL) was added dropwise and the mixture was stirred for 15 minutes or until the bright yellow colour disappeared. The solvent was removed *in vacuo* and the reaction was reconstituted in EtOAc and water in equal volumes. Extraction of the aqueous layer three times with EtOAc, pooling of organic phases, washing with brine and drying with Na_2SO_4 lead to a clear crude oil that was purified using flash chromatography (SiO_2, pure EtOAc as eluent). The pure product was a clear, colourless oil (0.154 mg, 75%). IR (CH_2Cl_2, cast film) 3301, 3089, 3019, 2933, 1683, 1658, 1550 cm^{-1}; ^{1}H-NMR ($CDCl_3$, 500MHz) **Diastereomer 1:** δ 6.22 (dd, J = 15.4, 10.5 Hz, 1H, H4) 6.24 (ddq, J = 14.7, 10.5, 1.3 Hz, 1H, H3), 5.94-5.80 (br s, 1H, NH), 5.72 (dq, J= 15.0, 7.0 Hz, 1H, H2), 5.52 (ddd, J = 15.2, 6.6, 0.5 Hz, 1H, H5), 4.44-4.40 (m, 1H, H6), 3.44-3.40 (m, 2H, H10), 3.08-2.96 (m, 2H, H9), 2.84-2.78 (m, 1H, H7), 2.50-2.46 (br s, 1H, OH), 1.95 (s, 3H, H12), 1.76 (d, 3H, H1), 1.21 (d, 3H, *J* = 7.0 Hz, H13) **Diastereomer 2:** δ 6.60 (ddd, 1H, *J* = 15.2, 11.0, 1.3 Hz, H4), 6.08-6.00 (m, 1H, H3), 5.94-5.80 (br s, 1H, NH), 5.62 (dd, 1H, *J* = 15.2, 6.4 Hz, H5), 4.45-4.46 (m, 1H, H6), 3.44-3.40 (m, 2H, H10), 3.08-2.96 (m, 2H, H9), 2.84-2.78 (m, 1H, H7), 2.57 (br s, 1H, OH), 1.95 (s, 3H, H12), 1.75 (d, 3H, *J* = , H12), 1.23 (d, 3H, *J* = 7.0 Hz, H13). ^{13}C-NMR (125 MHz, $CDCl_3$): **Diastereomer 1:** δ 203.2 (C8), 170.4 (C11), 132.4 (C4), 130.8 (C2), 130.5 (C3), 129.2 (C5) 73.3 (C6), 53.9 (C7), 39.3 (C10), 28.8 (C9), 23.2 (C2), 18.2 (C1), 12.0 (C13). **Diastereomer 2:** δ 203.2 (C8), 170.4 (C11), 131.5 (C5), 128.4 (C3), 127.7 (C2), 127.1 (C4), 73.3 (C6), 53.8 (C7),

39.3 (C10), 28.7 (C9), 23.2 (C2), 13.5 (C1), 11.9 (C13). HRMS (ES) calcd for $C_{13}H_{21}NO_3SNa$ 294.1134, found 294.1129 $[M+Na]^+$.

(4*E*, 6*E*)-*S*-2-acetamidoethyl-2-methyl-3-oxoocta-4,6-dienethiolate (115):

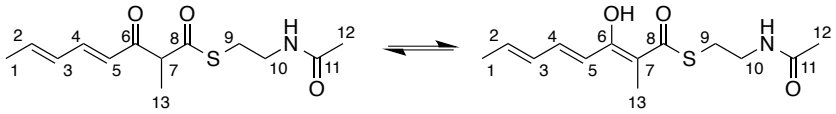

The synthesis of title compound **115** was adapted from a known procedure.[182] Oxalyl chloride (0.221 mmol, 19 µL) was cooled to -78°C and a solution of DMSO (dried over 4Å MS, 0.295 mmol, 21 µL) in 100 µL dry DCM was added dropwise. After 30 min at -78°C, a solution of **119** (20 mg, 0.074 mmol) in 250 µL of DCM was added dropwise and spun at -78°C for another 20 min. Diisopropylethylamine (dried over 4Å MS, 0.19 mL, 1.11 mmol) was added dropwise and the temperature was maintained for 20 min then warmed to -50°C for 20 min. The reaction was quenched with dH_2O (1 mL) and allowed to warm to room temperature. The aqueous was extracted with EtOAc (3 x 1 mL) and the organic was pooled, washed with $NaHCO_3$ (sat'd), brine and dried over Na_2SO_4. The reaction was concentrated *in vacuo* and the crude oil was purified by flash column chromatography (SiO_2, EtOAc) to yield a pure yellow oil (2.9 mg, 15%). Title compound was isolated as a single spot by TLC (SiO2, Rf = 0.5, EtOAc). (33:66 keto:enol) IR (CH_2Cl_2 cast) 3285, 2984, 2935, 1658, 1592, 1551 cm^{-1}; ^1H NMR (700 MHz, $CDCl_3$) δ 7.26 (m, 0.6H, enol-H4), 7.20 – 7.15 (m, 1H, keto-H4), 6.31 – 6.14 (m, 3.6H, H3+H5+keto-H2), 6.14 – 6.05 (m, 0.6H, enol-H2), 5.92 (br s, 0.3H, keto-N-H), 5.78 (br s, 0.6H, enol-N-H), 3.98 (q, *J* = 7.0 Hz, 0.3H, keto-H7), 3.53 – 3.36 (m, 2H, H10), 3.18 – 2.96 (m, 2H, H9), 1.97 (s, 2H, enol-H13), 1.95 (m, 3H, H12), 1.91 – 1.88 (m, 2H, enol-H1), 1.87 (dd, *J* = 6.9, 1.5 Hz, 1H, keto-H1), 1.42 (d, *J* = 7.0 Hz, 1H); ^{13}C-NMR (125 MHz, CH_2Cl_2): δ 197.2, 194.4, 170.2, 147.2, 145.2, 130.4, 125.4, 60.0, 39.1, 30.4, 23.3, 19.1, 14.0; HRMS (ESI) Calcd for $C_{13}H_{19}NO_3SNa$ 292.0978, found 292.0979 $[M+Na]^+$.

5-hexanoyl-2,2-dimethyl-1,3-dioxane-4,6-dione (122):

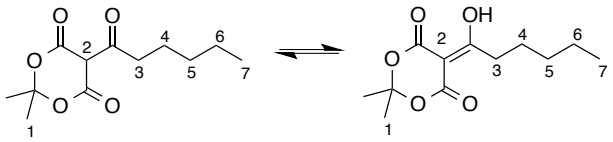

Compound **122** is a known compound[183] and was prepared using the established procedure. Freshly recrystallized Meldrum's acid (1.0 g, 6.9 mmol) and DMAP (1.70 g, 13.9 mmol) were dissolved in dry CH_2Cl_2 (10 mL) and stirred at room temperature for 5 minutes. Hexanoyl chloride (0.97 mL, 6.9 mmol) was added dropwise and the mixture was stirred for 16 h under Ar. A change in colour from colourless to bright yellow was noted. The solution was quenched with 1 M HCl (25 mL), the layers were separated and the aqueous was extracted (3x 20 mL CH_2Cl_2). The organic layers were pooled, washed with 1 M HCl (10 mL) brine and dried over anhydrous Na_2SO_4. The solvent was removed *in vacuo* to yield a crude yellow oil that was used immediately without purification (1.688 g, quant.). ^{1}H NMR (400 MHz, $CDCl_3$) δ 3.17 – 2.91 (m, 2H, H3), 1.82 – 1.53 (m, 6H, H1), 1.50 – 1.17 (m, 6H, H4+H5+H6), 1.01 – 0.77 (m, 3H, H7). ^{13}C-NMR (125 MHz, $CDCl_3$) δ 198.4, 104.8, 91.3, 35.7, 31.5, 26.8, 25.8, 22.3, 13.9.

***S*-2-acetamidoethyl 3-oxooctanethioate (120):**

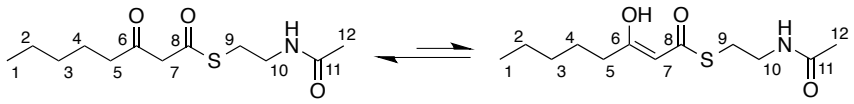

The title compound has been prepared previously[184] using a similar procedure as **61**. White powder (365 mg, 53%). (75:25 keto:enol) IR (CH_2Cl_2, cast): 3284.0, 2951.8, 2928.0, 2869.3, 1716.6, 1687.0, 1636.4, 1563.3 cm^{-1}; ^{1}H-NMR (400 MHz, $CDCl_3$): δ 6.00 (br s, 0.6H, NH), 5.90 (br s, 0.2H, enol-NH), 5.45 (s, 0.5H, enol-H7), 3.68 (s, 1.5H, keto-H7), 3.48-3.40 (m, 2H, H10), 3.10-3.07 (m, 2H, H9), 2.53 (app t, 1.5H, J = 7.6 Hz, keto-H5), 2.18-2.14 (app t, 0.5H, J = 7.5 Hz, enol-H5), 1.96 (s, 3H, H12), 1.65-1.56 (m, 2H, H4), 1.36-1.20 (m, 4H, H2+H3), 0.89-0.86 (m, 3H, H1); ^{13}C-NMR (125 MHz, $CDCl_3$): δ 202.3 (C6), 192.4 (C8), 176.4 (enol-C6), 170.4 (C11), 169.8 (enol-C11), 99.1 (enol-C7), 57.2 (keto-C7), 44.3 (enol-C5), 43.4 (keto-C5), 40.0 (enol-C10), 39.2 (keto-C10), 34.9 (enol-C4), 31.2 (enol-C3), 31.0 (keto-C3), 29.2 (keto-C9), 27.8 (enol-C4), 23.2 (keto-C2), 23.1 (enol-C2), 22.4 (keto-C1), 22.3 (enol-C1), 13.9 (keto-C12), 13.8 (enol-C12); HRMS (ESI) Calcd for $C_{12}H_{21}NO_3SNa$ ($[M+Na]^+$): 282.1134, found 282.1132.

3-hydroxy-2-methyl-1-(2-thioxothiazolindin-3-yl)octan-1-one (123):

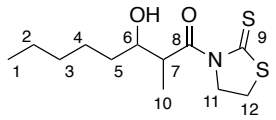

Known compound **123** was synthesized using a different procedure.[185] The procedure used was modified from the preparation of **118**. Bright yellow oil (0.943 g, 40%) IR (CH_2Cl_2, cast): 3453, 2932, 2858, 1699; ^{1}H-NMR (500MHz, $CDCl_3$): δ 4.62-4.50 (m, 3H, H7+H11), 4.01-3.96 (m, 1H, H6), 3.33-3.24 (m, 2H, H12), 2.57 (br s, 1H, OH), 1.58-1.49 (m, 1H, H5), 1.49-1.41 (m, 1H, H4), 1.41-1.36 (m, 1H, H5'), 1.36-1.26 (m, 5H, H2+H3+H4'), 1.21 (d, 3H, J = 7.0 Hz, H10), 0.88 (m, 3H, H1). ^{13}C-NMR (125 MHz, $CDCl_3$): δ 201.8 (C9), 179.3 (C8), 71.7 (C6), 56.4 (C7), 43.4 (C11), 34.0 (C5), 31.8 (C3), 28.2 (C12), 25.6 (C4), 22.6 (C2), 14.0 (C1), 10.2 (C13); HRMS (ESI) Calcd for $C_{12}H_{21}NO_2S_2Na$ ($[M+Na]^+$) 298.0906, found 298.0906.

***S*-2-acetamidoethyl 3-hydroxy-2-methyloctanethioate (124):**

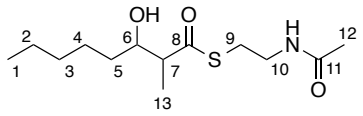

This compound has been prepared previously but by a different procedure.[186] The procedure used instead was identical to the preparation of compound **119**. Clear, colourless oil (0.249 g, 62%). IR (neat film): 3299, 2954, 2932, 2871, 2959, 1684, 1658 cm^{-1}; 1H-NMR (500 MHz, $CDCl_3$): **Major diastereomer (syn):** δ 5.90 (br s, 1H, NH), 3.94-3.88 (m, 1H, H6), 3.50-3.38 (m, 2H, H10), 3.06-2.94 (m, 2H, H9), 2.71 (qd, 1H, *J* = 7.2, 3.7 Hz, H7), 2.50 (br s, 1H, OH), 1.95 (s, 3H, H12), 1.56-1.43 (m, 2H, H5a + H4a), 1.42-1.36 (m, 1H, H5b), 1.36-1.24 (m, 5H, H2, H3, H4b), 1.21 (d, 3H, *J* = 7.0 Hz, H13), 0.87 (m, 3H, H1); **Minor diastereomer (anti)**: δ 5.90 (br s, 1H, NH), 3.73-3.66 (m, 1H, H6), 3.50-3.38 (m, 2H, H10), 3.06-2.94 (m, 2H, H9), 2.71 (qd, 1H, *J* = 7.2, 3.7 Hz, H7), 2.42-2.40 (br s, 1H, OH), 1.95 (s, 3H, H12), 1.56-1.43 (m, 2H, H5 + H4), 1.42-1.36 (m, 1H, H5'), 1.36-1.24 (m, 5H, H2, H3, H4'), 1.21 (d, 3H, *J* = 7.0 Hz, H13), 0.87 (m, 3H, H1); ^{13}C-NMR (125 MHz, $CDCl_3$) **Major diastereomer:** δ 204.2 (C8), 170.5 (C11), 72.2 (C6), 53.4 (C7), 39.4 (C10), 34.2 (C5), 31.7 (C3), 28.6 (C9), 25.7 (C4), 23.2 (C11), 22.6 (C2), 14.1 (C1), 11.1 (C12); **Minor diastereomer:** δ 204.2 (C8), 170.5 (C11), 73.9 (C6), 54.2 (C7), 39.4 (C10), 34.5 (C5), 31.7 (C3), 28.6 (C9), 25.1 (C4), 23.2 (C11), 22.6 (C2), 15.1 (C1), 11.1 (C12); HRMS (ESI) Calcd for $C_{13}H_{26}NO_3S$ 276.1628, found 276.1626 $[M+H]^+$.

***S*-2-acetamidoethyl-2-methyl-3-oxooctanethiolate (121):**

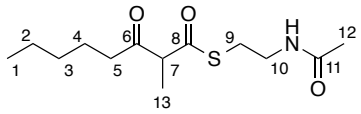

Compound **121** was constructed using an oxidation procedure published previously.[87] **124** (125 mg, 0.454 mmol) was dissolved in reagent grade DCM (15 mL) and spun at room temperature under Ar. Dess-Martin periodinane (289 mg, 0.681 mmol) was added in portions and the reaction was stirred at room temperature for 1.5 h. The solution was quenched with 15 mL 1:1 $Na_2S_2O_3$ (sat'd):$NaHCO_3$ (sat'd) and stirred for 15 min. The layers were then separated and the aqueous was extracted with DCM (3 x 15 mL). The organic was pooled, washed with 1:1 $Na_2S_2O_3$ (sat'd):$NaHCO_3$ (sat'd) (2 x 30 mL), brine and then dried over Na_2SO_4. The crude mixture was subjected to flash column chromatography (SiO_2, EtOAc) to yield a colourless oil (55.7 mg, 45%). Title compound isolated as a single spot by TLC (SiO_2, R_f = 0.6, EtOAc). (enol not detected by NMR) IR ($CHCl_3$, cast): 3292, 2956, 2934, 1723, 1676, 1678 cm^{-1}; ^1H NMR (500 MHz, $CDCl_3$) δ 5.79 (s, 1H, N-H), 3.78 (q, *J* = 7.1 Hz, 1H, H7), 3.55–3.34 (m, 2H, H10), 3.16–2.97 (m, 2H, H9), 2.67–2.40 (m, 2H, H5), 1.97 (s, 3H, H12), 1.62-1.54 (m, 2H, H4), 1.38 (d, *J* = 7.1, 3H, H13), 1.34 – 1.20 (m, 4H, H2+H3), 0.89 (t, *J* = 7.1 Hz, 3H, H1); ^{13}C NMR (126 MHz, $CDCl_3$) δ 205.0, 197.0, 170.3, 77.3, 77.2, 77.0, 76.8, 61.3, 41.3, 39.4, 31.2, 28.9, 23.2, 23.2, 22.4, 13.9, 13.6. HRMS (ESI) Calcd for $C_{13}H_{23}NO_3SNa$ 296.1291, found 296.1289 $[M+Na]^+$.

5-butyryl-2,2-dimethyl-1,3-dioxane-4,6-dione (145):

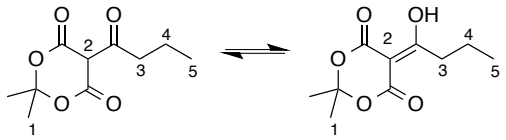

Compound **145** has been synthesized previously by a different procedure.[187] The procedure used is identical to the one used in synthesis of **122**. ^{1}H NMR (500 MHz, $CHCl_3$) δ 3.15 – 2.95 (m, 2H, H3), 1.84 – 1.62 (m, 8H, H1+H4), 1.03 (t, *J* = 7.4 Hz, 3H, H5). ^{13}C NMR (126 MHz, $CDCl_3$) δ 198.1, 104.8, 91.4, 77.3, 77.0, 76.8, 53.4, 37.5, 36.2, 27.6, 26.8, 19.7, 13.9.

***S*-2-acetamidoethyl 3-oxohexanethiolate (127):**

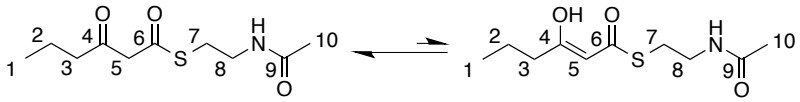

Compound **127** has been synthesized previously.[187] The procedure used was identical to **61**. White solid (704 mg, 75%) (70:30 keto:enol) IR ($CHCl_3$, cast) 3282.68, 3103, 2958, 2933, 1716, 1684, 1636 cm^{-1}; ^{1}H NMR (500 MHz, $CHCl_3$) δ 5.90 (s, 1H, N-H), 5.46 (s, 0.3H, enol-H5), 3.69 (s, 1.7H, keto-H5), 3.53 – 3.39 (m, 2H, H8), 3.09 (m, 2H, H7), 2.51 (t, *J* = 7.2 Hz, 1.4H, keto-H3), 2.16 (ddd, *J* = 8.0, 7.2, 0.6 Hz, 0.6H, enol-H3), 1.97 (s, 3H, H10), 1.70 – 1.52 (m, 2H, H2), 0.96 (t, J = 7.4 Hz, 0.9H), 0.93 (t, *J* = 7.4 Hz, 2.1H); ^{13}C NMR (126 MHz, $CDCl_3$) δ 213.0, 202.1, 194.3, 192.4, 177.4, 170.4, 170.2, 99.3, 77.3, 77.2, 77.0, 76.8, 57.2, 45.3, 39.9, 39.2, 36.8, 31.6, 29.2, 27.9, 23.3, 23.2, 19.6, 16.9, 13.6, 13.5. HRMS (ESI) Calcd for $C_{10}H_{17}NO_3SNa$ 254.0821, found 254.0825.

***S*-2-acetamidoethyl 2-methyl-3-oxohexanethiolate (128):**

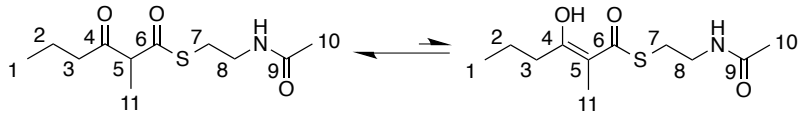

This compound has been synthesized previously and the procedure was used.[188] **127** (100 mg, 0.432 mmol) and potassium *tert*-butoxide (55.8 mg, 0.497 mmol) were dissolved in 15 mL of dry THF at 0°C. After stirring at the same temperature for 30 min, methyl iodide was added dropwise (0.16 mL, 2.55 mmol) and the reaction maintained at 0°C for 1 h. The reaction was then left to warm to room temperature over 16h. Quenching with 10 mL of HCl (0.1 M), separating, extracting the aqueous with EtOAc (3 x 10 mL) and drying the organic layer provided a crude colourless oil after concentration *in vacuo*. Purification by flash column chromatography provided the pure compound as a colourless oil (108 mg, 25%). (90:10 keto:enol) IR ($CHCl_3$, cast): 3291.4, 3078.0, 2964.5, 2937.0, 2876.3, 1723.0, 1675.7, 1546.2 cm^{-1}; ^{1}H-NMR (500 MHz, $CDCl_3$): δ 5.85 (br s, 0.1H, enol-NH), 5.80 (br s, 0.9H, keto-NH), 4.12 (q, 0.1H, enol-H5), 3.78 (q, 0.9H, keto-H5), 3.52-3.39 (m, 2H, H8), 3.13-3.02 (m, 2H, H7), 2.58-2.44 (m, 2H, H3), 1.97 (s, 2.7H, keto-H10), 1.88 (s, 0.3H, enol-H10), 1.67-1.56 (m, 2H, H2), 1.38 (d, 3H, J = 7.0 Hz, H11), 0.98 (m, 0.3H, H1), 0.91 (m, 2.7H, H1); ^{13}C-NMR (125MHz, $CDCl_3$) δ 204.8 (C4), 197.0 (C6), 170.3 (C9), 61.3 (C5), 43.5 (C3), 39.4 (C8), 28.9 (C7), 23.2 (C10), 17.0 (C2), 13.6 (C11), 13.5 (C1). HRMS (ESI) Calcd for $C_{11}H_{19}NO_3SNa$ ($[M+Na]^+$) 268.0978, found 268.0976.

(*R*)-4-benzyl-3-octanoyl-2-oxazolidinone (133):

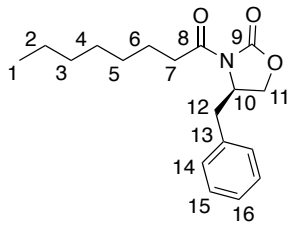

Compound **133** has been synthesized previously and their procedure was used for this synthesis.[189] (*R*)-4-benzyl-3-propionyl-oxazolidinone (0.50g, 2.82 mmol) was dissolved in 20 mL of dry THF and cooled to -78°C using a dry ice/acetone bath. *n*-BuLi (1.32 mL, 2.14 M) was then added dropwise and the reaction was maintained at -78°C for 15 min. Octanoyl chloride (0.53 mL, 3.10 mmol) was added via syringe and the reaction was allowed to warm over 16h. The solution was quenched with dH_2O (10 mL) and the bulk of the THF was removed *in vacuo*. The aqueous was then extracted with CH_2Cl_2 (3 x 10 mL) and the organic was pooled, washed with brine and dried over Na_2SO_4. The crude was concentrated and purified using flash column chromatography (SiO_2, 2:1 hexanes/EtOAc) to yield a clear colourless oil (0.699 g, 82%). $[\alpha]_D$ = -45.63 (*c* = 5.0 g/100mL, $CHCl_3$); IR ($CHCl_3$, cast): 2955, 2928, 2856, 1784, 1701, 1454, 1387, 1352 cm^{-1}; ^{1}H-NMR (700MHz, $CDCl_3$): δ 7.34-7.30 (m, 2H, H15), 2.27-2.24 (m, 1H, H16), 7.21-7.17 (m, 2H, H14), 4.63-4.68 (m, 1H, H10), 4.20-4.12 (m, 2H, H11), 3.28 (dd, 2H, *J* = 13.5, 3.2 Hz, H12a), 2.95 (ddd, 1H, *J* = 6.7, 8.5, 16.9 Hz, H7a), 2.88 (ddd, 1H, *J* = 6.7, 8.5, 16.9 Hz, H7b), 2.76 (dd, 1H, *J* = 9.6, 13.4 Hz, H12b), 1.73-1.64 (m, 2H, H6), 1.40-1.22 (m, 8H, H2 + H3 + H4 + H5), 0.88 (app t, 3H, *J* = 7.1 Hz, H1); ^{13}C-NMR (175 MHz, $CDCl_3$): δ 173.4 (C8), 153.4 (C9), 135.4 (C13), 129.4 (C14), 128.9 (C15), 127.3 (C16), 66.1 (C11), 55.1 (C10), 37.9 (C12), 35.5 (C7), 31.7 (C5), 29.1 (C3), 29.0 (C4), 24.3 (C6), 22.6 (C2), 14.1 (C1); HRMS (ES) Calcd for $C_{18}N_{26}NO_3$ ($[M+H]^+$) 304.1907, found 304.1906.

(*R*)-4-benzyl-3-((*R*)-2-methyloctanoyl)-2-oxazolidinone (134):

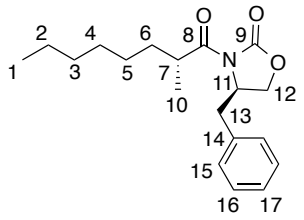

Compound **134** has been synthesized previously and the method was adapted for this synthesis.[190] A solution of **133** (0.50 g, 1.65 mmol) in 10 mL of dry THF was blanketed with argon and cooled to -78°C. NaHMDS (1.82 mL, 1 M) was added dropwise via syringe and the reaction was spun at -78°C for 30 minutes before methyl iodide was added. The reaction warmed to room temperature over 16h and was quenched with NH_4Cl (sat'd). The THF was removed *in vacuo* and replaced with 10 mL of EtOAc. The layers were separated and the aqueous was extracted with EtOAc (3 x 10 mL). The organic layers were then pooled, washed with brine and dried over Na_2SO_4. The reaction was concentrated *in vacuo* and purified by column chromatography (SiO_2, 6:1 hexanes/EtOAc) to yield a clear colourless oil (0.44g, 85%). $[\alpha]_D^{25}$ = 50.03 (*c* = 1.0 g/100mL, $CHCl_3$); IR ($CHCl_3$, cast): 2957.2, 2929.7, 2857.5, 1782.6, 1698.7, 1455.1, 1386.4, 1349.7 cm^{-1}; 1H-NMR (500 MHz, $CDCl_3$) 7.35-7.30 (m, 2H, H16), 7.30-7.24 (m, 1H, H17), 7.25-7.18 (m, 2H, H15), 4.70-4.64 (m, 1H, H11), 4.22-4.14 (m, 2H, H12), 3.74-3.67 (tq, 1H, *J* = 6.8, 6.8 Hz, 1H, H7), 3.28 (dd, 1H, *J* = 13.4, 3.3Hz, H13a), 2.77 (dd, 1H, *J* = 13.4, 9.5 Hz, H13b), 1.78-1.70 (m, 1H, H6a), 1.46-1.38 (m, 1H, H6b), 1.38-1.24 (m, 8H, H2-5), 1.22 (d, 3H, *J* = 6.2 Hz, H10), 0.88 (m, 3H, H1). ^{13}C-NMR (125MHz, $CDCl_3$): 177.5 (C8), 153.1 (C9), 135.4 (C14), 129.5 (C16), 129.0 (C15), 127.4 (C17), 66.0 (C12), 55.4 (C11), 38.0 (C7), 37.7 (C13), 33.5 (C6), 31.8 (C5), 29.4 (C4), 27.3 (C3), 22.6 (C2), 17.4 (C10), 14.1 (C1); HRMS (ES) Calcd for $C_{19}H_{27}NO_3Na$ $[M+Na]^+$ 340.1881, found 340.1883.

(2*R*)-2-methyl-1-hexanol (135):

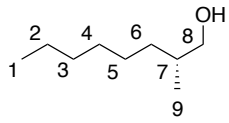

Compound **135** has been synthesized previously by an alternate method.[191] The method used is detailed in the synthesis of **68**. Clear, colourless oil (429 mg, 33%). $[\alpha]_D$ = 11.63 (*c* = 1.25, EtOH); IR ($CHCl_3$, cast) 3332, 2956, 2925, 2856 cm^{-1}; ^1H NMR (600 MHz, $CDCl_3$) δ 3.51 (dd, 1H, *J* = 10.4, 5.7 Hz, H8a), 3.42 (dd, 1H, *J* = 10.5, 6.5 Hz, H8b), 1.61 (m, 1H, H7), 1.48 – 1.21 (m, 10H, H2 + H3 + H4 + H5 + H6), 1.20 – 1.03 (m, 1H, OH), 0.92 (d, 3H, *J* = 6.7 Hz, H9), 0.88 (t, 3H, *J* = 6.8 Hz, H1); ^{13}C-NMR (125 MHz, $CDCl_3$) δ 68.4 (C8), 35.8 (C6), 33.2 (C7), 31.9 (C3), 29.6 (C4), 27.0 (C5), 22.7 (C2), 16.6 (C9), 14.1 (C1); HRMS (EI), Calcd for C_9H_{18} 126.1408, found 126.1406 $[M\text{-}H_2O]^+$.

***N*-acetyl-thiazolidine-2-thione (136)**

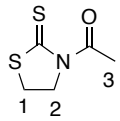

The procedure used to synthesize **117** was used to synthesize **136**. Bright yellow oil (88%). (SiO_2, 4:1 hexanes:EtOAc) yielded the product as a bright yellow oil (5.87 g, 87%). IR ($CHCl_3$, cast) 3002, 2940, 1696 cm^{-1}; ^1H NMR (400 MHz, $CHCl_3$) δ 4.57 (t, 2H, *J* = 7.5 Hz, H2), 3.28 (t, 2H, *J* = 7.5 Hz, H1), 2.77 (s, 3H, H3); ^{13}C NMR (101 MHz, $CDCl_3$) δ 201.4, 170.9, 76.8, 76.5, 76.2, 55.1, 27.6, 26.5. HRMS (ESI) Calcd for $C_5H_7NO_2S_2Na$ 183.9861, found 183.9858 $[M+Na]^+$.

(4*R*)-3-hydroxy-4-methyl-1-(2-thioxo-3-thiazolidinyl)decanone (137):

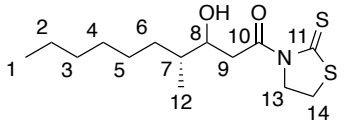

Oxalyl chloride (2.08 mmol, 0.18 mL) was cooled to -78°C and a solution of DMSO (dried over 4Å MS, 2.77 mmol, 0.2 mL) in 10 mL dry DCM was added dropwise. After 30 min at -78°C, a solution of **135** (100 mg, 0.692 mmol) in 1.5 mL of CH_2Cl_2 was added dropwise and spun at -78°C for another 20 min. Diisopropylethylamine (DIPEA; dried over 4Å MS, 1.81 mL, 10.4 mmol) was added dropwise and the temperature was maintained for 20 min then warmed to -50°C for 60 min. The reaction mixture was quenched with 10 mL NH_4Cl (sat'd) and allowed to warm to room temperature. The layers were separated and the organic was washed with 10 mL of $NaHCO_3$ (sat'd) and brine before drying on Na_2SO_4. The solvent was removed and the crude aldehyde was used immediately in the next step. A solution of **136** (74.3 mg, 0.461 mmol) in 5 mL of DCM was charged with $TiCl_4$ (1 M, 0.51 mL) at -78°C. After 30 minutes at -78°C, DIPEA (80 μL, 0.461 mmol) was added dropwise and a colour change was noted from bright orange-red to a deep red-brown. After 1 h at -78°C, the reaction was quenched with 10 mL NH_4Cl (sat'd) and allowed to warm to room temperature. Separation of the layers and extraction of the aqueous layer with CH_2Cl_2 (3 x 10 mL) led to the layers being pooled, washed with brine and dried on Na_2SO_4. The reaction was concentrated *in vacuo* and subjected to flash column chromatography (SiO2, 3:1 hexanes/EtOAc) to yield a bright yellow oil (75mg, 35%). IR (CH_2Cl_2, cast film): 3533, 2956, 2926, 1780, 1696 cm^{-1}; ^{1}H-NMR (400 MHz, $CDCl_3$): **Major diastereomer (*anti*)**: δ 4.66-4.54 (m, 2H, H13), 4.08-4.01 (m, 1H, H8), 3.50-3.32 (m, 4H, H9 + H14), 2.89 (br d, 1H, J = 3.8 Hz, OH), 1.60-1.52 (m, 1H, H7), 1.52-1.40 (m, 1H, H6), 1.40-1.22 (m, 8H, H2-H5), 1.22-1.10 (m, 1H, H6), 0.95-0.92 (d, 3H, J = 6.8 Hz, H12), 0.90-0.85 (m, H3,

H1); **Minor diastereomer (*syn*)**: δ 4.66-4.54 (m, 2H, H13), 4.00-3.94 (m, 1H, H8), 3.50-3.32 (m, 2H, H9 + H14), 2.84-2.80 (br s, 1H, OH), 1.70-1.60 (m, 1H, H7), 1.52-1.40 (m, 1H, H6), 1.40-1.22 (m, 8H, H2-H5), 1.22-1.10 (m, 1H, H6), 0.93-0.90 (d, 3H, J = 6.9 Hz, H12), 0.90-0.85 (m, 3H, H1); ^{13}C-NMR (125 MHz, $CDCl_3$): **Major diasteromer (*anti*):** δ 202.0 (C11), 174.8 (C10), 71.3 (C8), 55.8 (C13), 43.4 (C9), 38.2 (C7), 32.8 (C6), 31.9 (C5), 29.6 (C14) 28.4 (C4), 37.3 (C3), 22.7 (C2), 14.5 (C12), 14.1 (C1); **Minor diastereomer (*syn*):** δ 202.0 (C11), 174.9 (C10), 72.0 (C8), 55.8 (C13), 42.4 (C9), 38.3 (C7), 32.4 (C6), 31.8 (C5), 29.6 (C14), 28.4 (C4), 27.2 (C3), 22.7 (C2), 15.1 (C12), 14.1 (C1); HRMS (ES) Calcd for $C_{14}H_{25}NO_2S_2Na$ [M+Na]+ 326.1219, found 326.1216.

(4*R*)-*S*-2-acetamidoethyl 3-hydroxy-4-methyldecanethioate (138):

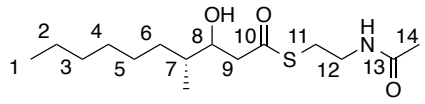

Compound **138** was constructed from **137** using the procedure used to assemble **119** from **118**. Clear colourless oil (37.5 mg, 64%). IR (CH_2Cl_2, cast): 3298.6, 2957.8, 2927.3, 2856.4, 1688.9, 1657.5, 1551.1 cm^{-1}; 1H-NMR (500MHz, $CDCl_3$): **Major diastereomer (anti)**: δ 5.89 (br s, 1H, NH), 4.02-4.00 (ddd, 8.9, 3.9, 3.9 Hz, 1H, H8), 3.52-4.45 (m, 2H, H12), 3.13-3.03 (m, 2H, H11), 2.79-2.68 (m, 2H, H9), 2.39 (br s, 1H, OH), 2.00 (s, 3H, H14), 1.58-1.51 (m, 1H, H7), 1.51-1.42 (m, 1H, H6), 1.42-1.21 (m, 10H, H2-H5) 1.20-1.10 (m, 1H, H6), 0.96-0.88 (m, 6H, H1+H15); **Minor diastereomer (syn)**: δ 5.89 (br s, 1H, NH), 3.98-3.94 (ddd, J = 5.4, 3.1, 3.1Hz, 1H, H8), 3.52-4.45 (m, 2H, H12), 3.13-3.03 (m, 2H, H11), 2.79-2.68 (m, 2H, H9), 2.39 (br s, 1H, OH), 2.00 (s, 3H, H14), 1.66-1.68 (m, 1H, H7), 1.51-1.42 (m, 1H, H6a), 1.42-1.21 (m, 10H, H2-H5) 1.20-1.10 (m, 1H H6b), 0.96-0.88 (m, 6H, H1+H15); ^{13}C-NMR (125MHz, $CDCL_3$): **Major diastereomer (anti)**: δ 200.1 (C10), 170.5 (C13), 72.0 (C8), 48.6 (C9), 39.4 (C12), 38.4 (C7), 32.8 (C5), 31.9 (C6), 29.6 (C11), 29.0 (C4), 27.3 (C3), 23.3 (C14), 22.7 (C2), 15.0 (C1), 14.2 (C15); **Minor diastereomer (syn)**: δ 200.2 (C10), 170.5 (C13), 72.7 (C8), 47.7 (C9), 39.4 (C12), 38.5 (C7), 32.8 (C5), 32.3 (C6), 29.6 (C11), 28.9 (C4), 27.1 (C3), 23.3 (C14), 22.7 (C2), 15.0 (C1), 14.2 (C15); HRMS (ES) Calcd for $C_{15}H_{29}NO_3SNa$ $[M+Na]^+$ 326.1760, found 326.1761.

(4*R*)-*S*-2-acetamidoethyl 4-methyl-3-oxo-decanethioate (131):

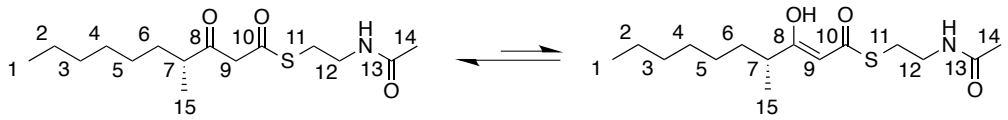

Compound **131** was oxidized from **138** using the procedure used to assemble **121** from **124**. Clear colourless oil, (8.4 mg, 34%). Title compound was isolated as a single spot by TLC (SiO2, Rf = 0.6, EtOAc). (70:30 keto:enol) $[\alpha]_D$ = 16.0 (*c* = 1.1 g/100mL, $CHCl_3$); IR ($CHCl_3$ cast): 3288.1, 2956.8, 2930.0, 2857.4, 1721.4, 1656.2, 1613.3, 1552.5 cm^{-1}; ^{1}H-NMR (500 MHz, CD_2Cl_2): δ 5.88 (br s, 1.3H, NH), 5.48 (s, 0.3H, enol-H9), 3.74 (s, 1.6H, keto-H9), 3.44-3.39 (m, 2H, H12), 3.08-3.05 (m, 2H, H11), 2.61 (tq, 0.7H, *J* = 6.8, 6.8 Hz, keto-H7), 2.19 (tq, 0.3H, *J* = 7.0 Hz, enol-H7), 1.91 (s, 3H, H14), 1.70-1.56 (m, 1H, H6), 1.42-1.20 (m, 10H, H2-5), 1.12 (d, 0.9H, *J* = 6.9 Hz, enol-H15), 1.08 (d, 2.1H, *J* = 6.9 Hz, keto-H15), 0.92-0.84 (m, 3H, H1); ^{13}C-NMR: δ 206.3 (C8), 194.8 (enol-C10), 192.7 (C10), 181.9 (enol-8), 170.3 (C13), 170.2 (enol-C13), 98.5 (enol-C9), 55.8 (C9), 47.4 (C7), 40.0 (enol-C7), 39.9 (enol-C12), 39.4 (C12), 34.5 (enol-C5), 32. 9 (C5), 32.1 (enol-C6) 32.0 (C6), 29.7 (C11), 29.6 (enol-C11), 29.5 (C4), 28.3 (enol-C4), 27.6 (enol-C3), 27.4 (C3), 23.3 (enol-C14), 23.2 (enol-2), 23.0 (C14), 29.9 (C2), 18.1 (enol-C15), 16.0 (C15), 14.2 (C1); HRMS (ES) Calcd for $C_{15}H_{28}NO_3S$ $[M+H]^+$ 302.1784, found 302.1785.

(4*R*)-3-hydroxy-2,4-dimethyl-1-(2-thioxo-3-thiazolidinyl)decanone (139):

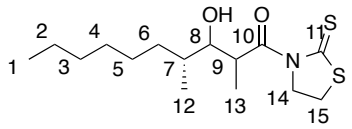

Compound **139** was prepared from **117** and **135** using the same method for preparation of **137** from **135** and **136**. Yellow, clear oil (3:1 mix of diastereomers; 75.3mg, 25% over two steps). IR ($CHCl_3$ cast) 3183, 2957, 2928, 2856, 1705, 1503 cm^{-1}; 1H-NMR (500MHz, $CDCl_3$) **Major diastereomer (syn):** δ 4.79 (qd, 1H, *J* = 6.9, 3.4 Hz, 1H, H9), 4.63-4.49 (m, 2H, H14), 3.70 (dd, 1H, *J* = 7.2, 3.9 Hz, H8), 3.34-3.23 (m, 2H, H15), 2.44 (br s, 1H, OH), 1.67-1.47 (m, 2H, H7, H6), 1.36-1.17 (m, 12H, H2 + H3 + H4 + H5 + H7' + H13), 1.17-1.04 (m, H6'), 0.97 (d, 3H, *J* = 6.6 Hz, H12), 0.90-0.82 (m, 3H, H1); **Minor diastereomer (anti):** δ 4.79-4.72 (m, 1H, H9), 4.63-4.49 (m, 2H, H14), 3.53 (m, 1H, H8), 3.34-3.23 (m, 2H, H15), 2.58 (br s, 1H, OH), 1.75-1.67 (m, 1H, H7), 1.36-1.17 (m, 13H, H2, H3, H4, H5, H6, H7', H13), 0.93 (d, 3H, *J* = 7.0 Hz, H12), 0.9-0.82 (m, 3H, H1); ^{13}C-NMR (125MHz, $CDCl_3$): **Major diastereomer:** δ 201.7, 179.4, 75.7, 56.5, 41.5, 35.8, 32.9, 31.9, 29.5, 28.3, 22.7, 15.3, 14.2, 11.2; **Minor diastereomer:** δ 201.7, 179.4, 80.1, 56.3, 41.6, 36.2,36.0, 32.0, 30.6, 29.6, 28.4, 27.2, 22.7, 16.7, 15.5, 11.2; HRMS (ES) Calcd for $C_{15}H_{27}NO_2S_2Na$ ($[M+Na]^+$) 340.1375, found 340.1372.

(4*R*)-*S*-2-acetamidoethyl 3-hydroxy-2,4-dimethyldecanethioate (140):

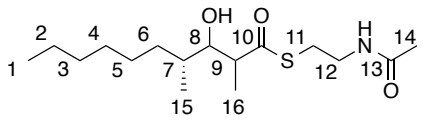

Compound **140** was synthesized from **139** using the same method used to **115** from **119**. Only *syn* diastereomer (major product) was purified as a single spot by TLC (SiO_2, R_f = 0.4, EtOAc). Clear, colourless oil (59 mg, 79%). IR (CH_2Cl_2, cast): 3299.9, 2959.9, 2928.2, 2857.2, 1683.1, 1658.7 cm^{-1}; ^{1}H-NMR (400MHz, $CDCl_3$): δ 5.75 (br s, 1H, NH), 3.70-3.65 (m, 1H, H8), 3.50-3.42 (m, 2H, H12), 3.06-3.01 (m, 2H, H11), 2.88 (qd, 1H, *J* = 7.0, 3.4 Hz, H9), 2.34 (br s, 1H, OH), 1.86 (s, 3H, H14), 1.73-1.64 (m, 1H, H7), 1.55-1.48 (m, 1H, H6), 1.44-1.34 (m, 1H, H5), 1.34-1.22 (m, 7H, H2+H3+H4+H6'), 1.20 (d, 3H, *J* = 7.0 Hz, H15), 1.18-1.08 (m, 1H, H5'), 0.91-0.84 (m, 6H, H1+H16); ^{13}C-NMR (100 MHz, $CDCl_3$) δ 204.7, 170.5, 76.3, 50.7, 39.5, 35.9, 32.1, 31.9, 29.7, 29.6, 28.6, 23.3, 22.7, 15.8, 14.1, 10.5; HRMS (ES) Calcd for $C_{16}H_{32}NO_3S$ ($[M+H]^+$) 317.2025, found 317.2026.

(4*R*)-S-2-acetamidoethyl 2,4-dimethyl-3-oxo-decanethioate (132):

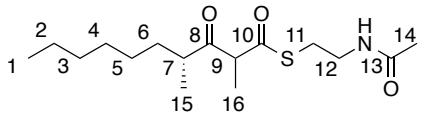

Compound **132** was prepared from **140** in the same manner as **131** from **138**. Clear, colourless oil (21.3 mg, 74%). Title compound was isolated as a single spot by TLC (SiO_2, R_f = 0.7, EtOAc). (5:1 keto:enol) IR (CH_2Cl_2, cast): 3289, 2931, 2857, 1722, 1663, 1659, 1550 cm^{-1}; ^{1}H-NMR (500MHz, $CDCl_3$) δ 6.00 (br s, 0.2H, enol-NH), 5.57 (br s, 1H, keto-NH), 3.94 (q, 1H, *J* = 7.0 Hz, H9), 3.53-3.36 (m, 2H, H12), 3.13-3.01 (m, 2H, H11), 2.78-2.70 (m, 1H, H7), 1.97 (s, 3H, H14), 1.89 (s, 0.6H, enol-H14), 1.70-1.62 (m, 1H, H6), 1.37 (m, 3H, H16), 1.35-1.17 (m, 9H, H2 + H3 + H4 + H5 + H6'), 1.12 (d, 0.6H, *J* = 6.9 Hz, enol-H15), 0.88 (m, 3H, H1); ^{13}C-NMR (125MHz, $CDCl_3$): (mix of keto and enol) δ 208.7, 208.6, 196.8, 196.6, 178.4, 170.5, 60.1, 59.8, 45.9, 45.7, 39.5, 32.1, 32.7, 31.7, 31.6, 29.4, 29.3, 29.2, 28.6, 27.2, 27.1, 23.1, 22.6, 22.5, 16.7, 16.4, 14.1, 14.0, 13.9, 13.8; HRMS (ES) Calcd for $C_{16}H_{29}NO_3SNa$ ($[M+Na]^+$) 338.1760, found 338.1760.

References

1. All natural. *Nat. Chem. Biol.,* **2007**, *3*, 351-351.
2. Newman, D. J.; Cragg, G. M. Natural products as sources of new drugs over the 30 years from 1981 to 2010. *J. Nat. Prod,* **2012**, *75*, 311-335.
3. Cragg, G. M.; Newman, D. J. Natural products: A continuing source of novel drug leads. *Biochim. Biophys. Acta, Gen. Subj.,* **2013**, *1830*, 3670-3695.
4. Karamehic, J.; Ridic, O.; Ridic, G.; Jukic, T.; Coric, J.; Subasic, D.; Panjeta, M.; Saban, A.; Zunic, L.; Masic, I. Financial aspects and the future of the pharmaceutical industry in the United States of America. *Mater. Sociomed.,* **2013**, *25*, 286-290.
5. Hay, M.; Thomas, D. W.; Craighead, J. L.; Economides, C.; Rosenthal, J. Clinical development success rates for investigational drugs. *Nat. Biotechnol.,* **2014**, *32*, 40-51.
6. DiMasi, J. A.; Grabowski, H. G.; Hansen, R. W. The cost of drug development. *N. Engl. J. Med.,* **2015**, *372*, 1972-1972.
7. Laxminarayan, R.; Duse, A.; Wattal, C.; Zaidi, A. K. M.; Wertheim, H. F. L.; Sumpradit, N.; Vlieghe, E.; Hara, G. L.; Gould, I. M.; Goossens, H.; Greko, C.; So, A. D.; Bigdeli, M.; Tomson, G.; Woodhouse, W.; Ombaka, E.; Peralta, A. Q.; Qamar, F. N.; Mir, F.; Kariuki, S.; Bhutta, Z. A.; Coates, A.; Bergstrom, R.; Wright, G. D.; Brown, E. D.; Cars, O. Antibiotic resistance—the need for global solutions. *Lancet Infect. Dis.,* **2013**, *13*, 1057-1098.
8. Staunton, J.; Weissman, K. J. Polyketide biosynthesis: a millennium review. *Nat. Prod. Rep.,* **2001**, *18*, 380-416.

9. Fischbach, M. A.; Walsh, C. T. Assembly-line enzymology for polyketide and nonribosomal peptide antibiotics: logic, machinery, and mechanisms. *Chem. Rev.,* **2006**, *106*, 3468-3496.

10. Hertweck, C. The biosynthetic logic of polyketide diversity. *Angew. Chem., Int. Ed.,* **2009**, *48*, 4688-4716.

11. Abraham, R. T.; Wiederrecht, G. J. Immunopharmacology of rapamycin. *Annu. Rev. Immunol.,* **1996**, *14*, 483-510.

12. De Clercq, E. Current lead natural products for the chemotherapy of human immunodeficiency virus (HIV) infection. *Med. Res. Rev.,* **2000**, *20*, 323-349.

13. Weisblum, B. Erythromycin resistance by ribosome modification. *Antimicrob. Agents Chemother.,* **1995**, *39*, 577-585.

14. Galm, U.; Hager, M. H.; Van Lanen, S. G.; Ju, J.; Thorson, J. S.; Shen, B. Antitumor antibiotics: bleomycin, enediynes, and mitomycin. *Chem. Rev.,* **2005**, *105*, 739-758.

15. Alberts, A. W.; Chen, J.; Kuron, G.; Hunt, V.; Huff, J.; Hoffman, C.; Rothrock, J.; Lopez, M.; Joshua, H.; Harris, E.; Patchett, A.; Monaghan, R.; Currie, S.; Stapley, E.; Albers-Schonberg, G.; Hensens, O.; Hirshfield, J.; Hoogsteen, K.; Liesch, J.; Springer, J. Mevinolin: a highly potent competitive inhibitor of hydroxymethylglutaryl-coenzyme A reductase and a cholesterol-lowering agent. *Proc. Natl. Acad. Sci. U.S.A.,* **1980**, *77*, 3957-3961.

16. Birch, A. J. Biosynthesis of polyketides and related compounds. *Science,* **1967**, *156*, 202-206.

17. Collie, J. N.; Chrystall, E. R. CLXX.-The production of orcinol derivatives from the sodium salt of ethyl acetoacetate by the action of heat. *J. Chem. Soc., Trans.,* **1907**, *91*, 1802-1806.

18. Collie, J. N. CLXXI.-Derivatives of the multiple keten group. *J. Chem. Soc., Trans.,* **1907**, *91*, 1806-1813.

19. Birch, A.; Massy-Westropp, R.; Moye, C. Studies in relation to biosynthesis. VII. 2-Hydroxy-6-methylbenzoic acid in *Penicillium griseofulvum*. *Aust. J. Chem.,* **1955**, *8*, 539-544.

20. Rittenberq, D.; Bloch, K. The utilization of acetic acid for fatty acid synthesis. *J. Biol. Chem.,* **1944**, *154*, 311-312.

21. Raper, H. S. CLXXV.-The condensation of acetaldehyde and its relation to the biochemical synthesis of fatty acids. *J. Chem. Soc., Trans.,* **1907**, *91*, 1831-1838.

22. Smith, S.; Tsai, S.-C. The type I fatty acid and polyketide synthases: a tale of two megasynthases. *Nat. Prod. Rep.,* **2007**, *24*, 1041-1072.

23. Malpartida, F.; Hopwood, D. A. Molecular cloning of the whole biosynthetic pathway of a Streptomyces antibiotic and its expression in a heterologous host. *Nature,* **1984**, *309*, 462-464.

24. Cortes, J.; Haydock, S. F.; Roberts, G. A.; Bevitt, D. J.; Leadlay, P. F. An unusually large multifunctional polypeptide in the erythromycin-producing polyketide synthase of *Saccharopolyspora erythraea*. *Nature,* **1990**, *348*, 176-178.

25. Tuan, J. S.; Weber, J. M.; Staver, M. J.; Leung, J. O.; Donadio, S.; Katz, L. Cloning of genes involved in erythromycin biosynthesis from *Saccharopolyspora erythraea* using a novel actinomycete-*Escherichia coli* cosmid. *Gene,* **1990**, *90*, 21-29.

26. Cane, D. E. Programming of erythromycin biosynthesis by a modular polyketide synthase. *J. Biol. Chem.,* **2010**, *285*, 27517-27523.

27. McDaniel, R.; Ebert-Khosla, S.; Hopwood, D. A.; Khosla, C. Engineered biosynthesis of novel polyketides. *Science,* **1993**, *262*, 1546-1550.

28. Lambalot, R. H.; Gehring, A. M.; Flugel, R. S.; Zuber, P.; LaCelle, M.; Marahiel, M. A.; Reid, R.; Khosla, C.; Walsh, C. T. A new enzyme superfamily — the phosphopantetheinyl transferases. *Chem. Biol.,* **1996**, *3*, 923-936.

29. Sattely, E. S.; Fischbach, M. A.; Walsh, C. T. Total biosynthesis: in vitro reconstitution of polyketide and nonribosomal peptide pathways. *Nat. Prod. Rep.,* **2008**, *25*, 757-793.

30. Stern, A.; Sedgwick, B.; Smith, S. The free coenzyme A requirement of animal fatty acid synthetase. Participation in the continuous exchange of acetyl and malonyl moieties between coenzyme a thioester and enzyme. *J. Biol. Chem.,* **1982**, *257*, 799-803.

31. Joshi, V. C.; Plate, C. A.; Wakil, S. J. Studies on the mechanism of fatty acid synthesis: XXIII. The acyl binding sites of the pigeon liver fatty acid synthetase. *J. Biol. Chem.,* **1970**, *245*, 2857-2867.

32. Kohli, R. M.; Walsh, C. T. Enzymology of acyl chain macrocyclization in natural product biosynthesis. *Chem. Commun.,* **2003**, 297-307.

33. Kopp, F.; Marahiel, M. A. Macrocyclization strategies in polyketide and nonribosomal peptide biosynthesis. *Nat. Prod. Rep.,* **2007**, *24*, 735-749.

34. Tsai, S.-C.; Miercke, L. J. W.; Krucinski, J.; Gokhale, R.; Chen, J. C.-H.; Foster, P. G.; Cane, D. E.; Khosla, C.; Stroud, R. M. Crystal structure of the macrocycle-forming thioesterase domain of the erythromycin polyketide synthase: Versatility from a unique substrate channel. *Proc. Natl. Acad. Sci. U.S.A.,* **2001**, *98*, 14808-14813.

35. Migita, A.; Watanabe, M.; Hirose, Y.; Watanabe, K.; Tokiwano, T.; Kinashi, H.; Oikawa, H. Identification of a gene cluster of polyether antibiotic lasalocid from *Streptomyces lasaliensis*. *Biosci., Biotechnol., Biochem.,* **2009**, *73*, 169-176.

36. Bililign, T.; Griffith, B. R.; Thorson, J. S. Structure, activity, synthesis and biosynthesis of aryl-C-glycosides. *Nat. Prod. Rep.,* **2005**, *22*, 742-760.

37. Kim, H. J.; Ruszczycky, M. W.; Choi, S.-h.; Liu, Y.-n.; Liu, H.-w. Enzyme-catalysed [4+2] cycloaddition is a key step in the biosynthesis of spinosyn A. *Nature,* **2011**, *473*, 109-112.

38. Cochrane, R. V. K.; Vederas, J. C. Highly selective but multifunctional oxygenases in secondary metabolism. *Acc. Chem. Res.,* **2014**, *47*, 3148-3161.

39. Rix, U.; Fischer, C.; Remsing, L. L.; Rohr, J. Modification of post-PKS tailoring steps through combinatorial biosynthesis. *Nat. Prod. Rep.,* **2002**, *19*, 542-580.

40. Cox, R. Oxidative rearrangements during fungal biosynthesis. *Nat. Prod. Rep.,* **2014**, *31*, 1405-1424.

41. John, U.; Beszteri, B.; Derelle, E.; Van de Peer, Y.; Read, B.; Moreau, H.; Cembella, A. Novel insights into evolution of protistan polyketide synthases through phylogenomic analysis. *Protist,* **2008**, *159*, 21-30.

42. Garg, A.; Xie, X.; Keatinge-Clay, A.; Khosla, C.; Cane, D. E. Elucidation of the cryptic epimerase activity of redox-inactive ketoreductase domains from modular polyketide synthases by tandem equilibrium isotope exchange. *J. Am. Chem. Soc.,* **2014**, *136*, 10190-10193.

43. Katz, L. In *Methods in Enzymology*; David, A. H., Ed.; Academic Press: 2009; Vol. Volume 459, p 113-142.

44. Heneghan, M. N.; Yakasai, A. A.; Williams, K.; Kadir, K. A.; Wasil, Z.; Bakeer, W.; Fisch, K. M.; Bailey, A. M.; Simpson, T. J.; Cox, R. J.; Lazarus, C. M. The programming role of trans-acting enoyl reductases during the biosynthesis of highly reduced fungal polyketides. *Chem. Sci.,* **2011**, *2*, 972-979.

45. Kennedy, J.; Auclair, K.; Kendrew, S. G.; Park, C.; Vederas, J. C.; Hutchinson, R. C. Modulation of polyketide synthase activity by accessory proteins during lovastatin biosynthesis. *Science,* **1999**, *284*, 1368-1372.

46. Chooi, Y.-H.; Tang, Y. Navigating the fungal polyketide chemical space: from genes to molecules. *J. Org. Chem.,* **2012**, *77*, 9933-9953.

47. Crawford, J. M.; Thomas, P. M.; Scheerer, J. R.; Vagstad, A. L.; Kelleher, N. L.; Townsend, C. A. Deconstruction of iterative multidomain polyketide synthase function. *Science,* **2008**, *320*, 243-246.

48. Xu, Y.; Zhou, T.; Zhou, Z.; Su, S.; Roberts, S. A.; Montfort, W. R.; Zeng, J.; Chen, M.; Zhang, W.; Lin, M.; Zhan, J.; Molnár, I. Rational reprogramming of fungal polyketide first-ring cyclization. *Proc. Natl. Acad. Sci. U.S.A.,* **2013**, *110*, 5398-5403.

49. Huitt-Roehl, C. R.; Hill, E. A.; Adams, M. M.; Vagstad, A. L.; Li, J. W.; Townsend, C. A. Starter unit flexibility for engineered product synthesis by the nonreducing polyketide synthase PksA. *ACS Chem. Biol.,* **2015**, *10*, 1443-1449.

50. Crawford, J. M.; Korman, T. P.; Labonte, J. W.; Vagstad, A. L.; Hill, E. A.; Kamari-Bidkorpeh, O.; Tsai, S.-C.; Townsend, C. A. Structural basis for biosynthetic programming of fungal aromatic polyketide cyclization. *Nature,* **2009**, *461*, 1139-1143.

51. Korman, T. P.; Crawford, J. M.; Labonte, J. W.; Newman, A. G.; Wong, J.; Townsend, C. A.; Tsai, S.-C. Structure and function of an iterative polyketide synthase thioesterase

domain catalyzing Claisen cyclization in aflatoxin biosynthesis. *Proc. Natl. Acad. Sci. U.S.A.,* **2010**, *107*, 6246-6251.

52. Dimroth, P.; Walter, H.; Lynen, F. Biosynthese von 6-methylsalicylsäure. *Eur. J. Biochem.,* **1970**, *13*, 98-110.

53. Fujii, I. Functional analysis of fungal polyketide biosynthesis genes. *J. Antibiot.,* **2010**, *63*, 207-218.

54. Moriguchi, T.; Kezuka, Y.; Nonaka, T.; Ebizuka, Y.; Fujii, I. Hidden function of catalytic domain in 6-methylsalicylic acid synthase for product release. *J. Biol. Chem.,* **2010**, *285*, 15637-15643.

55. Kage, H.; Kreutzer, Martin F.; Wackler, B.; Hoffmeister, D.; Nett, M. An iterative type I polyketide synthase initiates the biosynthesis of the antimycoplasma agent micacocidin. *Chem. Biol.,* **2013**, *20*, 764-771.

56. Sun, H.; Ho, C. L.; Ding, F.; Soehano, I.; Liu, X.-W.; Liang, Z.-X. Synthesis of (*R*)-mellein by a partially reducing iterative polyketide synthase. *J. Am. Chem. Soc.,* **2012**, *134*, 11924-11927.

57. Kasahara , K.; Miyamoto, T.; Fujimoto, T.; Oguri, H.; Tokiwano , T.; Oikawa, H.; Ebizuka, Y.; Fujii, I. Solanapyrone synthase, a possible Diels–Alderase and iterative type I polyketide synthase encoded in a biosynthetic gene cluster from *Alternaria solani*. *ChemBioChem,* **2010**, *11*, 1245-1252.

58. Winssinger, N.; Barluenga, S. Chemistry and biology of resorcylic acid lactones. *Chem. Commun.,* **2007**, 22-36.

59. Hertweck, C.; Luzhetskyy, A.; Rebets, Y.; Bechthold, A. Type II polyketide synthases: gaining a deeper insight into enzymatic teamwork. *Nat. Prod. Rep.,* **2007**, *24*, 162-190.

60. Levy, S. B.; McMurry, L. M.; Barbosa, T. M.; Burdett, V.; Courvalin, P.; Hillen, W.; Roberts, M. C.; Rood, J. I.; Taylor, D. E. Nomenclature for new tetracycline resistance determinants. *Antimicrob. Agents Chemother.,* **1999**, *43*, 1523-1524.

61. Pickens, L. B.; Tang, Y. Oxytetracycline biosynthesis. *J. Biol. Chem.,* **2010**, *285*, 27509-27515.

62. Bisang, C.; Long, P. F.; Cortes, J.; Westcott, J.; Crosby, J.; Matharu, A.-L.; Cox, R. J.; Simpson, T. J.; Staunton, J.; Leadlay, P. F. A chain initiation factor common to both modular and aromatic polyketide synthases. *Nature,* **1999**, *401*, 502-505.

63. Keatinge-Clay, A. T.; Maltby, D. A.; Medzihradszky, K. F.; Khosla, C.; Stroud, R. M. An antibiotic factory caught in action. *Nat. Struct. Mol. Biol.,* **2004**, *11*, 888-893.

64. Tang, Y.; Tsai, S.-C.; Khosla, C. Polyketide chain length control by chain length factor. *J. Am. Chem. Soc.,* **2003**, *125*, 12708-12709.

65. Katsuyama, Y.; Ohnishi, Y. In *Methods in Enzymology*; David, A. H., Ed.; Academic Press: 2012; Vol. Volume 515, p 359-377.

66. Morita, H.; Yamashita, M.; Shi, S.-P.; Wakimoto, T.; Kondo, S.; Kato, R.; Sugio, S.; Kohno, T.; Abe, I. Synthesis of unnatural alkaloid scaffolds by exploiting plant polyketide synthase. *Proc. Natl. Acad. Sci. U.S.A.,* **2011**, *108*, 13504-13509.

67. Austin, M. B.; Noel, J. P. The chalcone synthase superfamily of type III polyketide synthases. *Nat. Prod. Rep.,* **2003**, *20*, 79-110.

68. Austin, M. B.; Izumikawa, M.; Bowman, M. E.; Udwary, D. W.; Ferrer, J.-L.; Moore, B. S.; Noel, J. P. Crystal structure of a bacterial type III polyketide synthase and enzymatic control of reactive polyketide intermediates. *J. Biol. Chem.,* **2004**, *279*, 45162-45174.

69. Abe, I.; Morita, H. Structure and function of the chalcone synthase superfamily of plant type III polyketide synthases. *Nat. Prod. Rep.,* **2010**, *27*, 809-838.

70. Austin, M. B.; Bowman, M. E.; Ferrer, J.-L.; Schröder, J.; Noel, J. P. An aldol switch discovered in stilbene synthases mediates cyclization specificity of type III polyketide synthases. *Chem. Biol.,* **2004**, *11*, 1179-1194.

71. Yu , F.; Zaleta-Rivera, K.; Zhu, X.; Huffman, J.; Millet, J. C.; Harris, S. D.; Yuen, G.; Li, X.-C.; Du, L. Structure and biosynthesis of heat-stable antifungal factor (HSAF), a broad-spectrum antimycotic with a novel mode of action. *Antimicrob. Agents Chemother.,* **2007**, *51*, 64-72.

72. Chen, X.-H.; Vater, J.; Piel, J.; Franke, P.; Scholz, R.; Schneider, K.; Koumoutsi, A.; Hitzeroth, G.; Grammel, N.; Strittmatter, A. W.; Gottschalk, G.; Süssmuth, R. D.; Borriss, R. Structural and functional characterization of three polyketide synthase gene clusters in *Bacillus amyloliquefaciens* FZB 42. *J. Bacteriol.,* **2006**, *188*, 4024-4036.

73. Eley, K. L.; Halo, L. M.; Song, Z.; Powles, H.; Cox, R. J.; Bailey, A. M.; Lazarus, C. M.; Simpson, T. J. Biosynthesis of the 2-pyridone tenellin in the insect pathogenic fungus *Beauveria bassiana*. *ChemBioChem,* **2007**, *8*, 289-297.

74. Jeffs, L. B.; Khachatourians, G. G. Toxic properties of *Beauveria pigments* on erythrocyte membranes. *Toxicon,* **1997**, *35*, 1351-1356.

75. Jirakkakul, J.; Cheevadhanarak, S.; Punya, J.; Chutrakul, C.; Senachak, J.; Buajarern, T.; Tanticharoen, M.; Amnuaykanjanasin, A. Tenellin acts as an iron chelator to prevent iron-generated reactive oxygen species toxicity in the entomopathogenic fungus *Beauveria bassiana*. *FEMS Microbiol. Lett.,* **2015**, *362*, 1-8.

76. Song, Z.; Cox, R. J.; Lazarus, C. M.; Simpson, T. J. Fusarin C biosynthesis in *Fusarium moniliforme* and *Fusarium venenatum*. *ChemBioChem,* **2004**, *5*, 1196-1203.

77. Keatinge-Clay, A. T. The structures of type I polyketide synthases. *Nat. Prod. Rep.,* **2012**, *29*, 1050-1073.

78. Ma, S. M.; Li, J. W.-H.; Choi, J. W.; Zhou, H.; Lee, K. K. M.; Moorthie, V. A.; Xie, X.; Kealey, J. T.; Da Silva, N. A.; Vederas, J. C.; Tang, Y. Complete reconstitution of a highly reducing iterative polyketide synthase. *Science,* **2009**, *326*, 589-592.

79. Fisch, K. M.; Bakeer, W.; Yakasai, A. A.; Song, Z.; Pedrick, J.; Wasil, Z.; Bailey, A. M.; Lazarus, C. M.; Simpson, T. J.; Cox, R. J. Rational domain swaps decipher programming in fungal highly reducing polyketide synthases and resurrect an extinct metabolite. *J. Am. Chem. Soc.,* **2011**, *133*, 16635-16641.

80. Xu, W.; Cai, X.; Jung, M. E.; Tang, Y. Analysis of intact and dissected fungal polyketide synthase-nonribosomal peptide synthetase *in vitro* and in *Saccharomyces cerevisiae*. *J. Am. Chem. Soc.,* **2010**, *132*, 13604-13607.

81. Ugai, T.; Minami, A.; Fujii, R.; Tanaka, M.; Oguri, H.; Gomi, K.; Oikawa, H. Heterologous expression of highly reducing polyketide synthase involved in betaenone biosynthesis. *Chem. Commun.,* **2015**, *51*, 1878-1881.

82. Tagami, K.; Minami, A.; Fujii, R.; Liu, C.; Tanaka, M.; Gomi, K.; Dairi, T.; Oikawa, H. Rapid reconstitution of biosynthetic machinery for fungal metabolites in *Aspergillus oryzae*: total biosynthesis of aflatrem. *ChemBioChem,* **2014**, *15*, 2076-2080.

83. Liew, C. W.; Nilsson, M.; Chen, M. W.; Sun, H.; Cornvik, T.; Liang, Z.-X.; Lescar, J. Crystal structure of the acyltransferase domain of the iterative polyketide synthase in enediyne biosynthesis. *J. Biol. Chem.,* **2012**, *287*, 23203-23215.

84. Tang, Y.; Kim, C.-Y.; Mathews, I. I.; Cane, D. E.; Khosla, C. The 2.7-Å crystal structure of a 194-kDa homodimeric fragment of the 6-deoxyerythronolide B synthase. *Proc. Natl. Acad. Sci. U.S.A.,* **2006**, *103*, 11124-11129.

85. Weissman, K. J. Uncovering the structures of modular polyketide synthases. *Nat. Prod. Rep.,* **2015**, *32*, 436-453.

86. Whicher, J. R.; Dutta, S.; Hansen, D. A.; Hale, W. A.; Chemler, J. A.; Dosey, A. M.; Narayan, A. R. H.; Hakansson, K.; Sherman, D. H.; Smith, J. L.; Skiniotis, G. Structural rearrangements of a polyketide synthase module during its catalytic cycle. *Nature,* **2014**, *510*, 560-564.

87. Gao, Z.; Wang, J.; Norquay, A. K.; Qiao, K.; Tang, Y.; Vederas, J. C. Investigation of fungal iterative polyketide synthase functions using partially assembled intermediates. *J. Am. Chem. Soc.,* **2013**, *135*, 1735-1738.

88. Aldridge, D. C.; Burrows, B. F.; Turner, W. B. The structures of the fungal metabolites cytochalasins E and F. *J. Chem. Soc., Chem. Commun.,* **1972**, 148-149.

89. ten Hoopen, G. M.; Krauss, U. Biology and control of *Rosellinia bunodes*, *Rosellinia necatrix* and *Rosellinia pepo*: A review. *Crop Prot.,* **2006**, *25*, 89-107.

90. Buechi, G.; Kitaura, Y.; Yuan, S.-S.; Wright, H. E.; Clardy, J.; Demain, A. L.; Glinsukon, T.; Hunt, N.; Wogan, G. N. Structure of cytochalasin E, a toxic metabolite of *Aspergillus clavatus*. *J. Am. Chem. Soc.,* **1973**, *95*, 5423-5425.

91. Zhang, H.; Liu, H.-B.; Yue, J.-M. Organic carbonates from natural sources. *Chem. Rev.,* **2014**, *114*, 883-898.

92. Scherlach, K.; Boettger, D.; Remme, N.; Hertweck, C. The chemistry and biology of cytochalasans. *Nat. Prod. Rep.,* **2010**, *27*, 869-886.

93. Mookerjee, B. K.; Cuppoletti, J.; Rampal, A. L.; Jung, C. Y. The effects of cytochalasins on lymphocytes. Identification of distinct cytochalasin-binding sites in relation to mitogenic response and hexose transport. *J. Biol. Chem.,* **1981**, *256*, 1290-1300.

94. Udagawa, T.; Yuan, J.; Panigrahy, D.; Chang, Y.-H.; Shah, J.; D'Amato, R. J. Cytochalasin E, an epoxide containing *Aspergillus*-derived fungal metabolite, inhibits angiogenesis and tumor growth. *J. Pharmacol. Exp. Ther.,* **2000**, *294*, 421-427.

95. Graf, W.; Robert, J.-L.; Vederas, J. C.; Tamm, C.; Solomon, P. H.; Miura, I.; Nakanishi, K. Biosynthesis of the cytochalasans. Part III. 13C-NMR. of cytochalasin B (phomin) and cytochalasin D. Incorporation of [1-13C]- and [2-13C]-sodium acetate. *Helv. Chim. Acta,* **1974**, *57*, 1801-1815.

96. Binder, M.; Tamm, C. The cytochalasans: a new class of biologically active microbial metabolites. *Angew. Chem., Int. Ed. Eng.,* **1973**, *12*, 370-380.

97. Binder, M.; Kiechel, J. R.; Tamm, C. Zur biogenese des antibioticums phomin. 1. Teil: Die grundbausteine. *Helv. Chim. Acta,* **1970**, *53*, 1797-1812.

98. Robert, J.-L.; Tamm, C. Biosynthesis of cytochalasans. Part 5. the incorporation of deoxaphomin into cytochalasin B (phomin). *Helv. Chim. Acta,* **1975**, *58*, 2501-2504.

99. Schümann, J.; Hertweck, C. Molecular basis of cytochalasan biosynthesis in fungi: gene cluster analysis and evidence for the involvement of a PKS-NRPS hybrid synthase by RNA silencing. *J. Am. Chem. Soc.,* **2007**, *129*, 9564-9565.

100. Qiao, K.; Chooi, Y.-H.; Tang, Y. Identification and engineering of the cytochalasin gene cluster from *Aspergillus clavatus* NRRL 1. *Metab. Eng.,* **2011**, *13*, 723-732.

101. Qiao, K.; Zhou, H.; Xu, W.; Zhang, W.; Garg, N.; Tang, Y. A fungal nonribosomal peptide synthetase module that can synthesize thiopyrazines. *Org. Lett.,* **2011**, *13*, 1758-1761.

102. Vederas, J. C.; Nakashima, T. T. Biosynthesis of averufin by *Aspergillus parasiticus*; detection of 18O-label by 13C-NMR isotope shifts. *J. Chem. Soc., Chem. Commun.,* **1980**, 183-185.

103. Diakur, J.; Nakashima, T. T.; Vederas, J. C. Magnitudes of 18O isotope shifts in 13C nuclear magnetic resonance spectra of ketones and alcohols. *Can. J. Chem.,* **1980**, *58*, 1311-1315.

104. Hong, X.; Mejía-Oneto, J. M.; Padwa, A. Lewis acid-promoted α-hydroxy β-dicarbonyl to α-ketol ester rearrangement. *Tetrahedron Lett.,* **2006**, *47*, 8387-8390.

105. Rubin, M. B.; Inbar, S. Equilibria among anions of α-hydroxy-β-diketones and α-ketol esters. *J. Org. Chem.,* **1988**, *53*, 3355-3358.

106. Kim, M. Y.; Starrett, J. E.; Weinreb, S. M. Synthetic approach to cytochalasins. *J. Org. Chem.,* **1981**, *46*, 5383-5389.

107. Merifield, E.; J. Thomas, E. Total synthesis of cytochalasin D: total synthesis and full structural assignment of cytochalasin O. *J. Chem. Soc., Perkin Trans. 1,* **1999**, 3269-3283.

108. Stork, G.; Nakahara, Y.; Nakahara, Y.; Greenlee, W. J. Total synthesis of cytochalasin B. *J. Am. Chem. Soc.,* **1978**, *100*, 7775-7777.

109. Vedejs, E.; Reid, J. G. Total synthesis of carbocyclic cytochalasans. *J. Am. Chem. Soc.,* **1984**, *106*, 4617-4618.

110. Wang, J.-F.; Huang, Y.-J.; Xu, Q.-Y.; Zheng, Z.-H.; Zhao, Y.-F.; Su, W.-J. X-ray crystal structure of cytochalasin D produced by *Tubercularia sp*., a novel endophytic fungus of *Taxus mairei*. *J. Chem. Crystallogr.,* **2003**, *33*, 51-56.

111. Schreiber, J.; Eschenmoser, A. Über die relative Geschwindigkeit der Chromosäureoxydation sekundärer, alicyclischer Alkohole. Vorläufige Mitteilung. *Helv. Chim. Acta,* **1955**, *38*, 1529-1536.

112. Winstein, S.; Holness, N. J. Neighboring carbon and hydrogen. XIX. t-Butylcyclohexyl derivatives. Quantitative conformational analysis. *J. Am. Chem. Soc.,* **1955**, *77*, 5562-5578.

113. Krow, G. R. In *Organic Reactions*; John Wiley & Sons, Inc.: 2004.

114. Iida, M.; Ooi, T.; Kito, K.; Yoshida, S.; Kanoh, K.; Shizuri, Y.; Kusumi, T. Three new polyketide−terpenoid hybrids from *Penicillium sp*. *Org. Lett.,* **2008**, *10*, 845-848.

115. Hensens, O. D.; Giner, J. L.; Goldberg, I. H. Biosynthesis of NCS Chrom A, the chromophore of the antitumor antibiotic neocarzinostatin. *J. Am. Chem. Soc.,* **1989**, *111*, 3295-3299.

116. Hu, Y.; Dietrich, D.; Xu, W.; Patel, A.; Thuss, J. A. J.; Wang, J.; Yin, W.-B.; Qiao, K.; Houk, K. N.; Vederas, J. C.; Tang, Y. A carbonate-forming Baeyer-Villiger monooxygenase. *Nat. Chem. Biol.,* **2014**, *10*, 552-554.

117. Walsh, C. T.; Chen, Y. C. J. Enzymic Baeyer–Villiger oxidations by flavin-dependent monooxygenases. *Angew. Chem., Int. Ed. Eng.,* **1988**, *27*, 333-343.

118. Criegee, R. Die Umlagerung der dekalin-peroxydester als folge von kationischem sauerstoff. *Justus Liebigs Ann. Chem.,* **1948**, *560*, 127-135.

119. Leisch, H.; Morley, K.; Lau, P. C. K. Baeyer−Villiger monooxygenases: more than just green chemistry. *Chem. Rev.,* **2011**, *111*, 4165-4222.

120. Ryerson, C. C.; Ballou, D. P.; Walsh, C. Mechanistic studies on cyclohexanone oxygenase. *Biochemistry,* **1982**, *21*, 2644-2655.

121. Samuelsson, B. On the incorporation of oxygen in the conversion of 8,11,14-eicosatrienoic acid to prostaglandin E1. *J. Am. Chem. Soc.,* **1965**, *87*, 3011-3013.

122. Ryhage, R.; Samuelsson, B. The origin of oxygen incorporated during the biosynthesis of prostaglandin E1. *Biochem. Biophys. Res. Commun.,* **1965**, *19*, 279-282.

123. Kakule, T. B.; Lin, Z.; Schmidt, E. W. Combinatorialization of fungal polyketide synthase–peptide synthetase hybrid proteins. *J. Am. Chem. Soc.,* **2014**, *136*, 17882-17890.

124. Yue, S.; Duncan, J. S.; Yamamoto, Y.; Hutchinson, C. R. Macrolide biosynthesis. Tylactone formation involves the processive addition of three carbon units. *J. Am. Chem. Soc.,* **1987**, *109*, 1253-1255.

125. Cane, D. E.; Yang, C. C. Macrolide biosynthesis. 4. Intact incorporation of a chain-elongation intermediate into erythromycin. *J. Am. Chem. Soc.,* **1987**, *109*, 1255-1257.

126. Oikawa, H.; Katayama, K.; Suzuki, Y.; Ichihara, A. Enzymatic activity catalysing exo-selective Diels-Alder reaction in solanapyrone biosynthesis. *J. Chem. Soc., Chem. Commun.,* **1995**, 1321-1322.

127. Auclair, K.; Sutherland, A.; Kennedy, J.; Witter, D. J.; Van den Heever, J. P.; Hutchinson, C. R.; Vederas, J. C. Lovastatin nonaketide synthase catalyzes an intramolecular Diels−Alder reaction of a substrate analogue. *J. Am. Chem. Soc.,* **2000**, *122*, 11519-11520.

128. Kato, N.; Nogawa, T.; Hirota, H.; Jang, J.-H.; Takahashi, S.; Ahn, J. S.; Osada, H. A new enzyme involved in the control of the stereochemistry in the decalin formation during equisetin biosynthesis. *Biochem. Biophys. Res. Commun.,* **2015**, *460*, 210-215.

129. Hashimoto, T.; Hashimoto, J.; Teruya, K.; Hirano, T.; Shin-ya, K.; Ikeda, H.; Liu, H.-w.; Nishiyama, M.; Kuzuyama, T. Biosynthesis of versipelostatin: identification of an enzyme-catalyzed [4+2]-cycloaddition required for macrocyclization of spirotetronate-containing polyketides. *J. Am. Chem. Soc.,* **2015**, *137*, 572-575.

130. Witter, D. J.; Vederas, J. C. Putative Diels−Alder-catalyzed cyclization during the biosynthesis of lovastatin. *J. Org. Chem.,* **1996**, *61*, 2613-2623.

131. Tian, Z.; Sun, P.; Yan, Y.; Wu, Z.; Zheng, Q.; Zhou, S.; Zhang, H.; Yu, F.; Jia, X.; Chen, D.; Mándi, A.; Kurtán, T.; Liu, W. An enzymatic [4+2] cyclization cascade creates the pentacyclic core of pyrroindomycins. *Nat. Chem. Biol.,* **2015**, *11*, 259-265.

132. Fujii, R.; Minami, A.; Gomi, K.; Oikawa, H. Biosynthetic assembly of cytochalasin backbone. *Tetrahedron Lett.,* **2013**, *54*, 2999-3002.

133. Podust, L. M.; Sherman, D. H. Diversity of P450 enzymes in the biosynthesis of natural products. *Nat. Prod. Rep.,* **2012**, *29*, 1251-1266.

134. Yonemitsu, O.; Elghanian, K.-i.; Hart, A. C. In *Encyclopedia of Reagents for Organic Synthesis*; John Wiley & Sons, Ltd: 2001.

135. Hansen, D. B.; Starr, M.-L.; Tolstoy, N.; Joullié, M. M. A stereoselective synthesis of (2S,4R)-δ-hydroxyleucine methyl ester: a component of cyclomarin A. *Tetrahedron: Asymmetry,* **2005**, *16*, 3623-3627.

136. Taylor, R. E.; Chen, Y.; Galvin, G. M.; Pabba, P. K. Conformation-activity relationships in polyketide natural products. Towards the biologically active conformation of epothilone. *Org. Biomol. Chem.,* **2004**, *2*, 127-132.

137. Maryanoff, B. E.; Reitz, A. B. The Wittig olefination reaction and modifications involving phosphoryl-stabilized carbanions. Stereochemistry, mechanism, and selected synthetic aspects. *Chem. Rev.,* **1989**, *89*, 863-927.

138. Ando, K. A mechanistic study of the Horner−Wadsworth−Emmons reaction: computational investigation on the reaction pass and the stereochemistry in the reaction of lithium enolate derived from trimethyl phosphonoacetate with acetaldehyde. *J. Org. Chem.,* **1999**, *64*, 6815-6821.

139. Maggon, K. Best-selling human medicines 2002-2004. *Drug Discovery Today,* **2005**, *10*, 739-742.

140. Mulder, K. C. L.; Mulinari, F.; Franco, O. L.; Soares, M. S. F.; Magalhães, B. S.; Parachin, N. S. Lovastatin production: From molecular basis to industrial process optimization. *Biotechnol. Adv.,* **2015**, *in press*.

141. Goldstein, J. L.; Brown, M. S. Regulation of the mevalonate pathway. *Nature,* **1990**, *343*, 425-430.

142. Endo, A.; Hasumi, K. HMG-CoA reductase inhibitors. *Nat. Prod. Rep.,* **1993**, *10*, 541-550.

143. Endo, A.; Kuroda, M.; Tsujita, Y. ML-236a, ML-236b, and ML-236c, new inhibitors of cholesterogenesis produced by *Penicillium citrinum J. Antibiot.,* **1976**, *29*, 1346-1348.

144. Chen, Y.-P.; Tseng, C.-P.; Liaw, L.-L.; Wang, C.-L.; Chen, I. C.; Wu, W.-J.; Wu, M.-D.; Yuan, G.-F. Cloning and characterization of monacolin K biosynthetic gene cluster from *Monascus pilosus*. *J. Agric. Food Chem.,* **2008**, *56*, 5639-5646.

145. Barriuso, J.; Nguyen, D. T.; Li, J. W. H.; Roberts, J. N.; MacNevin, G.; Chaytor, J. L.; Marcus, S. L.; Vederas, J. C.; Ro, D.-K. Double oxidation of the cyclic nonaketide dihydromonacolin L to monacolin J by a single cytochrome P450 monooxygenase, LovA. *J. Am. Chem. Soc.,* **2011**, *133*, 8078-8081.

146. Campbell, C. D.; Vederas, J. C. Biosynthesis of lovastatin and related metabolites formed by fungal iterative PKS enzymes. *Biopolymers,* **2010**, *93*, 755-763.

147. Xu, W.; Chooi, Y.-H.; Choi, J. W.; Li, S.; Vederas, J. C.; Da Silva, N. A.; Tang, Y. LovG: The thioesterase required for dihydromonacolin L release and lovastatin nonaketide synthase turnover in lovastatin biosynthesis. *Angew. Chem., Int. Ed.,* **2013**, *52*, 6472-6475.

148. Xie, X.; Meehan, M. J.; Xu, W.; Dorrestein, P. C.; Tang, Y. Acyltransferase mediated polyketide release from a fungal megasynthase. *J. Am. Chem. Soc.,* **2009**, *131*, 8388-8389.

149. Jiménez-Osés, G.; Osuna, S.; Gao, X.; Sawaya, M. R.; Gilson, L.; Collier, S. J.; Huisman, G. W.; Yeates, T. O.; Tang, Y.; Houk, K. N. The role of distant mutations and allosteric regulation on LovD active site dynamics. *Nat. Chem. Biol.,* **2014**, *10*, 431-436.

150. Xie, X.; Pashkov, I.; Gao, X.; Guerrero, J. L.; Yeates, T. O.; Tang, Y. Rational improvement of simvastatin synthase solubility in *Escherichia coli* leads to higher whole-cell biocatalytic activity. *Biotechnol. Bioeng.,* **2009**, *102*, 20-28.

151. Gao, X.; Xie, X.; Pashkov, I.; Sawaya, M. R.; Laidman, J.; Zhang, W.; Cacho, R.; Yeates, T. O.; Tang, Y. Directed evolution and structural characterization of a simvastatin synthase. *Chem. Biol.,* **2009**, *16*, 1064-1074.

152. Wagschal, K.; Yoshizawa, Y.; Witter, D. J.; Liu, Y.; Vederas, J. C. Biosynthesis of ML-236C and the hypocholesterolemic agents compactin by *Penicillium aurantiogriseum* and lovastatin by *Aspergillus terreus*: determination of the origin of carbon, hydrogen and oxygen atoms by 13C NMR spectrometry and observation of unusual labelling of acetate-derived oxygens by 18O2. *J. Chem. Soc., Perkin Trans. 1,* **1996**, 2357-2363.

153. Yoshizawa, Y.; Witter, D. J.; Liu, Y.; Vederas, J. C. Revision of the biosynthetic origin of oxygens in mevinolin (lovastatin), a hypocholesterolemic drug from *Aspergillus terreus* MF 4845. *J. Am. Chem. Soc.,* **1994**, *116*, 2693-2694.

154. Moore, R. N.; Bigam, G.; Chan, J. K.; Hogg, A. M.; Nakashima, T. T.; Vederas, J. C. Biosynthesis of the hypocholesterolemic agent mevinolin by *Aspergillus terreus*. Determination of the origin of carbon, hydrogen, and oxygen atoms by carbon-13 NMR and mass spectrometry. *J. Am. Chem. Soc.,* **1985**, *107*, 3694-3701.

155. Chan, J. K.; Moore, R. N.; Nakashima, T. T.; Vederas, J. C. Biosynthesis of mevinolin. Spectral assignment by double-quantum coherence NMR after high carbon-13 incorporation. *J. Am. Chem. Soc.,* **1983**, *105*, 3334-3336.

156. Treiber, L. R. R., R. A.; Rooney, C. S.; Ramjit, H. G. Origin of monacolin L from *Aspergillus terreus* cultures. *J. Antibiot.,* **1989**, *42*, 30-36.

157. Nakamura, T. K., D.; Murakawa, S.; Sakai, K.; Endo, A. Isolation and biosynthesis of 3α-hydroxy-3,5-dihydromonacolin L. *J. Antibiot.,* **1990**, *43*, 1597-1600.

158. Burr, D. A.; Chen, X. B.; Vederas, J. C. Syntheses of conjugated pyrones for the enzymatic assay of lovastatin nonaketide synthase, an iterative polyketide synthase. *Org. Lett.,* **2007**, *9*, 161-164.

159. Abe, Y.; Suzuki, T.; Ono, C.; Iwamoto, K.; Hosobuchi, M.; Yoshikawa, H. Molecular cloning and characterization of an ML-236B (compactin) biosynthetic gene cluster in *Penicillium citrinum*. *Mol. Gen. Genomics,* **2002**, *267*, 636-646.

160. Hopwood, D. A.; Sherman, D. H. Molecular genetics of polyketides and its comparison to fatty acid biosynthesis. *Annu. Rev. Genet.,* **1990**, *24*, 37-62.

161. David, H. K.; Schulz, F. The stereochemistry of complex polyketide biosynthesis by modular polyketide synthases. *Molecules,* **2011**, *16*, 6092-6115.

162. Schönherr, H.; Cernak, T. Profound methyl effects in drug discovery and a aall for new C-H methylation reactions. *Angew. Chem., Int. Ed.,* **2013**, *52*, 12256-12267.

163. Gui, J.; Zhou, Q.; Pan, C.-M.; Yabe, Y.; Burns, A. C.; Collins, M. R.; Ornelas, M. A.; Ishihara, Y.; Baran, P. S. C–H methylation of heteroarenes inspired by radical SAM methyl transferase. *J. Am. Chem. Soc.,* **2014**, *136*, 4853-4856.

164. Olmstead, W. N.; Bordwell, F. G. Ion-pair association constants in dimethyl sulfoxide. *J. Org. Chem.,* **1980**, *45*, 3299-3305.

165. Bordwell, F. G. Equilibrium acidities in dimethyl sulfoxide solution. *Acc. Chem. Res.,* **1988**, *21*, 456-463.

166. Crimmins, M. T.; Chaudhary, K. In *Encyclopedia of Reagents for Organic Synthesis*; John Wiley & Sons, Ltd: 2001.

167. Ge, H.-M.; Huang, T.; Rudolf, J. D.; Lohman, J. R.; Huang, S.-X.; Guo, X.; Shen, B. Enediyne polyketide synthases stereoselectively reduce the β-ketoacyl intermediates to β-

d-hydroxyacyl intermediates in enediyne core biosynthesis. *Org. Lett.,* **2014**, *16*, 3958-3961.

168. Kumagai, A.; Nagaoka, Y.; Obayashi, T.; Terashima, Y.; Tokuda, H.; Hara, Y.; Mukainaka, T.; Nishino, H.; Kuwajima, H.; Uesato, S. Tumor chemopreventive activity of 3-O-acylated (−)-epigallocatechins. *Bioorg. Med. Chem.,* **2003**, *11*, 5143-5148.

169. Minko, Y.; Pasco, M.; Lercher, L.; Botoshansky, M.; Marek, I. Forming all-carbon quaternary stereogenic centres in acyclic systems from alkynes. *Nature,* **2012**, *490*, 522-526.

170. Pi, N.; Leary, J. A. Determination of enzyme/substrate specificity constants using a multiple substrate ESI-MS assay. *J. Am. Soc. Mass Spectrom.,* **2004**, *15*, 233-243.

171. Armarego, W. L. F.; Chai, C. L. L. In *Purification of Laboratory Chemicals (Fifth Edition)*; Chai, W. L. F. A. L. L., Ed.; Butterworth-Heinemann: Burlington, 2003, p xi-xii.

172. Still, W. C.; Kahn, M.; Mitra, A. Rapid chromatographic technique for preparative separations with moderate resolution. *J. Org. Chem.,* **1978**, *43*, 2923-2925.

173. Healy, A. R.; Vinale, F.; Lorito, M.; Westwood, N. J. Total synthesis and biological evaluation of the tetramic acid based natural product harzianic acid and its stereoisomers. *Org. Lett.,* **2015**, *17*, 692-695.

174. Meiries, S.; Bartoli, A.; Decostanzi, M.; Parrain, J.-L.; Commeiras, L. Directed studies towards the total synthesis of (+)-13-deoxytedanolide: simple and convenient synthesis of the C8-C16 fragment. *Org. Biomol. Chem.,* **2013**, *11*, 4882-4890.

175. Marin, J.; Didierjean, C.; Aubry, A.; Casimir, J. R.; Briand, J. P.; Guichard, G. Synthesis of enantiopure 4-hydroxypipecolate and 4-hydroxylysine derivatives from a common 4,6-dioxopiperidinecarboxylate precursor. *J. Org. Chem.,* **2004**, *69*, 130-141.

176. Hoffmann, Reinhard W.; Göttlich, R.; Schopfer, U. Conformation induction between neighboring dimethylpentane segments. *Eur. J. Org. Chem.,* **2001**, *2001*, 1865-1871.

177. DeBoef, B.; Counts, W. R.; Gilbertson, S. R. Rhodium-catalyzed synthesis of eight-membered rings. *J. Org. Chem.,* **2007**, *72*, 799-804.

178. Burke, L. T.; Dixon, D. J.; Ley, S. V.; Rodriguez, F. Total synthesis of the *Fusarium* toxin equisetin. *Org. Biomol. Chem.,* **2005**, *3*, 274-280.

179. Czuba, I. R.; Zammit, S.; Rizzacasa, M. A. Total synthesis of the marine sponge metabolites (+)-rottnestol, (+)-raspailol A and (+)-raspailol B. *Org. Biomol. Chem.,* **2003**, *1*, 2044-2056.

180. Pronin, S. V.; Martinez, A.; Kuznedelov, K.; Severinov, K.; Shuman, H. A.; Kozmin, S. A. Chemical synthesis enables biochemical and antibacterial evaluation of streptolydigin antibiotics. *J. Am. Chem. Soc.,* **2011**, *133*, 12172-12184.

181. Verbeure, B.; Lacey, C. J.; Froeyen, M.; Rozenski, J.; Herdewijn, P. Synthesis and cleavage experiments of oligonucleotide conjugates with a diimidazole-derived catalytic center. *Bioconjugate Chem.,* **2002**, *13*, 333-350.

182. Li, S.; Liang, S.; Tan, W.; Xu, Z.; Ye, T. Total synthesis of emericellamides A and B. *Tetrahedron,* **2009**, *65*, 2695-2702.

183. McInnis, C. E.; Blackwell, H. E. Thiolactone modulators of quorum sensing revealed through library design and screening. *Bioorg. Med. Chem.,* **2011**, *19*, 4820-4828.

184. Arthur, C.; Cox, R. J.; Crosby, J.; Rahman, M. M.; Simpson, T. J.; Soulas, F.; Spogli, R.; Szafranska, A. E.; Westcott, J.; Winfield, C. J. Synthesis and characterisation of acyl carrier protein bound polyketide analogues. *ChemBioChem,* **2002**, *3*, 253-257.

185. Mukaiyama, T.; Kobayashi, S. In *Organic Reactions*; John Wiley & Sons, Inc.: 2004.

186. Harvey, C. J. B.; Puglisi, J. D.; Pande, V. S.; Cane, D. E.; Khosla, C. Precursor directed biosynthesis of an orthogonally functional erythromycin analogue: selectivity in the ribosome macrolide binding pocket. *J. Am. Chem. Soc.,* **2012**, *134*, 12259-12265.

187. Piasecki, Shawn K.; Taylor, Clint A.; Detelich, Joshua F.; Liu, J.; Zheng, J.; Komsoukaniants, A.; Siegel, Dionicio R.; Keatinge-Clay, Adrian T. Employing modular polyketide synthase ketoreductases as biocatalysts in the preparative chemoenzymatic syntheses of diketide chiral building blocks. *Chem. Biol.*, *18*, 1331-1340.

188. Piasecki, S. K.; Keatinge-Clay, A. T. Monitoring biocatalytic transformations mediated by polyketide synthase enzymes in cell lysate via fluorine NMR. *Synlett,* **2012**, *23*, 1840-1842.

189. Hu, Z.; Jiang, X.; Han, W. Synthesis of novel analogues of antimycin A3. *Tetrahedron Lett.,* **2008**, *49*, 5192-5195.

190. Zhang, T.; Ma, W.-L.; Li, T.-R.; Wu, J.; Wang, J.-R.; Du, Z.-T. A facile asymmetric synthesis of (S)-14-methyl-1-actadecene, the sex pheromone of the peach leafminer moth. *Molecules,* **2013**, *18*, 5201.

191. Yadav, J. S.; Gayathri, K. U.; Thrimurtulu, N.; Prasad, A. R. Stereoselective synthesis of 10,14-dimethyloctadec-1-ene, 5,9-dimethyloctadecane, and 5,9-dimethylheptadecane, the sex pheromones of female apple leafminer. *Tetrahedron,* **2009**, *65*, 3536-3544.